Radio over fibre techniques for backhaul and fronthaul

---

vorgelegt von
Jessé Gomes dos Santos, M. Sc.
geb. in Itamaraju/Bahia – Brasilien

von der Fakultät IV – Elektrotechnik und Informatik
der Technischen Universität Berlin
zur Erlangung des akademischen Grades

Doktor der Ingenieurwissenschaften
– Dr.-Ing. –

genehmigte Dissertation

Promotionsausschuss:

Vorsitzender:	Prof. Dr.-Ing. Slawomir Stanczak
Gutachter:	Prof. Dr.-Ing. Hans-Joachim Grallert
Gutachter:	Prof. Marcelo Vieira Segatto, PhD
Gutachter:	Prof. Paulo Miguel N. P. Monteiro, PhD

Tag der wissenschaftlichen Aussprache: 27. October 2017

Berlin 2017

Abstract

The 5^{th} generation of the mobile network, foreseen to work commercially from 2020, promises to offer significant improvements when compared to previous mobile generations. Among these advances, the minimum experienced user throughput in uplink 50 [Mbps] and downlink 100 [Mbps] stands out. Such new requirements will lead to an exponential growth of aggregation network traffic. To address such theme, this dissertation presents the state-of-the-art subjects directly related to the collection and distribution of signal in access networks, besides the traffic in fronthaul segment. The theoretical background begins by presenting the main features of 4G/5G mobile dense heterogeneous networks using millimetre wave and massive MIMO. It continues showing the evolution from the Distributed Radio Access Network (D-RAN) to the Centralized Radio Access Network (C-RAN), which creates the fronthaul segment, their requirements, and Radio-over-Fibre (RoF) techniques capable of carrying signals between Remote Radio Head (RRH) and Base Band Unit (BBU), are also presented.

The use of such technologies altogether with Common Public Radio Interface (CPRI) translates into a huge increase in data traffic in the fronthaul segment. In order to minimize these effects, three main

techniques have been suggested, one belonging to the analogue domain Analogue Radio over Fibre (A-RoF), and the other two (I/Q compression and functional split) concerning the digital domain. In addition to the previously mentioned demands, the integration between the fronthaul and backhaul segments, contained in the aggregation network, is already a beneficial factor for the proper functioning of the aggregation networks. This integration is supported by Software Defined Network (SDN) and Virtual Radio Access Network (V-RAN).

After collaborating with the beginning readings, showing a deep description about the state of the art design and trends, this dissertation contributes to the currents discussion on front/back-haul presenting a quantitative analysis on the traffic generated in fronthaul, considering the CPRI interface and five different spaces of subcarriers, to confirm the exponential data traffic between the BBU and the RRH.

Numeric evaluations demonstrate the gains offered by compression techniques, which were shown with the potential of saving up to 75% in the amount of data transported in fronthaul. Still in the digital domain, the results of the quantitative analysis regarding to the functional split technique demonstrates an even more relevant saving than the one offered by the compression. In order to verify the performance of the transmission in the analogue domain, the experiment using Analogue Radio over Fibre (A-RoF) shows the feasibility of using this technological option, even though it is hindered by non-linear effects produced by the transceivers present in this transmission model. The main points of design proposed by the 5G-Crosshaul project is presented in the annex.

Zusammenfassung

Die 5. Generation des Mobilfunknetzes verspricht deutliche Verbesserungen im Vergleich zu früheren Mobilgenerationen. Vorgesehen ist, dass sie 2020 kommerziell verwendet wird. Unter den Fortschritten sind insbesondere die minimale Datenrate im Uplink 50 [Mbps] und Downlink 100 [Mbps] hervorzuheben. Diese neuen Anforderungen führen zu einem exponentiellen Wachstum des Datenverkehrs im Aggregationsnetzwerk. Diese Thesis stellt die State-of.the-Art-Themen vor, die sich, neben dem Datenverkehr im Fronthaul-Segment, direkt mit der Sammlung und Verteilung von Signalen im Zugangsnetz beschäftigen. Der theoretische Hintergrund beginnt mit der Präsentation der Main-Features von dichten, heterogenen 4G- und 5G-Mobilfunknetzen, die Milimeterwellen und Massive MIMO nutzen. Es folgt eine Übersicht über die Entwicklung von Distributed Radio Access Network (D-RAN) zu Centralized Radio Access Network (C-RAN), durch die das Fronthaul-Segment entstanden ist. Seine Anforderungen und Radio-over-Fibre (RoF), die eine Signalübertragung zwischen Remote Radio Head (RRH) und Base Band Unit (BBU) ermöglichen, werden ebenso vorgestellt.

Die Verwendung solcher Technologien zusammen mit dem Common Public Radio Interface (CPRI) führt zu einer enormen Zunahme des

Datenverkehrs im Fronthaul-Segment. Um diese Effekte zu minimieren, wurden drei grundlegende Techniken vorgeschlagen. Eine dieser Techniken Analogue Radio over Fibre (A-RoF) erfolgt auf analoger Ebene, die anderen zwei (Kompression und Functional Split) auf digitaler Ebene. Zusätzlich zu den erwähnten Anforderungen ist die Integration zwischen den im Aggregationsnetz enthaltenen Fronthaul- und Backhaul-Segmenten bereits ein nützlicher Faktor für das einwandfreie Funktionieren der Aggregationsnetzwerke. Diese Integration wird durch Software Defined Network (SDN) und Virtual Radio Access Network (V-RAN) unterstützt.

Außer der gemeinsamen Arbeit an den zu Beginn vorgestellten Themen, daher die detailreiche Beschreibung von State-of.the-Art-Design und –Trends, trägt diese Thesis eine quantitative Analyse des Datenverkehrs im Fronthaul-Segment zu den aktuellen Diskussionen um Front- und Backhaulnetze bei. Die durchgeführte Analyse bestätigt den exponentiellen Datenverkehr zwischen BBU und RRH. Sie berücksichtigt dabei die CPRI-Schnittstelle und fünf verschiedene Abstände zwischen den einzelnen Subcarriern.

Simulationen zeigen die durch Kompressionstechniken ermöglichten Gewinne, die eine Reduzierung von bis zu 75% der Datenmenge im Fronthaul-Bereich ermöglichen. Im digitalen Bereich zeigen die Resultate der quantitativen Analyse der Functional Split-Technik sogar eine noch größere Reduzierung als die Kompressionstechnik. Die Analyse der Nutzung von Analogue Radio over Fibre (A-RoF) verifiziert die Leistung der Übertragung im analogen Bereich und zeigt, dass auch diese Technik möglich ist, obwohl sie unter nichtlinearen Effekten leidet, die durch die Empfänger hervorgerufen werden. Die Haupt-Designpunkte, die das 5G-Crosshaul Projekt vorgeschlagen hat, werden im Anhang vorgestellt.

Contents

Abbreviations

1G	First Generation
2G	Second Generation
3G	Third Generation
ADC	Analogue to Digital Converter
AF	Adaptation Function
AgN	Aggregation Network
AMPS	Advanced Mobile Phone Services
AN	Access Network
AON	Active Optical Network
APD	Avalanche Photo Diode
API	Application Programming Interface
A-RoF	Analogue Radio over Fibre
ATM	Asynchronous Transfer Mode
AxC	antenna-carriers

AWG	Arbitrary Waveform Generator
BBM	Base Band Module
BBU	Base Band Unit
BGP	Border Gateway Protocol
BTS	Base Transceiver Station
BS	Base Station
CA	Carrier Aggregation
CapEx	Capital Expenditure
CCM	Control and Clock Module
CD	Chromatic Dispersion
CDF	Cumulative Distribution Function
CN	Core Network
CO	Central Office
CoMP	Coordinated MultiPoint
CPRI	Common Public Radio Interface
C-RAN	Centralized Radio Access Network
CRC	Cyclic Redundancy Check
CSI	Channel State Information
CWDM	Coarse Wavelength Division Multiplexing
D2D	Device to Device
DAC	Digital to Analog Converter
DAS	Distributed Antenna System

DwPTS	Downlink Pilot Time Slot
DML	Direct Modulated Laser
D-RoF	Digital Radio of Fibre
D-RAN	Distributed Radio Access Network
DWDM	Dense Wavelength Division Multiplexing
EBI	Eastbound Interface
eCPRI	enhanced Common Public Radio Interface
EDGE	Enhanced Data rates for GSM Evolution
E/O	Electrical-to-Optical
EMBB	Enhanced Mobile BroadBand
EPC	Evolved Packet Core
EPON	Ethernet Passive Optical Network
ETSI	European Telecommunications Standards Institute
EVM	Error Vector Magnitude
FDD	Frequency Division Duplexing
FFT	Fast Fourier Transform
FPGA	Field Programmable Gate Array
FTTH	Fibre To The Home
FTTP	Fibre To The Premisse
GP	Guard Period
GPON	Gigabit Passive Optical Network
GPRS	General Packet Radio Service

GPS	Global Positioning System
GSM	Global System for Mobile Communications
HARQ	Hybrid automatic Repeat request
HSPA	High Speed Packet Access
IQ	In-phase, Quadrature
IF	Intermediate Frequency
IFB	Intermediate Frequency-band
IF-over-fibre	Intermediate Frequency over fibre
IMD	Inter-Modulation Distortion
IP	Intelectual Property
IoE	Internet of Everything
ISAZ	Integrated Services Access Zone
ICS	Indoor Coverage System
ISI	Inter Symbol Interference
ITU-T	International Telecommunication Union - Telecommunication Standardization Sector
JT	Joint Transmission
LTE	Long Term Evolution
LTE-A	Long Term Evolution Advanced
MANO	Management and Orchestration
MIMO	Multiple Input Multiple Output
MMIMO	Massive Multiple Input Multiple Output

mmWave	Millimeter Wave
MFH	Mobile FrontHaul
MTC	Machine Type Communication
MPLS	MultiProtocol Label Switching
NBI	Northbound Interface
NB-IoE	Narrow Band Internet of Everthings
NFV	Network Function Virtualization
NGFI	Next Generation Fronthaul Interface
NGMN	Next Generation Mobile Networks
NG-PON	Next Generation Passive Optical Network
TSP	Telecommunication Service Provider
OADM	Optical Add&Drop Multiplexer
OBSAI	Open Base Station Architecture Initiative
ODL	Open Daylight
ODN	Optical Distribution Network
OEM	Original Equipment Manufacturers
OFDM	Orthogonal Frequency Division Multiplexing
OLT	Optical Line Terminal
ONU	Optical Network Unit
ONOS	Open Nerwok Operating System
OpEx	Operational Expenditure
ORI	Open Radio equipment Interface

OWS	Optical Wireless System
OTN	Optical Transport Network
OXC	Optical Cross-Connect
PA	Power Amplifier
PAPR	Peak-to-Average Power Ratio
PON	Passive Optical Network
QoE	Quality of Experience
QoS	Quality of Service
RAN	Radio Access Network
RAT	Radio Access Technology
RAU	Radio Access Unit
RGU	Radio Aggregation Unit
RB	Resource Block
RCC	Remote Cloud Center
RE	Radio Equipment
REC	Radio Equipment Control
RF	Radio Frequency
RFM	Radio Frequency Module
ROADM	Reconfigurable Optical Add&Drop Multiplexer
RoE	Radio over Ethernet
RoF	Radio-over-Fibre
RP	Reference Point

RRH	Remote Radio Head
RRS	Remote Radio System
RRU	Remote Radio Unit
SBI	Southbound Interface
SDN	Software Defined Network
SFP	Small Form-factor Pluggable
SISO	Single Input Single Output
SSMF	Standard Single Mode Optical Fibre
SNR	Signal Noise Ratio
TAE	Time Accuracy Error
TDD	Time Division Duplexing
TDM	Time Division Multiplexing
TDM-PON	Time Division Multiplexing Passive Optical Network
TM	Transport Module
TVWS	Television White Space
TWDM	Time and Wavelength Division Multiplexing
TWDM-PON	Time and Wavelength Division Multiplexing Passive Optical Network
UMTS	Universal Mobile Telephone Service
URLLC	Ultra-Reliable and Low-Latency Communications
UpPTS	Uplink Pilot Time Slot

UTRA-FDD	(Universal Mobile Telecommunications System) Terrestrial Radio Access - Frequency Division Duplexing
V-RAN	Virtual Radio Access Network
VDSL	Very High Speed Digital Subscriber Line
VEA	Variable Electrical Attenuator
ViLTE	Video over LTE
VLAN	Virtual Local Area Network
VoLTE	Voice over LTE
XCF	5G-Crosshaul Common Frame
XCI	5G-Crosshaul Control Infrastructure
XCSE	5G-Crosshaul Circuit Switching Element
XFE	5G-Crosshaul Forwarding Element
XPFE	5G-Crosshaul Packet Forwarding Element
XPU	5G-Crosshaul Processing Unit
WCDMA	Wideband Code Division Multiple Access
WDM	Wavelength Division Multiplexing
WDM-PON	Wavelength Division Multiplexing Passive Optical Network
WiMAX	Worldwide Interoperability for Microwave Access
WLAN	Wireless Local Area Network
WBI	Westbound Interface
WWWW	World Wide Wireless Web

List of Figures

List of Tables

Acknowledgements

Firstly, I would like to thank Jesus Christ for opening this important door for me and therefore fulfilling a promise that had been made to me when I was a child and reconfirmed in February 2012. I also thank my family, in particular my grandfather Manoel Ferreira de Souza, for his constant spiritual support. I also thank Dr. Thomas Haustein for receiving me at the Franhoufer-HHI and also to the research institutes who both directly and indirectly helped me.Thanks also to Professor Doctor Hans-Joachim Grallert for being my guide and for always showing me patience and respect. I also want to thank Luiz Anet Neto for his promptness and numerous help in the course of writing and experiments. I thanks also to Coordenação de Aperfeiçoamento de Pessoal de Nível Superior (CAPES) by the financial support.

1 Introduction

This chapter is divided into three sections. Section 1.1 introduces the reasons for the accomplishment of this academic research. Section 1.2 highlights the focus and the main contributions of this research. Section 1.3 presents the structure of this dissertation.

1.1 Motivation

Since 1980, when the first analogue cellular networks were deployed, mobile networks have experienced a splendid growth in mobile traffic. This growth has required one continuous expansion of existing mobile networks to ensure the high rate of users upload and download. Achieving such severe constraints, requires the existence of, not only

macro cells, but also small cell and wi-fi zones in the new generations of wireless mobile networks [Fre13, VIAa].

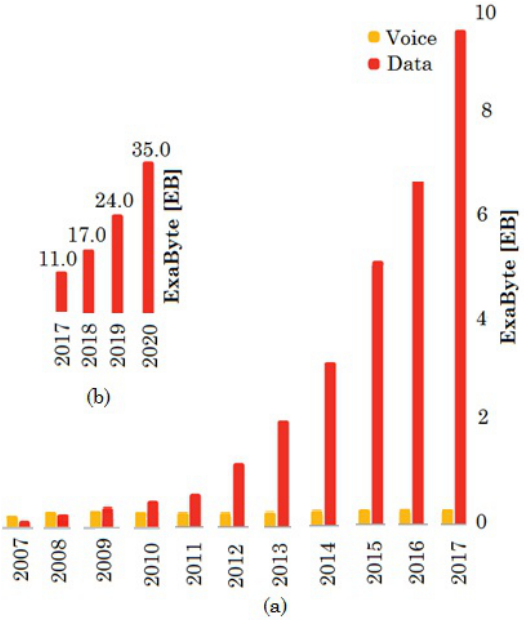

Figure 1.1: Mobile telecommunication statistics: a) Total quarterly mobile voice and data traffic as measured by Ericsson between 2007 and Q1/2017; b) Cisco forecast of data traffic between 2017 and 2020 [Eri16, CIS17].

Figure 1.1(a) shows this exponential growth, which started in 2007. In the end of 2009 the total (uplink + downlink) mobile network traffic becomes mostly data-based, and in the 2017 this traffic is almost 10 Exabytes (Figure 1.1.b). Those responsible for such growth are addition of new smartphone subscriptions altogether with average data volume per subscription, which are fuelled by consumption of multimedia contents with high and ultra high-quality. In the same

period, mobile voice traffic has grown at much more modest rates [Eri16].

Studying this mobile traffic, it is observed that 80% has been used for indoor applications such as homes, offices, shopping malls, hotels or other indoor venues, and 90% of this value is handled by less than 10% of the cells [Fre13, VIAa]. Considering the forecast presented in 1.1(b) it is possible to conclude that the traffic in 2020 will be 1000-fold more than predicted in 2010 [IHD+14, Aya16, PSS16].

Table 1.1: Strategies about achieving 1000x capacity increase.

Institution	Additional Spectrum	Spectral Efficiency	Connection Density	Total
KTH and RWTH	3x	5x	67x	1,005x
JDSU	3x	6x	56x	1,008x
Nokia	10x	10x	10x	1,000x
NTT DoCoMo	2.8x	24x	15x	1,008x
Qualcomm	10x	1x	100x	1,000x

Source:[ZM13]

To satisfy this massive demand, market players and academic research institutes have proposed different strategies. Some of them are showed in table 1.1 [ZM13, BLM+14, Hus14]. It is observed that the demand

for new spectrum ranges between 2.8x and 10x, the spectral efficiency should be improved by up to 24x, and densification should reach values to the order of 100x.

Table 1.2 [MET15] shows different strategies that can be used to meet the foreseen throughput. Massive MIMO, use of dynamic Time Division Duplexing (TDD), cells coordination, device to device (D2D) are used together with additional spectrum and densification allowing to meet the foreseen 1000x throughput.

Table 1.2: New promising techniques and their respective impact.

Description of technique	**Impact**
Additional spectrum bands	3.4x
Densification of system together with use of RRH	3.65x
Strong use of dynamic Time Division Duplexing (TDD)	1.67x
Cells coordination	1.21x
Massive MIMO using 256 x 256 antenna elements	20x
Device to Device (D2D) increase of localized traffic flow	2x
Total	1,003.1x

Source:[MET15]

1.2 Research focus and contributions

In accord with shown in section 1.1, since the launch of Long Term Evolution (LTE) a exponential grow in mobile data traffic has been observed, and predictions point to even more aggressive growth in the coming years. Such access networks data traffic growth is reflected in aggregation networks, especially on fronthaul segment, requiring much larger capacity than the currently available.

To avoid this, some technologies to minimize this huge quantity of data transmitted between Base Band Unit (BBU) and Remote Radio Head (RRH) are investigated in this dissertation, which presents as main contributions:

1. In section 5.1, the numerical analysis evaluation showing the quantity of data demanded on fronthaul segment using Common Public Radio Interface (CPRI), considering number of bands and number of Multiple Input Multiple Output (MIMO) antennas elements;

2. In section 5.2, the gains produced by compression techniques using the decrease of the number of sampling bits alone or associated with redundant spectral data remotion is shown through numerical simulations. Also in section 5.2.1 are presented I/Q compression experimental results showing evolution of Error Vector Magnitude (EVM) as the number of sampling bit rate is decreased.

3. In section 5.3 is done a numerical analysis about fronthaul transmission using different functional split options. Such analysis shows the percentage of savings data traffic provided by the functional split.

4. In section 5.4, analogue transmission is approached through experiments done in laboratory aiming to present the EVM value obtained in this third option, useful to minimize the data traffic in fronthaul and non-linearity EVM performance produced Direct Modulated Laser (DML) when the RF power of input of the laser are increased for laser non-linear region.

1.3 Structure of this dissertation

Aiming to facilitate the understanding of beginning readers there is an ample state-of-the-art of the technologies considered as trends for the new access 5G network. Figure 1.2 shows the organization of this dissertation.

Chapter 2 considers the essential technologies to be used on 5^{th} mobile access network generation, which are: Dense Heterogeneous Network, (Dense HetNet), millimetre wave (mmWave), and Massive MIMO (MMIMO).

Chapter 3 presents an overview about the technologies Distributed Radio Access Network (D-RAN) and Centralized Radio Access Network (C-RAN), Analogue Radio over Fibre (A-RoF) and Digital Radio over Fibre (D-RoF) transmission altogether with their respective interfaces.

Chapter 4 presents the features of Software Defined Network (SDN) and Virtual Radio Access Network (V-RAN) transmission using Radio over Ethernet (RoE).

Chapter 5 starts investigating, in section 5.1, a study about quantity of data demanded by digital fronthaul transmission considering five

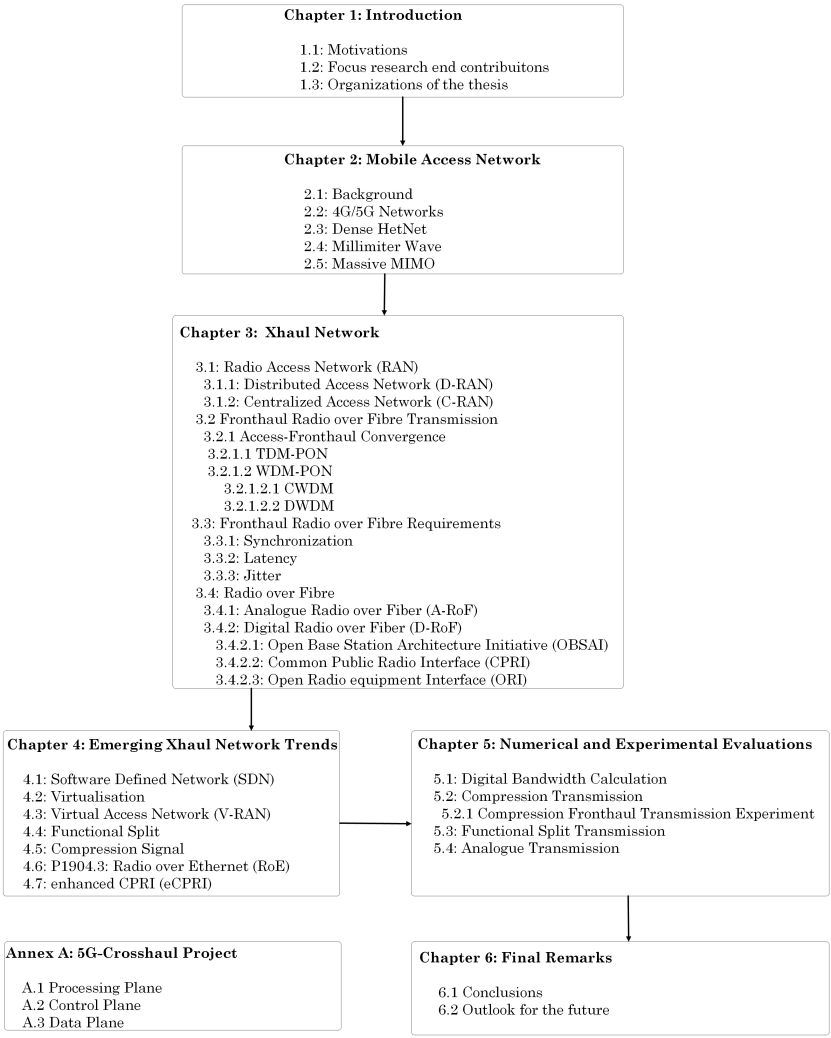

Figure 1.2: Organisation of the dissertation.

different potential 5G spacing subcarrier. In the following section 5.2, a numerical analysis showing the gains produced by different compression technique options altogether with Error Vector Magnitude (EVM) experiment results measured in Fraunhofer Heinrich Hertz Institute laboratory using an off-line transmission and lossy compression technique. Next, the section 5.3 shows the positive impact caused by four different functional split options. Section 5.4 presents the feasibility of analogue transmission in the fronthaul segment even considering non linearity effects.

Chapter 6 starts presenting the summary and conclusions obtained in the face of the studies carried out, and ends up presenting potential research topics directly related to the study under discussion.

Annex A presents the concept of new system researched on 5G Crosshaul project.

2

Mobile Access Network

This chapter is divided into five sections. It starts introducing, in section 2.1, the main features contained in Core Network (CN), Aggregation Network (AgN) and Access Network (AN). Section 2.2 presents the main features of 4G and 5G network system architecture. Section 2.3 is dedicated to showing the main characteristics of Mobile Heterogeneous Network densification (Dense HetNet). Millimetre Wave (mmWave) is the object of study in section 2.4, while section 2.5 has the description of the features belonging to massive Multiple Input Multiple Output (mMIMO).

2.1 Background

The current mobile network architecture can be divided as follows [Hai16, VGMM14, PPP15, Sau14]:

1. Core Network (CN), user of Ethernet based packet switched topology;
2. Aggregation Network (AgN), divided in two segments:
    a) Fronthaul segment, a currently user of Open Base Station Architecture Initiative (OBSAI) or Common Public Radio Interface (CPRI), which is a circuit switched technology;
    b) Backhaul segment, an adept of same technologies adopted by access and core networks. Currently there are some technologies being used as backhaul link: copper-based twisted pair cable using E-1 timeslot-based architecture (2 Mbps) to connect Global System for Mobile Communications (GSM) cell site. The second option, used by Universal Mobile Telephone Service (UMTS), is Asynchronous Transfer Mode (ATM) connectivity with 155.52 Mbps. For Long Term Evolution (LTE), there is Very High Speed Digital Subscriber Line (VDSL) which can offer up to 100 Mbps, high speed Ethernet-based microwave enabling, up to 1 Gbps, or optical fibre offering dozens of Gbps.
3. Access Network (AN) also known as Radio Access Network (RAN), operates in two environments:
    a) Indoor, where predominates Wi-Fi calling technology using Wi-Fi standard, (IEEE 802.11 a/b/g/n/ac) an adept of Ethernet based packet switched topology. Telecommunication

Service Provider (TSP) has used massive amounts of Wi-Fi access points in order to extend, transparently to the user, the reach of service Voice over LTE (VoLTE) and Video over LTE (ViLTE);

b) Outdoor, where Wi-Fi access points can also be found but are predominantly controlled by mobile technology (2G, 3G, and 4G).

The use of mobile technologies began in the early 1980s with the implementation of the First Generation (1G) commercial cellular systems, called Advanced Mobile Phone Services (AMPS), which stands out because of its use of frequency modulated analogue voice transmission providing speed of up to 2.4 kbps and a very small quantity of base stations, which illuminated a large area [Cat15, Hu16].

A digital version of the 1G systems appeared 10 years later, called Second Generation (2G), whose commercial name is Global System for Mobile Communications (GSM), unifying autonomous national systems in Europe. Similarly to 1G, 2G was designed to provide only voice traffic, and its maximum data speed is 64 kbps. The advent of the technologies for the General Packet Radio Service (GPRS) (2.5G) and Enhanced Data rates for GSM Evolution (EDGE) enabled 2G to offer data traffic with a maximum network speed of 64-144 kbps [Cat15, Hu16].

The popularization of the Internet was the catalysing source for the Third Generation (3G). Launched in the early of 2000s, Universal Mobile Telephone Service (UMTS) offers enhanced support for data traffic along with the traditional voice services. The introduction of 3G improved data transmission speed from 144 kbps to 2 Mbps. Later versions of 3G, named High Speed Packet Access (HSPA) and HSPA+,

have improved this feature, enabling speeds of up to 336 Mbps, but always using carrier bandwidth equal to 5 MHz [Cat15, Hu16].

2.2 4G/5G Networks

In 2008 the voice traffic centralization paradigm was broken due to a new Radio Access Technology (RAT) interface being presented to the world, named Long Term Evolution (LTE). LTE emerged only focused on data traffic (with voice only being transmitted by the 2G or 3G networks). LTE promises theoretic peak experienced throughput of up to 300 Mbps. In 2010, Long Term Evolution Advanced (LTE-A) expanded user experienced throughput from 300 Mbps to up 1 Gbps [Cat15, Hu16]. Figure 2.1 depicts the correlation between number of antennas or streams, radio frequency (RF) bandwidth and respective 4G/5G standards.

Figure 2.1 shows that LTE system, which starts using a maximum MIMO of 4x4 in single carrier, has evolved to enable the use up to 256 antennas (in Massive MIMO) and 100 MHz (in Bandwidth Aggregation). The figure 2.1 also shows that for 5G the bandwidth available can to achieve up to 7 GHz.

LTE can be deployed using two types of frame structure Time Division Duplexing (TDD) and Frequency Division Duplexing (FDD). In TDD there are uplink (UL) and downlink (DL) configurations. UL and DL are separated in time domain, being that some subframes carrier for downlink and other for uplink. Between them there are special subframe to transmit Downlink Pilot Time Slot (DwPTS), Uplink Pilot Time Slot (UpPTS), Guard Period (GP) [OJFM11].

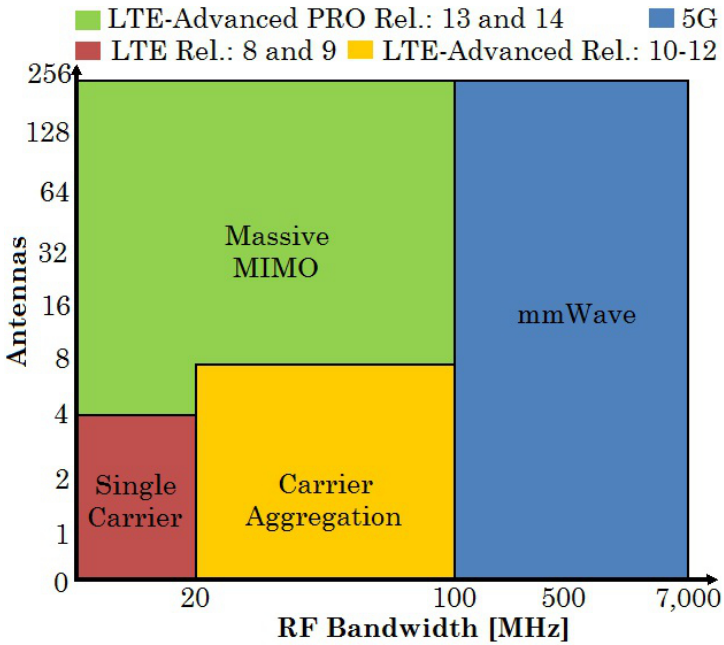

Figure 2.1: Spectrum division.

TDD has seven UL/DL options. Each one of this option is chosen according to the demand of each area. If in a given region, the higher demand is download, then the configuration used will have predominance of subframes for downlink, and vice versa. If the demand is equal, a configuration that meets this situation is used. TDD uses frame structure type 2, which period of frame, subframe, slot duration, and resource blocks (pairs) quantity are the same used in FDD mode [OJFM11].

In FDD, occurs the separation of uplink/downlink in frequency domain, and each frame, with duration of 10 ms, is composed by 10 subframes during 1 ms. Each subframe is composed of two slots having

0.5 ms of duration. In a normal cyclic prefix, each slot is one Resource Block (RB) and has 7 OFDM symbols. In frequency domain there are 12 subcarriers, and each subcarrier is spaced of 15 kHz. Two RB is named resource block pair in time domain. In time and frequency domains each one Orthogonal Frequency Division Multiplexing (OFDM) symbol are housing by one Radio Equipment (RE), and the number of resource elements (N_{RE}) of each air channel bandwidth is calculated by [OJFM11]

$$N_{RE} = N_{RB} \cdot N_{RB-pairs} \cdot N_{Time-RE} \cdot N_{Freq-RE}. \tag{2.1}$$

LTE Frequency Division Duplexing (FDD) uplink user experienced peak spectral efficiency ($\mathrm{SE_{pFDD,U}}$) can be calculated by [OJFM11]

$$SE_{p-FDD,Up} = 2^m \cdot N_A \cdot N_B \cdot N_{bps} \cdot N_{RB} \cdot N_{DM-RS} \cdot \frac{6}{7} \cdot \frac{(N_{RE} - N_{PUCCH} - N_{PRACH})}{T_F}. \tag{2.2}$$

The factor 6/7 used in equation 2.2 is due to one of seven symbols are used to carrier demodulation reference signal (DM-RS). For Frequency Division Duplexing (FDD) downlink user experienced peak spectral efficiency ($\mathrm{SE_{pFDD,D}}$) per sector is found through equation 2.3 [OJFM11]

$$SE_{p-FDD,Dw} = 2^m \cdot N_A \cdot N_B \cdot N_{bps} \cdot N_{RB} \cdot \frac{(N_{RE} - N_{DRS} - N_{PBCH} - N_{SCH} - N_{L1/L2CS})}{T_F}. \tag{2.3}$$

where,

$N_{RB-pairs}$ = Number of resource blocks pair in time domain,
$N_{Time-RE}$ = Number of resource elements in time domain,
$N_{Freq-RE}$ = Number of resource elements in frequency domain,
2^m = Scale factor comes from 5G, where m is an integer positive or negative number,
N_A = Number of antennas,
N_B = Number of frequency bands,
N_{bps} = Number of data bits per symbol,
N_{RB} = Number of resource blocks in frequency domain,
N_{DM-RS} = Number of demodulation reference signal,
N_{RE} = Number of resource elements,
N_{PUCCH} = Number of Physical Uplink Shared Channel,
N_{PRACH} = Number of Physical Random Access Channel,
N_{PRACH} = Number of Physical Random Access Channel,
N_{DRS} = Number of Downlink Reference Signal,
N_{PBCH} = Number of Physical Broadcast Channel,
N_{SCH} = Number of Synchronization signals,
$N_{L1/L2CS}$ = Number of L1/L2 Control Signal,
T_F = Period of frame.

Table 2.1: Downlink physical layer parameters comparison between LTE and 5G systems.

Var.	Feature	4G						5G	Formula
S_R	Sampling rate [MHz]	1.92	3.84	7.68	15.36	23.04	30.72	122.88	$S_S \times T_S$
C_B	Air channel bandwidth [MHz]	1.4	3	5	10	15	20	80	$G_B + M_B$
M_B	Measurement bandwidth [MHz]	1.08	2.7	4.5	9	13.5	18	72	$S_S \times U_S$
G_B	Guard band [MHz]	0.32	0.3	0.5	1	1.5	2	8	-
T_S	Total subcarriers	128	256	512	1024	1536	2048	2048	$U_S + Z_P$
Z_P	Zero padding	56	76	212	424	636	848	848	-
U_S	Useful subcarriers	72	180	300	600	900	1200	1200	$P_{RB} \times S_{PRB}$
P_{RB}	Physical Resource Block [PRB]	6	15	25	50	75	100	100	-

Continues on next page

Table 2.1 : *Continued from previous page*

Var.	Feature	4G						5G	Formula
C_{FS}	Cyclic Prefix of first symbol	10	20	40	80	120	160	160	-
C_{OS}	Cyclic Prefix of other symbols	9	18	36	72	108	144	144	-
S_{SL}	Samples per slot	960	1920	3840	7680	11520	15360	15360	$C_{FS} + (6 \times C_{OS}) + (7 \times T_S)$
S_S	Subcarrier spacing [kHz]	15						$2^{m1} \times 15$	-
N_F	Number of frames	10						40	-
S_{PRB}	Sub carrier at each PRB	12							-
N_B	Number of frequency band	1,..,5						1,...,8	-
N_{Sym}	Number symbol per PRB	7							-

Continues on next page

[1] m is an integer number (i.e. ... -2, -1, 0,1,2,...), 5G uses m = 2

Table 2.1 : *Continued from previous page*

Var.	Feature	4G	5G	Formula
N_{bps}	Number of data bit per symbol	2, 4, 6, 8		-
N_A	Number of SISO or MIMO antennas elements	1x1, 2x2, 4x4, 8x8		-
T_F	Duration of frame [ms]	10		$10 \times T_{TTI}$
N_{fps}	Number of frame per second	100		$1 / T_F$
T_{TTI}	Duration of Subframe [ms]	1	0.25	$20 \times T_{Slot}$
T_{Slot}	Duration of slot [ms]	0.5	0.125	$T_{FS} + (6 \times T_{OS})$
T_{SoCP}	Duration of symbol without cyclic prefix [µs]	66.67	16.67	$1 / S_S$

Continues on next page

Table 2.1 : *Continued from previous page*

Var.	**Feature**	**4G**	**5G**	**Formula**
N_{SpF}	Number of slot per frame	20	80	T_F / T_{Slot}
T_{fs}	Duration of first Symbol [µs]	71.87	17.97	T_{SoCP} + C_{fs} / ($S_S \times T_S$)
C_{fs}	Duration of other Symbols [µs]	71.36	17.84	T_{SoCP} + C_{OS} / ($S_S \times T_S$)

Table 2.1 presents a description of the variables and values used in LTE and 5G systems [TR14, NK16]. It shows that LTE has a scalable air channel bandwidth and it allows the signal to be coded by Binary Phase Shift Keying (BPSK), Quadrature Phase-Shift Keying (QPSK) and Quadrature Amplitude Modulation (QAM). The LTE guard band, reserved for filter edge roll-off is about 10% of the air channel bandwidth. The last column in table 2.1 shows that sampling frequency (S_R) can be calculated multiplying subcarrier spacing (S_S) by total subcarrier (T_S); Channel bandwidth (C_B) is the sum of Guard band (G_B) plus Measurement bandwidth (M_B); Measurement bandwidth (M_B) can be obtained multiplying subcarrier spacing (S_S) by Useful subcarrier (U_S). Total subcarrier (T_S) is the product of Physical Resource Block (P_{RB}) and subcarriers in each Physical Resource Block (S_{PRB}).

Table 2.2 [NK16] shows that LTE admits signals to be coded by BPSK, QPSK, and QAM.

Table 2.2: Maximum EVM requirements for different modulation schemes in LTE-Advanced [Section 6.5.2 TS 36.104].

Constellation Size	**Maximum EVM**
BPSK/QPSK	17.5%
16-QAM	12.5%
64-QAM	8%
256-QAM	3.5%

The frequency domain Error Vector Magnitude (EVM), a measure of

deviation of constellation points from their ideal locations and which calculates the distortion only over part of the bandwidth carrier useful information, ranges from 3.5% to 17.5% and can be calculated by [SNRZ17]

$$EVM_{FD}(\%) = \sqrt{\frac{\sum_{n\in\beta|\tilde{s}_{IN}(n)-\tilde{s}_{OUT}(n)|^2}}{\sum_{n\in\beta|\tilde{s}_{IN}(n)|^2}}} \times 100, \tag{2.4}$$

where $\tilde{s}_{IN}(n)$ and $\tilde{s}_{OUT}(n)$ are transformed signals by Fast Fourier Transform (FFT) for input and output respectively, and β is the collection of indices corresponding to the utilized bandwidth [SNRZ17].

The next generation of mobile phone system (5G) will present a degree of complexity much higher than those observed so far (1G, 2G, 3G, 4G), because 5G devices should be able to operate in several spectrum bands, from Radio Frequency (RF) to Millimeter Wave (mmWave), and also be compatible with existing technologies such as 2G (GPRS/EDGE), 3G (WCDMA/HSPA/HSPA+), 4G (LTE/LTE-Advanced/Worldwide Interoperability for Microwave Access (WiMAX)), Wireless Local Area Network (WLAN), Television White Space (TVWS) networks, Optical Wireless System (OWS), Machine Type Communication (MTC)s, Fibre To The Premisse (FTTP), Active Optical Network (AON) and Passive Optical Network (PON) [HH15, ODK16]. This involvement in various Radio Access Technology (RAT), containing dynamic cell sizes, will accredit the 5G as the true World Wide Wireless Web (WWWW) [ODK16].

5G network can also been resumed as a fibre-like user experience due to required capabilities such as low latency and massive capacity. It is based on three main features: ubiquitous connectivity, extremely low latency and ultra-high speed data rate [BNP16, CNG+17].

According to [Uni17] there are 13 technical performance requirements defined for IMT-2020 which are: peak data rate, peak spectral efficiency, user experienced data rate fifth percentile user spectral efficiency, average spectral efficiency, area traffic capacity, latency, energy efficiency, reliability, mobility, mobility interruption time, bandwidth.

1. Peak data rate [Mbps]: the maximum achievable received data rate under error-free conditions attributed to a single mobile station [Uni17].

$$R_p = \sum_{n=1}^{k} W_n \times SE_p \tag{2.5}$$

   where, W_n and SE_{p_n} (n = 1, ..., k) are the air channel bandwidth and peak spectral efficiency in that band. The minimum requirements for peak data rate as follows: in uplink peak data rate is 10 Gbps while downlink peak data rate is 20 Gbps.

2. Peak spectral efficiency [in bit/s/Hz]: the maximum data rate ideal conditions normalised by air channel bandwidth. The minimum requirements for peak spectral efficiencies are: in uplink peak spectral efficiency using 4 spatial layers (stream) is 15 bit/s/Hz while downlink peak data rate with 8 spatial layers (stream) is 30 bit/s/Hz.

3. User experienced throughput [Mbps]: the 5% point of the Cumulative Distribution Function (CDF) of the user throughput. The target values for the user experienced data rate as follows: in uplink user experienced throughput is at least 50 Mbps while downlink user experienced throughput rate is at least 100 Mbps.

4. Fifth percentile user spectral efficiency: the 5% point of the CDF of the number of correctly received bits. The table 2.3 [Uni17] shows the minimum requirements for fifth percentile user.

Table 2.3: Fifth percentile user spectral efficiency.

Test environment	**Uplink [bit/s/Hz]**	**Downlink [bit/s/Hz]**
Indoor Hotspot	0.21	0.3
Dense Urban	0.15	0.225
Rural	0.045	0.12

5. Average spectral efficiency (SE_{avg}): the aggregate throughout of all users divided by the air channel bandwidth of a specific band divided by the number of transmission reception points (TRxPs). The SE_{avg} is calculated by [Uni17]

$$SE_{avg} = \frac{\sum_{n=1}^{k} R_n(T)}{T \cdot W \cdot M} \tag{2.6}$$

where $R_n(T)$ is the number of correctly received by user n (downlink) or from user n (uplink) in a system with N users. Furthermore, T is the time over which the data bits are received, M is the transmission reception points and the alredy known W. The table 2.4 [Uni17] shows the minimum requirements for Average spectral efficiency (SE_{avg}).

Table 2.4: Average spectral efficiency.

Test environment	**Uplink [bit/s/Hz/TRxP]**	**Downlink [bit/s/Hz/TRxP]**
Indoor Hotspot	6.75	9.0
Dense Urban	5.4	7.8
Rural	2.1	3.3

6. Area traffic capacity (C_{area}) [Mbps/m^2]: the total traffic throughput available per geographic area. The relation with average spectral efficiency (SE_{avg}) is given by [Uni17]

$$C_{area} = \alpha \times W \times SE_{avg} \tag{2.7}$$

where (α) is the transmission reception point density [TRxP/m^2] and the already known W. For indoor environment the target value in downlink is 10 [Mbps/m^2].

7. Latency [ms]: two types of latency are considered, i) user plane latency, which is the contribution given by the radio network to the time since the emitter send the packet up to the receive side (in ms), and ii) control plane latency, which refers to transition time between idle state and active state. Considering user plane latency, the maximum value for Enhanced Mobile BroadBand (EMBB) is 4 ms, while for Ultra-Reliable and Low-Latency Communications (URLLC) is 1 ms, since that unloaded conditions for uplink and downlink. For control plane latency,

this maximum value is 20 ms, but the companies are being encouraged to consider lower values such as 10 ms.

8. Connection density [Device/Km^2]: total number of devices performing a determinate Quality of Service (QoS) per unit area. For this item, the minimum value is 1,000,000 per km^2.

9. Energy efficiency: the capability of one or more radio interface technology to minimize energy consumption in the radio access network. This requirement evaluate the Enhanced Mobile BroadBand (EMBB) usage scenario and must be defined.

10. Reliability: Capacity of transmit, with high success probability, a quantity of traffic in predetermined time. This requirement evaluate the Ultra-Reliable and Low-Latency Communications (URLLC) usage scenario and the requirement is 10^{-5} success probability of transmitting 32 bytes within 1 ms.

11. Mobility interruption time [ms]: the shortest time duration by one system during which a user terminal cannot exchange user plane packets with any base station during transitions. This requirement evaluates Enhanced Mobile BroadBand (EMBB) and Ultra-Reliable and Low-Latency Communications (URLLC) scenarios. The value required is 0 ms.

12. Bandwidth [Hz]: the maximum aggregated system range supported by single or multiple radio frequency carriers. The minimum value is 100 MHz, but it also to reach 1 GHz.

13. Mobility [km/h]: maximum mobile station speed at which a predefined QoS can be achieved. Requirement defined to evaluate

Enhanced Mobile BroadBand (EMBB) is shown in table 2.5.

Table 2.5: Traffic channel link data rates normalized by bandwidth.

Test environment		**Normalized traffic channel link data rate [bit/s/Hz]**	**Maximum Mobility [km/h]**
Indoor Hotspot [2]		1.5	10
Dense Urban [3]		1.12	30
Rural	Pedestrian	0.8	120
	Train	0.45	500

[2] Stationary, Pedestrian
[3] Stationary, Pedestrian, Vehicular

Key Performance Indicators (KPIs), available in table 2.6 [Hai16], indicate that in 5G networks items such as achievable user data rate, latency and massive number of devices connection density will improve up to 100x compared to the 3G network. 5G will have ultra-high: reliability (99.9999%), coverage (10^6 devices / km^2), device/network energy efficiency (100x), and mobility (being able of to allow a connection to users which are travelling at speeds to 500 km/h).

Table 2.6: CPRI options data rate and applications in mobile broadband.

Feature	3G	4G	5G
Achievable user data rates [Mbps]	20	1,000	20,000
Traffic Capacity	Low	High	Massive
Mobility and coverage	High	High	Ultra-High
Network and device energy efficiency	High	High	Ultra-High
Massive number of devices [Billions]	0.5	16	28
Reliability	High	High	Ultra-High
Latency [ms]	100	10	1
Spectrum and bandwidth flexibilty	Low	High	Ultra-High

2.3 Mobile Dense Heterogeneous Network (Dense HetNet)

The tremendous growth of data traffic foreseen for the 5G requires considerable expansion in the current mobile networks. The achievement of this objective requires that 5G mobile networks have several frequency bands, not only macro cells and small cells with a licensed band, but also Wi-Fi zones using an unlicensed band [Hu16].

The inter operation among these devices will provide a mosaic coverage,

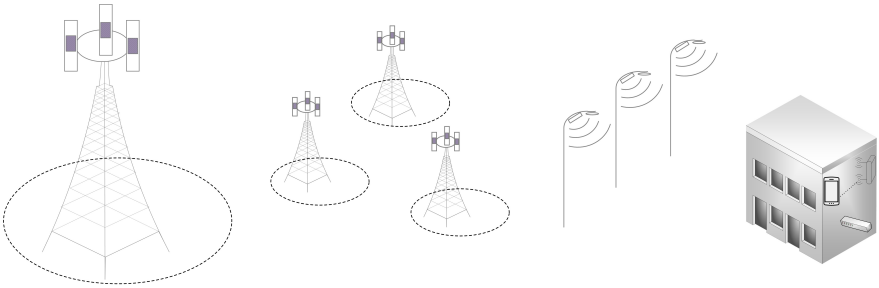

(a) (b) (c) (d)

Figure 2.2: Mobile Dense Heterogeneous Networks: (a) Macro Cell; (b) Micro cell; (c) Pico Cell; (d) Femtocell.

as illustrated in figure 2.2, allowing the hand off capability between these network elements and justifying the replacement of homogeneous mobile network by heterogeneous mobile networks (HetNet), which consists of a macro cell overlay and various small cells (micro, pico and femto cells) underlay, whose concepts are presented to follow [Iva13, Fre13, LCCV13, GJJ17]:

1. Macro Cell: used only in outdoors environments, can achieve a coverage radius of kilometres required and thus can hold a current between 200 to 1000+ users, but for this to be possible it is essential that antennas located in these large cells, have an unobstructed view over buildings, to be able to emit a power output of typically 40W (46 dBm). Its fronthaul/backhaul is achieved by fibre or microwave;

2. Micro cell: this technology can support up to 200 subscribers by using output power of 5W (37 dBm). Its maximum cell radius is 2 km. It possesses two macro cell features: the use must be only in an outdoor environment and the fronthaul can be achieved by fibre or microwave;

3. Pico cell: this technique can be used at indoor (shopping mall) or outdoor environments. Indoor cells, however, present the advantage of improving data rates. Its maximum cell radius of 200 meter and output power of 2W (33 dBm) can support up to 128 clients;

4. Femto cell: presented only in indoor places, are designed to hold up to 16 wireless users, and for this purpose uses 0.1W (20 dBm) with a maximum cell radius equalling 50 m. It is also used in Wi-Fi/3G/4G technology, and fronthaul/backhaul can be achieved by DSL, cable or fibre.

According to [Fre13], the heterogeneity of the network has been presented as the form in which the 5G will emerge. This is due to the fact that HetNet has been identified as a technology capable of enhancing spectral efficiency of mobile networks by the implantation of antennas targeted to specific subscriber groups, therefore enhancing the systems performance in comparison to the traditional macro cellular network [Fre13].

Therefore, while macro cells, provide mobility, and ensure coverage that meets the demands of low speed services, and downsizes cells; the use of small cells (micro, pico and femtocells) boost capacity and increases the spectral efficiency, below 5 GHz, through the spatial reuse of spectrum by the use of millimetre wave, but also increase inter-cell interference and hand-off, demanding application of a technique named Coordinated MultiPoint (CoMP), which is the main element on the LTE roadmap beyond Release 9 and it is as a tool to improve coverage, cell-edge throughput, and system efficiency [EaG13, LZZ+13, LZ16, KLH13].

2.4 Millimeter Wave

The millimetre-wave band allows extremely fast transmissions because millimetre bands can provide individual quantities of spectrum not less than 1.3 GHz, while band frequencies below 6 GHz offer a total spectrum of 657.2 MHz [Hai16].

Among these frequencies, it is important to highlight, 28 GHz, 60 GHz (license-free band used at IEEE 802.11ad - V-band) and 71–76 GHz along with 81–86 GHz (E-band) as shown in figure 2.3 [PK11, BHL+14, Str16]. The use of these high frequencies, however, provides a pretty short reach [Gui12].

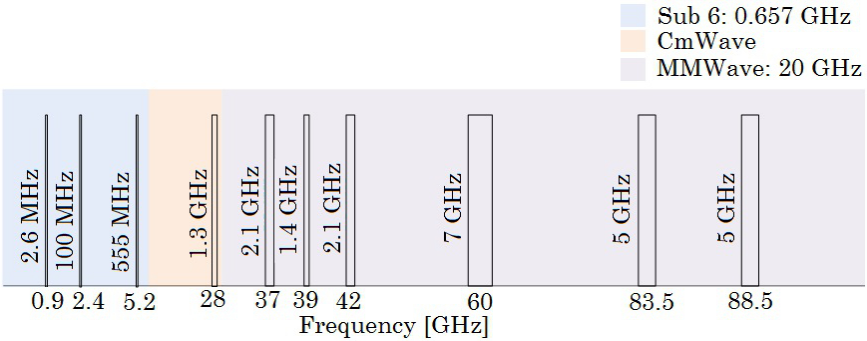

Figure 2.3: Available spectrum in sub 6 GHz and millimetre wave.

Despite numerous utilities, mm Wave imposes challenges such as [TvWA+16, LLJ+15]:

1. Channel modelling, because it is difficult to take channel measurements over longer distances and therefore obtaining the required information;

2. Architecture and integration, because requires changes in current mobile network system or a substitution for a whole new architecture;

3. Radio interface design, because it is compared to sub 6 GHz frequencies and link budget constraints lead to the need for multiple antenna transmitters and/or receivers and the corresponding direction transmission;

4. High attenuation, because sensitivity to signal blockage and fast channel variations require innovative solutions in different aspects such as communications algorithms, network protocol and network architecture engineering.

2.5 Massive MIMO

Modern communication systems have been characterized by using multiple antennas in both the transmitter and receiver. Multiple Input Multiple Output (MIMO) is a technology that has been the subject of research in the past two decades. The research about Multiple Input Multiple Output (MIMO) systems frequently describes this technology as a user of OFDM, a technique that uses of multiples of narrow carriers. Therefore, the drawbacks of OFDM signals, which makes MIMO a complex technology, include high Peak-to-Average Power Ratio (PAPR), Inter Symbol Interference (ISI), and the high computational load required for the execution of the Fourier transform, caused by the large amount of antennas. Due to this, single carrier has been studied for the use in MIMO systems. Another feature of MIMO is its use of the Time Division Duplexing (TDD) mode, by its proficiency to estimate channels and to give feedback on issues, however the use of

the Frequency Division Duplexing (FDD) mode is also possible using Channel State Information (CSI) [LLS+14, JMZ+14].

The initial MIMO focus was point-to-point links (both devices with multiple antennas communicating with each other). After this, the focus is on multi-user MIMO (MU-MIMO) systems, which consist of a Base Station (BS) with multiple antennas that serve many users, by using a single antenna. In this context, expensive equipment is only needed on the Base Station (BS). The latest research focus in this area has been on Massive Multiple Input Multiple Output (MMIMO) where the number of antennas, used in base stations, has achieved more than 100 units [LLS+14, JMZ+14, LZ16].

In order to improve the data rate and robustness of the link, MMIMO has adopted spatial multiplexing and space-time block codes, respectively. The combination of these two techniques can increase system capacity up to 10 times or more, and the system radiated energy efficiency is upgraded by to 100 times; this aggregation of technologies, allows the antenna to be considered smart [Hu16, LZ16, LETM14].

Massive MIMO presents as main advantages: the ability to provide uniform feeding to everyone in the cell, to boost spectral efficiencies compared to current standards, to enable a significant reduction of latency on the air interface, the simplification of the multiple access layer, and the ability to increase the robustness against both unintended man-made interference and intentional jamming; On the other hand, Massive MIMO also has several limitations, such as: pilot contamination, which is caused by the use of non-orthogonal pilot sequences by users in adjacent cells due to pilot reuse, and channel reciprocity, which occurs when the measured uplink/downlink channels are not only determined by the propagation channels, but are also influenced by the RF devices, also known as RF chains [SL15, LETM14].

mMIMO is a multi user MIMO with a much number of antennas (M) larger than the number of devices (N), such that $(N \ll M)$. It can be used in the configurations cylindrical, linear, rectangular, spherical, and distributed, as depicted in figure 2.4 [BHL+14, LZ16, LETM14, RVR15].

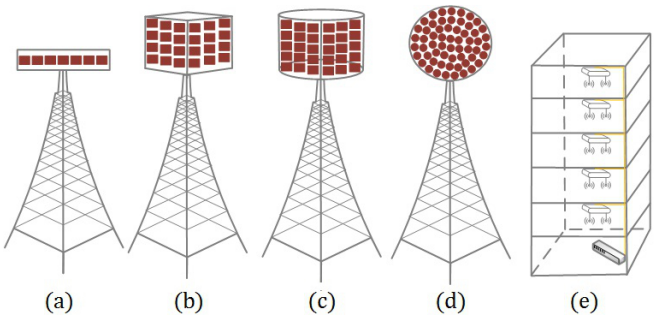

Figure 2.4: Massive MIMO antenna array configurations: (a) Linear; (b) Rectangular; (c) Cylindrical; (d) Spherical; (e) Distributed.

Distributed (also know as cell-free) configuration is a potential improvement of Massive MIMO over larger areas, such as the roof of the building. This type of antenna is beneficial for positioning due to its better spatial diversity [SL15]. The rectangular, spherical and cylindrical antenna array belong to the 3D antenna array, while linear is a 2D antenna array [ZOY14].

Different of Multiple Input Multiple Output (MIMO) systems, which uses between two and eight antennas, Massive MIMO is based on tens or even hundreds arrays of antenna elements, all operating on higher frequencies larger than 10 GHz, and are spread around the cell site and connected to the central office via optical fibres [WHG+14]. Massive MIMO super-scales convectional MIMO by up to 100 times, which therefore generates enormous quantities of baseband data that are to be carried to the central office, demanding, therefore, a high

optical fronthaul network bandwidth [SKGR15].

3

Xhaul Network

This chapter is divided into three sections. Section 3.1 describes the still predominant Distributed Radio Access Network (D-RAN) and introduces a relative new technology named Centralized Radio Access Network (C-RAN). Section 3.1.1 presents the transition from coaxial cable connections to fibre used in D-RAN, while subsection 3.1.2 highlights the rise of C-RAN and the creation of new separate transport network segment called fronthaul, which is completely incompatible to the backhaul in terms of physical interfaces, user, control and management plane. Section 3.2 introduces the different types of candidates Passive Optical Network (PON) techniques for fronthaul. Section 3.3 presents the three requirements (Synchronisation, Latency, Jitter) of fronthaul segment. Section 3.4 explain the main features distinguishing Analogue Radio over Fibre (A-RoF) and Digital Radio of Fibre (D-RoF). It shows also the difference among the three main digital fronthaul interface named: Common Public Radio Interface (CPRI), Open Base Station Architecture Initiative (OBSAI), and Open Radio equipment Interface (ORI).

3.1 Radio Access Network

Radio Access Network (RAN) is connected with aggregation network using three different categories of connections:

1. Backhaul, when the links join a radio base station and a network controller gateway site;
2. Fronthaul, if the links connects a remote radio head and a base band unit;
3. Midhaul, when a carrier Ethernet link is used between two radio base stations or base band units, especially if one of the site is a small cell.

In terms of technology (e.g., 2G, 3G, 4G, Wi-Fi), cell ranges (e.g., macro-/micro-/pico-/femto-cells) and density levels (e.g., from macro-cell Base-Station to tens or hundreds small cells) RAN is classified as a heterogeneous network and it can be classified into Distributed Radio Access Network (D-RAN) and Centralized Radio Access Network (C-RAN) [VGMM14, PPP15].

3.1.1 Distributed Radio Access Network (D-RAN)

Until 2009 wireless access network was characterized as having a D-RAN architecture which is divided in two phases. Figure 3.1 (a) shows that initially, each sector antenna is connected to the Radio Access Unit (RAU) by coaxial cables RG 19U, which are bulky, expensive, and presenting attenuation of up to 280 dB/km [Hun84, Yos13, Haq14, CPC+13]. RAU, in turn, is connected, by copper cable or fibre, directly to the core network (backhaul) through an IP/Ethernet based network [Yos13]. In this traditional radio access network, all functionalities

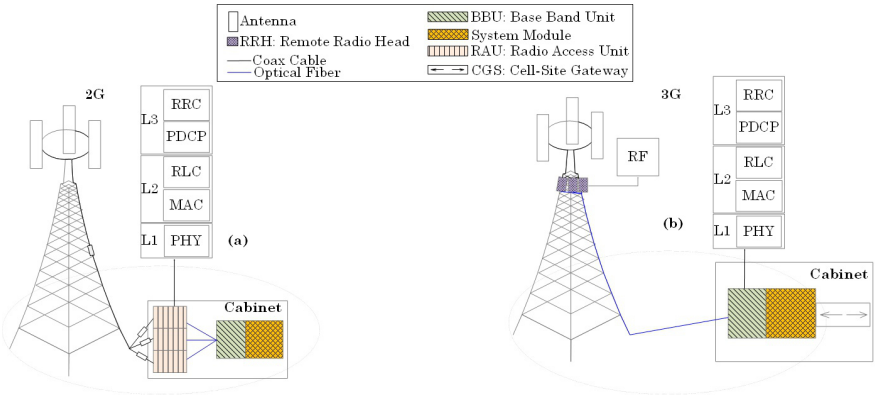

Figure 3.1: The evolution of the connection between RRH and BBU: a) macro cell interconnected with the RRU / BBU via coaxial cable antennas; b) RRH next to antenna, and BBU located in a street cabinet, and connection between both done via fibre transmitting digital signal [PCSD15].

are processed at cell site, which brings several limitations such as: limited scalability and flexibility, increased CaPEx to acquire new base stations (BSs) and OpEx due to underutilized resources, increased management costs, lack of modularity and limited density as the system is complex to resize after deployment, inefficient power delivery as the BSs processing power cannot be shared [PHV15, TAS+16].

Figure 3.1 (b) shows that, in a second moment, functions performed by RAU are divided between RRH and BBU. In this context, RRH consists of down-/up converters, analogue transceivers, and analogue-to-digital converters, while BBU performs functions, such as, whole protocol stack sheltering, self-organizing network and scheduling functionalities, radio resource management, and also physical layer processing such as detection, decoding, frequency up-conversion, carrier modulation, multiplexing, analogue transceivers and analogue-to-digital

converters and BBU is responsible for the full signal baseband processing [BF14, BCA+13].

The second architecture allows RRH to be located at the mast-head next to the antenna enabling use of short coaxial jumper cables to connect to sectoral antennas, which produces low RF losses, flexibility performance improvements and costs saving. The connection between RRH and BBU is being achieved by the use of an optical single mode fibre [BF14, CPC+13]. Optical fibre provides large bandwidth, low attenuation loss, reduced energy consumption, and immunity to radio frequency interference [BCA+13, LGN+16].

3.1.2 Centralized Radio Access Network (C-RAN)

In D-RAN architecture, static configuration and deployment are used. However, this approach is inefficient in handling any spatio-temporal fluctuations of the traffic demand [RIG+17]. Beyond, the increasing number of base stations implies proportional increase of the initial investment, site support/rental, and management support [Ins]. Aiming to subtract these costs, a new network architecture called C-RAN was proposed in 2009 and tested for the first time by China Telecom, in 2010 [CPC+13, IHD+14, Ins].

Figure 3.2 shows that C-RAN consists of displacing individual BBUs from cell site cabinets to a new place named Central Office (CO). Connections between RRH and BBU are done via fibres, and the links between them are called Mobile FrontHaul (MFH). This kind of mobile operator's entity connection allows that several BBUs to be co-located in the same place, generating operational efficiency, and that each BBU manages one or more RRHs at individual cell site.

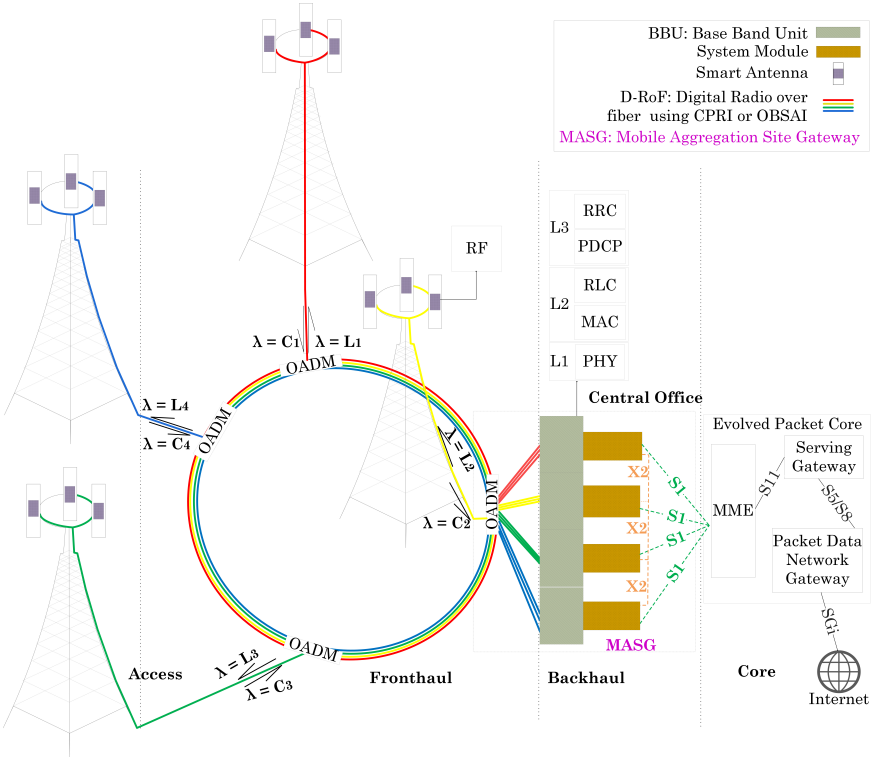

Figure 3.2: C-RAN with BBU hostelling [PCSD15].

On the other hand, the BBUs co-location at same place, produced by C-RAN, permits BBUs to communicate quickly with each other over standardized *X2* interfaces. The interconnection between BBU and Evolved Packet Core (EPC) is done by *S1* interfaces. The C-RAN architecture contributes strongly to two goals, which have to be achieved [CPC+13, ADABV15, MKTO16]:

1. Performing handover avoiding the use of core network;

2. Implementing Coordinated MultiPoint (CoMP), allowing exchanges information between BBUs about resource allocation and network structure.

From the field trial it was observed that, with C-RAN methodology, Capital Expenditure (CapEx) is reduced by 30% and Operational Expenditure (OpEx) by 53%. An important item inserted in this economy is the construction cycle, because while in D-RAN traditionally about 77 days are needed, C-RAN demands around 30 days [IHD+14].

In terms of coverage, figure 3.3 shows that C-RAN can be classified into four options: City-wide, Central Office based, Master macro site based, and Local.

Figure 3.3(a) shows that in city-wide based C-RAN, thousands of RRHs are managed by a BBU pooling (an agnostic server) placed in a regional central office.

Figure 3.3(b) depicts that in central office based C-RAN, hundreds of RRHs are controlled by BBU pooling located in a local Central Office (CO).

Figure 3.3(c) shows that in master macro site based C-RAN, tens of RRHs ruled by BBU pooling deployed in a macro cell site (being RRHs and BBU linked by CPRI interface).

Figure 3.3 (d) shows that local C-RAN over Distributed Radio Access Network (D-RAN), small cell RRHs are aggregated, by BBU pooling, via CPRI fronthaul and macro cells continues using D-RAN architecture [Ins].

Figure 3.3: C-RAN coverage classifications: (a) City-wide; (b) Central Office based; (c) Master macro site based; (d) Local.

Figure 3.4 shows that there are three options available to implement C-RAN: full, partial, and hybrid centralized [IHD+14].

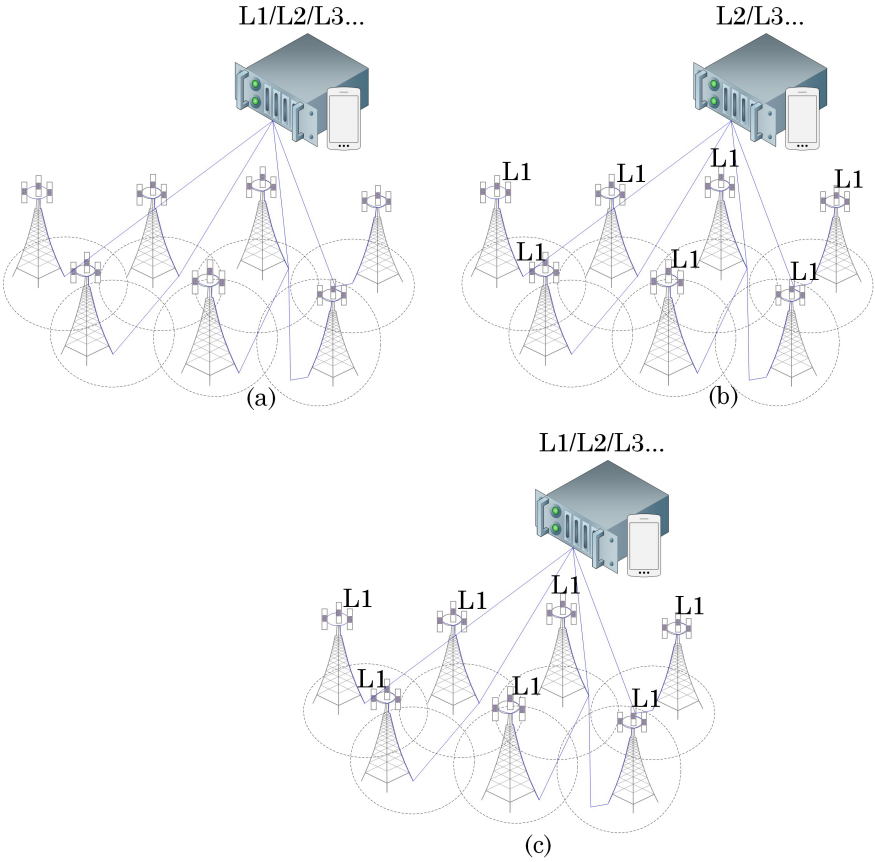

Figure 3.4: C-RAN architecture centralized: (a) Full; (b) Partial; (c) Hybrid [Ins, Sal16].

In the full scheme, figure 3.4 (a), L1, L2, L3 and Operation and Maintenance (O&M) functions are located in BBU enabling easy

upgrades, network capacity expansions, and Software Defined Network (SDN) deployments. This last feature allows air interface standards to be upgraded only by software, better capability for supporting multi-standard operation, maximum resource sharing, and more convenient to support multi-cell collaborative signal processing. However, full centralization has the disadvantage of demanding highest bandwidth on fronthaul due to digital transmission interface inefficiency [IHD+14, Ins].

In partial centralization, figure 3.4 (b), just collaborative function (L2/L3 scheduling, and wireless resource allocation) are performed in BBU, while L1 remains in RRH. The main advantage of this C-RAN implementation is the need for a lower bandwidth, but the disadvantages of this setup are: the requirement of remote equipment rooms, the delay impact produced during information exchanges, which can affect system performance, and also the fact that this type of base station is not preferred in the perspective of system management and future upgrade [IHD+14, Ins].

In hybrid centralized, figure 3.4 (c), a percentage of the physical layer functions are transferred to RRH, which will execute cell specific actions linked mainly with signal processing. This layout can allow more resource sharing flexibility, reducing energy consumptions, and communication overhead in BBUs [Sal16].

3.2 Fronthaul Radio over Fibre Transmission

With the advent of C-RAN, a new network transport segment between RRH and BBU, called fronthaul, was created [CPC+13]. In this segment, which also is considered as backplane extension of RAN

[CNG+17], the maximum distance depends on an upper limit on tolerable fronthaul latency, which is composed by [Car15]:

1. Fronthaul signals adequacy inside of the transport network caused by CPRI/OBSAI interfaces and additional functions asked by optional lower-layer transport (i.e. buffering, re-framing, mu/demultiplexing, error-correction);

2. Signal propagation through RAN.

Figure 3.5 identifies the different processing delays in RRH, BBU and End Switch that must be considered when calculating the maximum time available for the transit of signals in the fronthaul segment (t_{fs}) which calculus is done by equation 3.1 [ZM13].

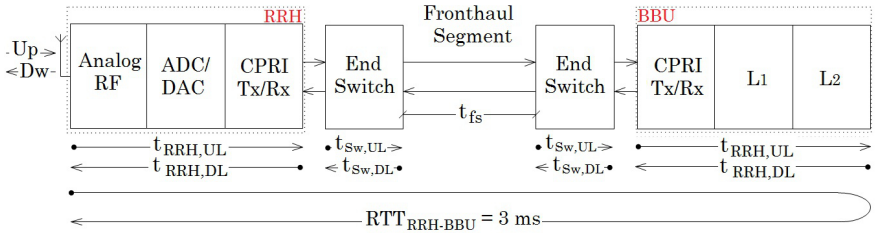

Figure 3.5: Delay contributions along fronthaul segment [Car15].

$$t_{fs} = RTT_{RRH-BBU} - t_{RRH,UL} - t_{RRH,DL} - 2 \cdot (t_{Sw,UL} + t_{Sw,DL}) - t_{BBU,UL} - t_{BBU,DL} \quad (3.1)$$

To find the maximum fronthaul segment distance, equation 3.2 [ZM13] is used.

$$D_{mfs} = t_{fs}/(2 \times t_{fpd}) \tag{3.2}$$

Table 3.1 shows the description of variables and respective values practised today. Using equations 3.1 and 3.2 and typical commercial values, presented in Table 3.1, it is possible to verify that fronthaul maximum distance is 25 km. However, according [STP+13], in European urban areas 99% of all fronthaul links are shorter than 20 Km.

Table 3.1: Maximum delay contributions values along fronthaul segment.

Var.	**Description**	**Value [µs]**
$t_{RRH,UL}$	RRH uplink time	15
$t_{RRH,DL}$	RRH uplink time	25
$t_{Sw,UL}$	End switch uplink time	2.5
$t_{Sw,DL}$	End switch downlink time	2.5
$t_{BBU,UL}$	BBU uplink time	1350
$t_{BBU,UL}$	BBU downlink time	1350
t_{cf}	Total fronthaul time fibre propagation delay	250
t_{fpd}	Fronthaul time fibre propagation delay per kilometre	5
$RTT_{RRH\text{-}BBU}$	**Round Trip Time**	**3000**

The 3 ms assigned to the Round Trip Time (RTT) is the narrower BBU upper latency limitation considered in FDD radio interface. This value comes from the fact that once received, the uplink data packet, at radio frame number i, must send back a correspondent acknowledgement (ACK) and/or negative-acknowledgement (NACK) answers at frame number (i+3) as show figure 3.6 [Car15, PCSD15].

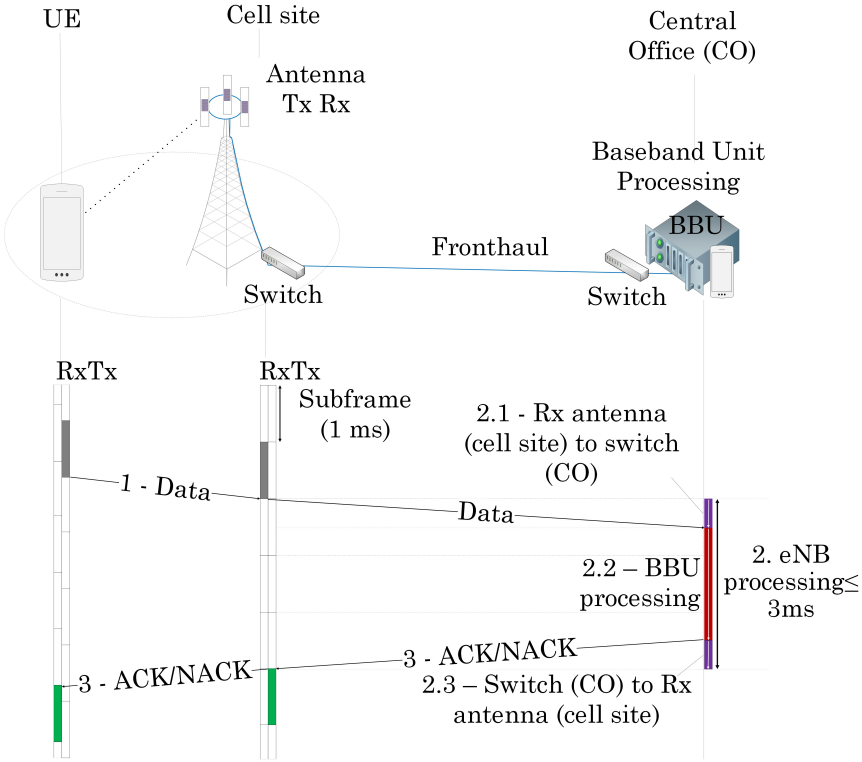

Figure 3.6: Impact of fronthaul delay in C-RAN [SS14].

Although 3 ms meets much of the demand for services already known,

figure 3.7 shows that new demands will require a round trip equal to 1 ms, which is expected to be reached in 5G networks. However, achieving this goal requires a substantial subtraction of the processing time spent by BBU and RRH.

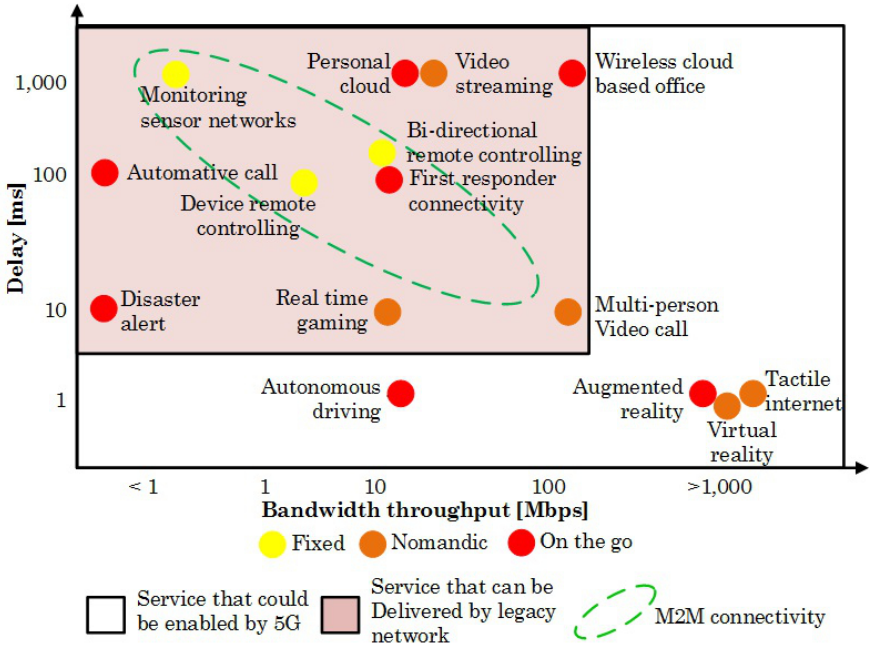

Figure 3.7: Services and their respective delays [Gar17].

Experiments done during the 1960s proved the feasibility of performing transport of information encoded in light signals over a cylindrical glass waveguide, named optical fibre. This element consists of two main parts: inner core and outer cladding. These two elements, imprison the light inside the fibre enabling the transmission of the light for considerably long distances before the signal degrades in quality [RRS09].

There are two types of fibre: single-mode fibre and multi mode fibre multi-mode has a diameter range from 50 to 85 µm, and single-mode has a relatively small core of about 8 to 10 µm [RRS09].

Among the existing optical network topologies, Passive Optical Network (PON) is a potential option for Common Public Radio Interface (CPRI) transport. PON is composed of three main parts: Optical Line Terminal (OLT), placed at the central office to provide the interface between backbone network and PON, Optical Network Unit (ONU), located near RRH, and Optical Distribution Network (ODN) connecting OLT and ONUs [AZ13]. PON can be divided into three types: Time Division Multiplexing Passive Optical Network (TDM-PON), Wavelength Division Multiplexing Passive Optical Network (WDM-PON) and Time and Wavelength Division Multiplexing Passive Optical Network (TWDM-PON) [TKT+14, TKK+14].

3.2.1 Time Division Multiplexing-Passive Optical Network (TDM-PON)

Time Division Multiplexing Passive Optical Network (TDM-PON) it was the first fibre sharing technique used in residential optical access, Fibre To The Home (FTTH), with the use of TDM-PON to share up to 128 subscribers using a Gigabit Passive Optical Network (GPON) [TGC+16].

TDM-PON, depicted in figure 3.8, is considered the most cost-effective, offering data rates up to 10 Gbps, however its bandwidth utilization efficiency and latency are poor (because is necessary to wait all costumers send their packets), and its rigid architecture hinders any easy and dynamic adaptability and scalability, limiting C-RAN resource pooling [TKT+14, JITT16].

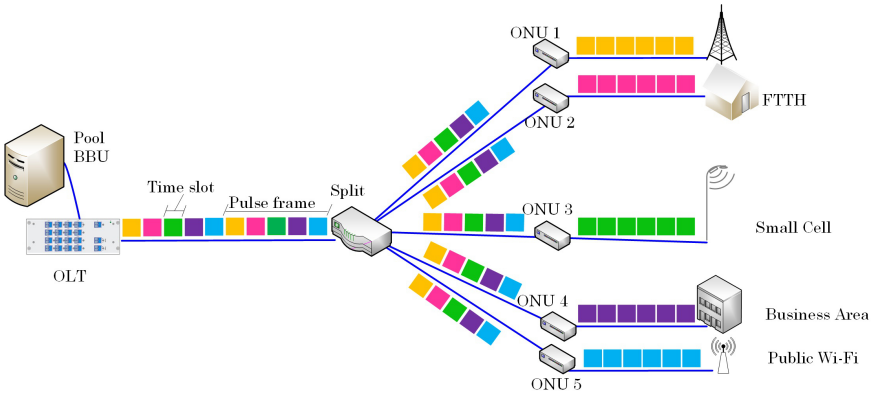

Figure 3.8: TDM system diagram.

TDM-PON can provides different data rates using Ethernet Passive Optical Network (EPON) and Gigabit Passive Optical Network (GPON) [AZ13, BET+12, KH16, TSF+17, HvVH17, Hua10].

1. EPON is a point to multipoint topology (P2MP) based on Ethernet technologies and standardized by IEEE 802.3ah. It is implemented using passive optical splitters and optical fibres. EPON can reach up to 10 km with maximum split ratio of 1:32 or 20 km using split ration of 1:16. Recently it was standardized by IEEE 802.3av a 10G-EPON technology, which offers a symmetric-rate of 10 Gbps in upstream and downstream. The wide 10G-EPON communication bandwidth allows to accommodate multiple services such as business, high-resolution video distribution and mobile xhaul. Nowadays the IEEE P802.3a task force works on standardization of 25, 50 and 100G EPON.

2. GPON, standardized by International Telecommunication Union - Telecommunication Standardization Sector (ITU-T) recommendation G.984, is based on P2MP architecture. In practice,

it is available in market using asymmetric speed access peak rate. In downstream transmission, GPON can be made available through single fibre operating in 1490 nm, offering 2.5 Gbps and serving up to 64 customers. In upstream the maximum data rate is 1.25 Gbps. GPON can reach up 20 km if the maximum budget equal to 28 dB is used. Considering only bit rates, it has little transmission capacity for D-RoF transport. After finished GPON recommendation, ITU-T concentrated in the study of Next Generation Passive Optical Network (NG-PON). This technology it was divided in two phase: NG-PON1 an enhanced TDM-PON technology, and NG-PON2 a Time and Wavelength Division Multiplexing (TWDM) technology. NG-PON1, a mid-term upgrade, is compatible with legacy GPON ODNs. It is required by operators that NG-PON1 have larger bandwidth, higher capacity and long reach. NG-PON1 can be an asymmetric technology offering data rates of 10 Gbps in downstream and 2.5 Gbps in upstream (XG-PON1), or symmetric offering 10 Gbps in up/down-stream (XG-PON2). XG-PON1 (G.987.2) offers high aggregate capacity, it can reach a nominal line rate of 2.48832 Gbps in upstream, operating in wavelength range of 1260-1280 nm, and 9.95328 Gbps in downstream using wavelength range of 1575-1580 nm.

3.2.2 Wavelength Division Multiplexing-Passive Optical Network (WDM-PON)

Wavelength Division Multiplexing (WDM), represented by the figure 3.9, is a transmission media ruled by recommendation G.694.2, which is established by ITU-T [Tel03].

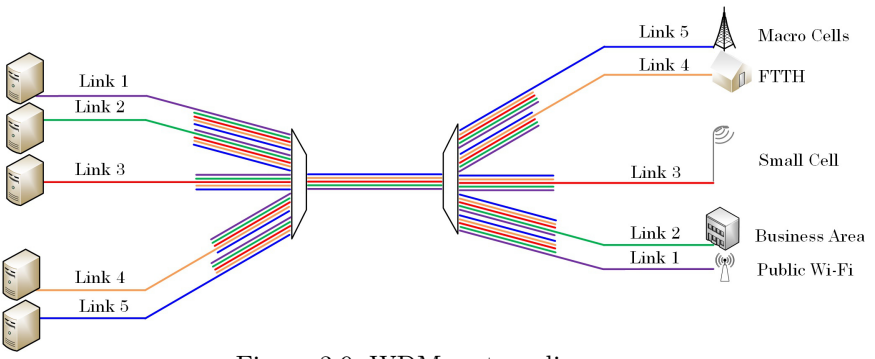

Figure 3.9: WDM system diagram.

WDM uses MUX and DEMUX devices to combine lights from different fibres and wavelengths into a single fibre [BCA+13]. WDM provides scalability, dynamism and adaptive resource allocation at a low latency. These features translate to a potential reduction in fibre links and lower capital expenditure. However Wavelength Division Multiplexing (WDM) devices continue to be very costly, reducing Capital Expenditure (CapEx), and it is not fully gained at this stage [JITT16].

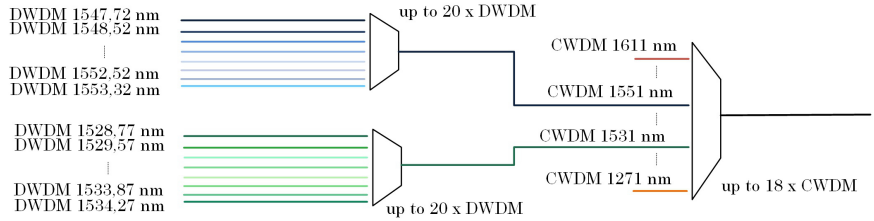

Figure 3.10: DWDM and CWDM channel space.

Figure 3.10 depicts the two methods to share resources in Wavelength Division Multiplexing (WDM): Coarse Wavelength Division Multiplexing (CWDM) and Dense Wavelength Division Multiplexing (DWDM)

[SHL+14].

3.2.2.1 Coarse Wavelength Division Multiplexing (CWDM)

CWDM is one of the most cost effective ways to connect BBU and RRH, because it combines or separates different wavelength signals from or to distinct optical fibres [SHL+14, PSL+16, Tel03].

CWDM grid wavelength ranges from 1271 nm to 1611 nm totalling 18 channels, with a channel spacing of 20 nm and source wavelength variation between 6 and 7nm, both for more and less [SHL+14, PSL+16, Tel03]. Recent researches [DGP+15] have presented a solution using a single optical fibre bidirectional symmetrical link, which promises to connect up to 18 RRHs using optical fibre over 20 km. This method uses a Cooled Single Channel (CSC)-Small Form Factor Pluggable (SFP) to divide 20nm CWDM in two sub-channels of 2.4576 Gbps performing at 4.9152 Gbps, with enough capacity to transmit a LTE signal with, one sector, one band of 20 MHz, and antennas using MIMO 4x4.

3.2.2.2 Dense Wavelength Division Multiplexing (DWDM)

DWDM is a technology capable of transporting various optical carriers at the same time obtaining a more efficiently use of fibre [INF12, Tel12]. In DWDM the channel spacing is equal 0.8 nm, this narrow space enables the insertion of 20 duplex channels in a single CWDM channel, allowing the creation of a super channel, which can provide data rates of up to 400 Gbps [KRM+16, CGS13]. According to [Wik14, Net16], DWDM has the following advantages:

1. Very few cores to transmit/receive high capacity data;

2. A single core fibre cable can support multiple channels;
3. Easy network expansion, because it is not necessary to replace components;
4. It supports long span lengths;
5. It presents low latency and enables the ability to transport simultaneously, multiple services to RRH.

In contrast, in accord with [WIK16, Net16] DWDM presents the following disadvantages :

1. Not cost-effective for low channel numbers;
2. More complex transmitters and receivers;
3. CapEx and OpEx high;
4. Requires high quality optics and well cooled and stable lasers.
5. It is not a flexible network, therefore, it needs to use a Reconfigurable Optical Add&Drop Multiplexer (ROADM);
6. High losses, attenuation can achieve up to 10 dB.

3.2.3 Time Wavelength Division Multiplexing-Passive Optical Network (TWDM-PON)

TWDM-PON is the third sharing resources technology, proposed in [IKT13] to transmit a signal using optical fibre. It is a mix of TDM-PON and WDM-PON.

TWDM-PON, presented in figure 3.11, can provide up to 40 Gbps through 4 x 10 Gbps WDM channels divided in time to each costumer [Mit14]. TWDM-PON meets CPRI data rates, however jitter delays

and latencies, in order to synchronize the transmissions across massive RRHs, are still a challenge for the use of C-RAN [OOF+14, PSL+16]. Specification G.989.1 recommends use of 4 to 8 TWDM channels. For upstream wavelengths in C band ranging from 1524 nm to 1544 nm with 5 nm of space and for downstream between 1595 nm and 1625 nm in the band L are used [OOF+14].

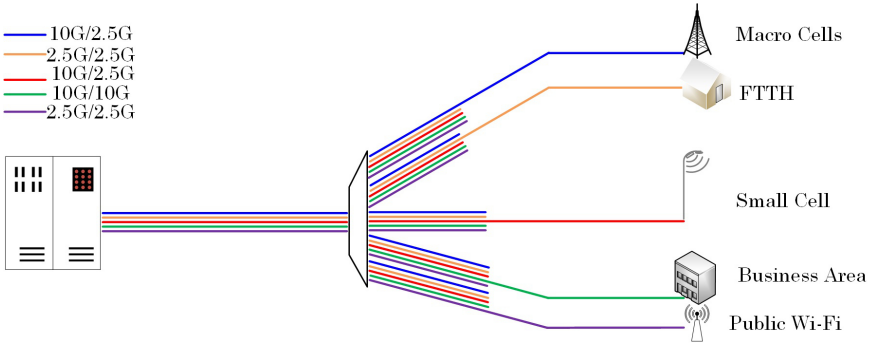

Figure 3.11: TWDM system diagram.

TWDM-PON is the base for the NG-PON2, a PON long-term solution, which improves the rate to 40 Gbps. NG-PON2, standardized by ITU-T recommendation G.989, is available in market with asymmetric aggregate rates (40 Gbps in downstream and 10 Gbps in upstream) or symmetric 40 Gbps in both direction. It can serve up to 64 costumers in a maximum distance of 20 km. It has a high price and transmission capacity for D-RoF transportation [Hua10].

3.3 Fronthaul Radio over Fibre Requirements

Besides bandwidth, previously discussed, mobile fronthaul has the following requirements: synchronization, latency, and jitter.

3.3.1 Synchronisation

Base Band Unit (BBU) is hypersensitive to discrepancy between transmitter and receiver clock frequencies, bit errors, and variation in clock phase (jitter). The synchronization process is usually performed in two steps: acquisition, which consists of initiating the process of alignment between the two signals, and tracking, which continuously maintain the best alignment [GCTS13, CJCB15].

In a traditional Base Transceiver Station (BTS) there is a real time single clock signal used for all the elements, whereas in Centralized Radio Access Network (C-RAN) clock signals generated in BBU must be sent to Remote Radio Head (RRH) [Hai16]. In current fronthaul networks it is possible the following synchronisation approaches [GCTS13, CJCB15, LHDG17]:

1. Traditional method using phase and frequency synchronisation provided by Global Positioning System (GPS);
2. SyncE user of frequency synchronization;
3. IEEE 1588 also user of frequency and phase synchronisation;
4. Precision time protocol synchronisation via aggregation network.

In traditional approach every station receives a GPS. This option has high cost, difficult maintenance, and limited indoor deployment. Clocks are synchronised in frequency when the time between two rising edges of the clock match; while for phase synchronisation, the rising edges must happen at the same time [LHDG17].

For 3G/4G, synchronization requirement is $\pm$ 1500ns. Time synchronization can be impacted by Carrier Aggregation (CA), Joint Transmission (JT) and short frame. 3GPP TS 36.104 has defined the following Time Accuracy Error (TAE) requirement for CA [LHDG17]:

1. Intra-band contiguous carrier aggregation, with or without MIMO or TX diversity: 130 ns;
2. Intra-band non-contiguous carrier aggregation, with or without MIMO or TX diversity: 260 ns;
3. Inter-band contiguous carrier aggregation, with or without MIMO or TX diversity: 260 ns;

For Joint Transmission (JT), there is no specification for TAE, however, simulation has shown that this value must be within 260 ns. The 5G frame structure has been considered a shocking factor, because 5G cyclic prefix length will be much shorter than in 4G, resulting in a more stringent synchronization accuracy than observed in 4G [I17, LHDG17].

3.3.2 Latency

Latency is the time which a packet spends to go from one point to another and it can be divided in two parts [Hai16]:

1. Occurred as a result of the adjustment of fronthaul signals inside of RAN infrastructure services, which can be generated by CPRI/OBSAI transmission/reception interfaces and existing functions at optional layer transport technologies (i.e. multiplexing/demultiplexing, buffering, re-framing and error correction);
2. Caused by the signal propagation along the fronthaul segment, entailing a limitation on the maximum length between BBU hostels and RRH managed cell sites.

The fronthaul segment associated with CPRI/OBSAI protocols demand very low latency, which often can shorten the reach of such

network segment [Hai16]. This imposes to C-RAN to meet stringent performance requirements on fronthaul aggregation network [ATC+15, WAS15, JITT16, Cvi14].

There are two items which impact fronthaul latency: user plane latency and Hybrid automatic Repeat request (HARQ). The data plane latency varies according to the service, and it can range from 0.5ms for Ultra-Reliable and Low-Latency Communications (URLLC) to 4 ms for Enhanced Mobile BroadBand (EMBB). Because HARQ is located at low-MAC, it is not advisable to carry out a functional split in this region [I17].

3.3.3 Jitter

Jitter is the variation of the time required for data to be transmitted between BBU and RRH. Jitter can be influenced by two aspects: Buffering space reserved by BBU and RRH to compensate this fluctuation (the greater the jitter is, the bigger data caching will be demanded), and by the processing time sequence of BBU and RRH (the greater the jitter is, the faster the processing should be). Transmission on fronthaul segment using Ethernet will increase jitter because of the presence of transport nodes, and to meet this jitter, devices must be optimized [oEE16].

Table 3.2 [Hai16] does a comparison between CPRI and Ethernet requirements. Analysing CPRI fronthaul jitter and considering reference clock frequency of BBU for 30.72 MHz (2 ppb represents 0.06144 Hz).

Table 3.2: CPRI and Ethernet requirements.

Properties	**CPRI**	**Ethernet**
Latency budget between BBU and RRH without cable [µs]	5	
Maximum frequency error contribution [ppb]	2	
Maximum Bit Error Rate (BER)	10^{-12}	
Transmission mode	Continuous	Burst
Transport interface	Synchronous	Asynchronous
Link status	Always On	Can be idle
Latency budget considering propagation delay from fibre length [µs]	100-250	50
Maximum variation in delay	65 ns	5µs or 10% End-to-End

3.4 Radio-over-Fibre (RoF)

Radio-over-Fibre (RoF) can be Analogue Radio over Fibre (A-RoF) and Digital Radio of Fibre (D-RoF). A-RoF has not been standardized yet, while digital radio over fibre (D-RoF) has as main interfaces Open Base Station Architecture Initiative (OBSAI), Common Public Radio Interface (CPRI) and Open Radio Equipment Interface (ORI). There

is also ongoing work in IEEE 1904.3 to define a new solution called radio over Ethernet. The main features of RoF are: preservation of the waveform and tolerance to electromagnetic interference. [FSM+15].

3.4.1 Analogue Radio over Fibre (A-RoF)

In A-RoF, the transmission of wireless signals can be modulated, onto an optical carrier, directly or externally. This results in an optical double side band signal. This wireless signal is recovered via direct detection using a photodetector, which can be: photo conductors, junction photodetectors, and avalanche photodiodes [Tan16].

There are three fundamental architectures for the transmission of analogue signals: RF band subcarrier, Intermediate Frequency-band (IFB), and reference frequency signals. Compared to the IF-band, RF transmission presents a worst optical bandwidth efficiency because RF frequencies is higher than intermediate frequencies. Reference frequency signals is similar to IF-band, except by the fact that reference frequency is provided from the local office end, and it is delivered to the remote antenna site [IT15]. The configuration of analogue RoF transmission is depicted in figure 3.12.

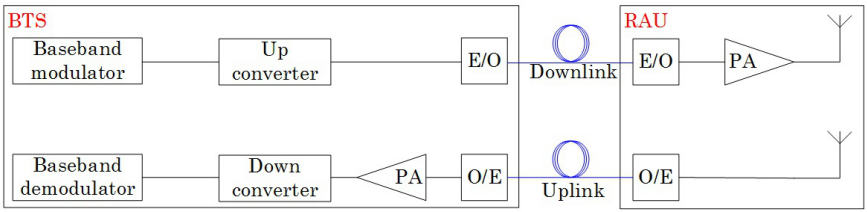

Figure 3.12: Analogue Radio over Fibre (A-RoF) scheme [Tan16].

Figure 3.12 shows that in downlink, the baseband signal, generated in Base Transceiver Station (BTS), is modulated, up converted to other

level frequency, and sent to an electrical-to-optical converter where it is modulated directly or externally onto an optical carrier, resulting in an optical double side band signal. After transmission over optical fibre, the signal is recovered in Radio Access Unit (RAU) via a direct detection using a photodetector (such as photo conductors, junction photodetectors, and avalanche photodiodes), amplified using a Power Amplifier (PA) and forwarded to antenna.

In uplink, after being captured by the antenna, the wireless signal is converted to the optical domain and transmitted over optical fibre. In BTS, the signal is changed to the electrical domain, amplified by a Power Amplifier (PA), then down converted returning to original frequency and electrically demodulated [Tan16].

Analogue Radio over Fibre (A-RoF) transmission scheme differs from digital presenting advantages such as: the avoidance of the digitization process, because it removes the need for sampling, the simplicity of an access point and centralized control at the Central Office (CO), reduced power consumption, and dynamic resource allocation [NW13, BCA+13].

The simplest A-RoF scheme is adversely affected by: the required high-speed optical modem techniques at high frequencies (10 GHz or more), the lack of control and management capabilities, non-compatibility with TDM-PON, Inter-Modulation Distortion (IMD), and Chromatic Dispersion (CD). Inter-modulation distortion results from non linearities that exist in optical and electronic components [YLLN13, LPJ13, LN10, KPSD10, NW13]. Nevertheless, techniques presented in [ZSL14] can minimize these harmful effects. Chromatic dispersion originates from the optical fibre limits the dynamic range of the optical link owing to attenuation, which increases directly with the distance between two points [NW13].

In the Radio-over-Fibre (RoF), signals are carried on fibre with the same wireless carrier frequency [NW13]. The main difference in terms of implementation between digital and analogue transmission is in the down-conversion part. In digital, it contains Analogue to Digital Converter (ADC) and Digital to Analog Converter (DAC) while in analogue there is an electrical mixer and a local oscillator [JL13].

3.4.2 Digital Radio of Fibre (D-RoF)

In current fronthaul transport network, digital transmission is the scheme which wireless signals are converted to digital baseband signals using Analogue to Digital Converter (ADC) and afterwards are optical modulated through an Electrical-to-Optical (E/O) conversion. After these procedures, the optical signal can be dislocated, with negligible losses, over distances higher than analogue transmission [LPJ13]. However, this asks for constrained jitter and quantization [JL13].

A digital transmission is created by using a digitized Intermediate Frequency over fibre (IF-over-fibre) [BF14, CPC+13, YLLN13]. IF-over-fibre is a type of transport scheme in which wireless signal is optically modulated, by a lower Intermediate Frequency (IF) (<10 GHz), before transmission over fibre. On the opposite side, optical signal is up-converted to Radio Frequency (RF) in antenna before radiation through the air [LN10, BCA+13].

IF-over-fibre transmission presents as advantages: the use of low cost components, transmission of multiple channels at the same radio carrier frequency over a single link, using, simple intensity modulation direct detection scheme, and direct modulation of semiconductor laser diodes [WNG10].

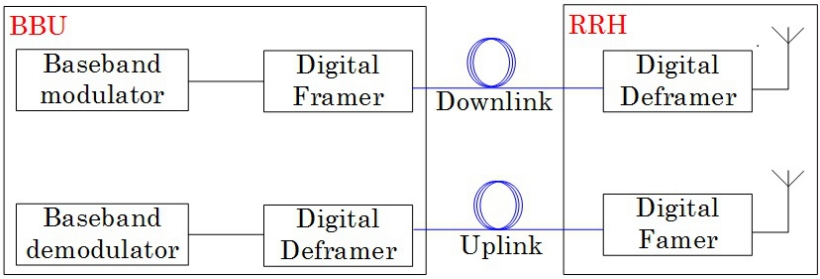

Figure 3.13: Digital Radio of Fibre (D-RoF) scheme [Tan16].

The main difference in terms of implementation between digital and analogue transmission is in down-conversion area. In digital, it contains an ADC and a DAC, while in analogue there is an electrical mixer and a local oscillator [JL13]. D-RoF scheme digitizes the wireless signal producing a sampled digital data stream in a serial format, which can directly modulate the optical source [LLN15]. In digital transmission, shown in Figure 3.13, all basic analogue areas are replaced by digital framer or de-framer.

This change results in scalability, energy efficiency, and low implementation cost. In D-RoF the digital Framer/De-framer is made using three types of typical generic industry agreement high speed serial communication interfaces, which produces high throughput and low latency: Common Public Radio Interface (CPRI) and Open Base Station Architecture Initiative (OBSAI) semi proprietary solutions, and a non proprietary solution currently under development named Open Radio equipment Interface (ORI) [Tan16, PSL+16].

3.4.2.1 Open Base Station Architecture Initiative (OBSAI)

OBSAI is the first to be launched in 2002 by Hyundai Syscomm, LG Electronics, Nokia, Samsung Electronics and ZTE Corporation

[RM13]. This interface objected to overcome an excessive pressure on the research and development activities of the Original Equipment Manufacturers (OEM). This pressure has occurred due to high demands for state-of-the-art equipment from the operators. This situation forced sellers to present quickly released products, which resulted in missed deadlines [Sah09].

Figure 3.14 shows the four main logical blocks performing in access network. These blocks can be composed of up to 12 modules, which represent a set of functions and attributes.

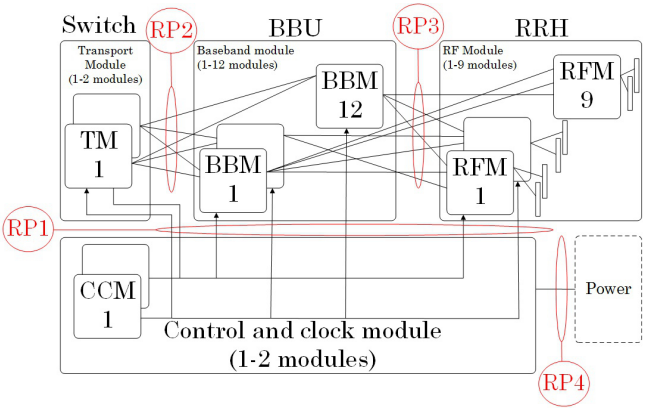

Figure 3.14: OBSAI functional blocks reference architecture [VIAc].

The Transport Module (TM) makes the interface with external network, it offers security, synchronization and Quality of Service (QoS). Base Band Module (BBM) does the base band processing for the air interface (i.e en/de-coding, interleaving, spreading, modulation, de/multiplexing de/ciphering, protocol frame processing, and MIMO processing).

The Radio Frequency Module (RFM) propitious conditions for competing operation of two or more air interfaces, for Global System for

Mobile Communications (GSM), Wideband Code Division Multiple Access (WCDMA), HSPA, Worldwide Interoperability for Microwave Access (WiMAX) and Long Term Evolution (LTE), using different air channel bandwidth as a multiple of 1.25, 1.5, and 1.75 canning to reach up to 20 MHz. Among the many functions performed in this module, are: amplification, antenna interface, digital to analogue conversion, and RF filtering.

The fourth module is named Control and Clock Module (CCM). It is responsible for supervising all activities, monitoring status and reports performance. Links among these modules are achieved using three agents, called Reference Point (RP). RP1 is the interface which communicates control and the clock module with the other three modules. RP2 connects baseband and transport modules. RP3 interconnects baseband and radio frequency modules by carrying control data and the data generated by the user. RP4 provides the DC power interface between the internal modules and DC power source [RM13, VIAc, SEN+06].

RP3 offers two main topologies to connect Base Band Module (BBM) and Radio Frequency Module (RFM) (Figure 3.15). Figure 3.15(a) presents a mesh topology, which is configured with (N) baseband and (M) RF modules. Figure 3.15 (b) depicts star topology. In this option, connections between the baseband module and the RF module are agglomerated in a combiner and distributor (CD) [SEN+06].

RP3 is a point-to-point serial data interface structure both for uplink and downlink, and it is the most important reference point. It is based on messages, fundamentally divided in these distinct phases: sampling, messaging and framing as shown in figure 3.16. [SEN+06].

In the sampling phase, for LTE Downlink and Uplink Data Mapping, each high (H) or low (L) byte, representing the real (I) and imaginary

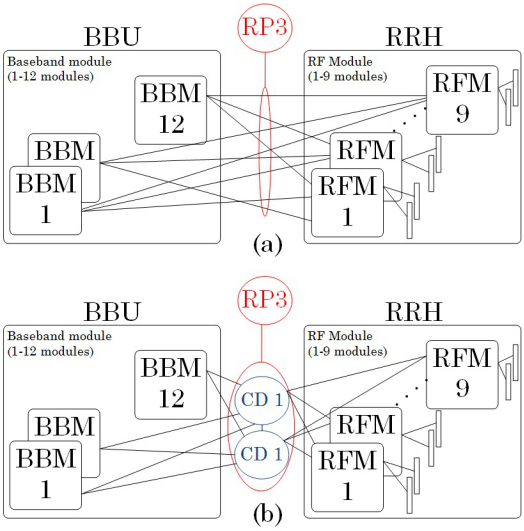

Figure 3.15: OBSAI topology: (a) mesh; (b) star [VIAc].

(Q) parts of stream, are firstly up converted using 8 bits; then the four [(I_H,I_L);(Q_H,I_L)] are stored in one of 4 samples fields, using 32 bits each, belonging to the payload [SEN+06].

Figure 3.16 also shows that, in messaging phase besides the Payload field which is composed of a maximum of 128 bits, there are three other fields, namely: Time stamp identifying time instance, Type classifying type of message using codes available in table 12, available in [SEN+06], and Address routing and to specifying the node where the payload must be delivered [SEN+06].

Figure 3.16 shows yet in framing phase a maximum quantity of the 1,920 message group, containing 20 messages, 1 code (C_n) marking the end of a message group, and 20 idle codes that are transmitted consecutively over an OBSAI frame, which has a duration of 10 ms

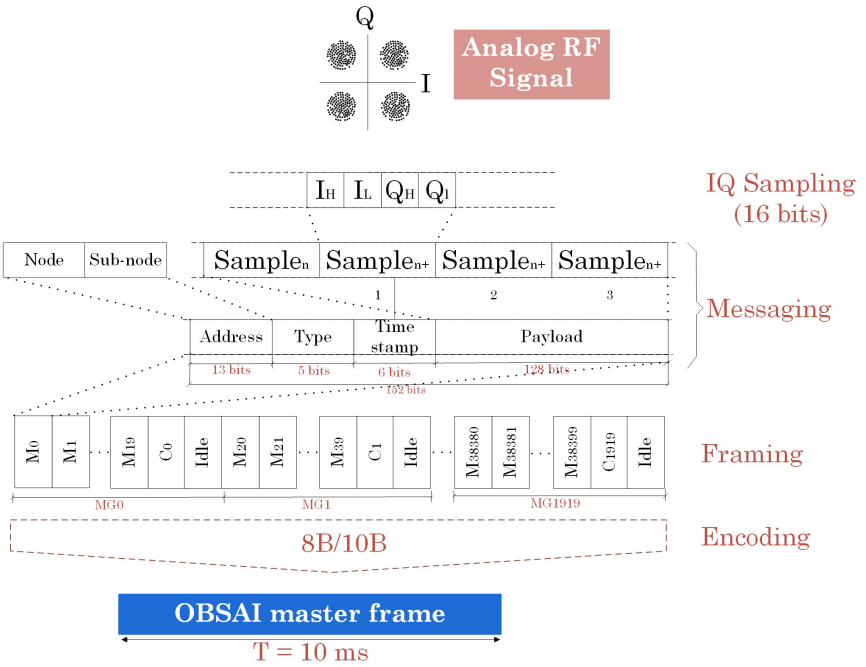

Figure 3.16: OBSAI RP3 interface structure [VIAc, SEN+06].

[SEN+06].

As shown in the figure 3.16 in messaging phase, data is transported, from the baseband module to the RF module or vice-versa, in the format of IQ data flows. Each data flow represents the data from one antenna to one carrier. Table 3.3 shows the maximum number of antenna-carriers (AxC) containers that will fit into a given virtual RP3 link given a specific LTE data rate and a determined bandwidth.

Table 3.3: Maximum number of antenna-carriers (AxC) containers that fit into a Virtual RP3 link basic frame (247,395 ns) considering each OBSAI data rate option available and each LTE data rate profile using 256-QAM.

Channel bandwidth [MHz]	**Sampling rate [MHz]**	**Number of AxC containers**			
LTE data rate [Mbps]		*50*	*100*	*250*	*500*
OBSAI data rate [Mbps]		*768.8*	*1,536.0*	*3,072.0*	*6,144.0*
OBSAI option		*1*	*2*	*3*	*4*
1,4	1,92	8	16	32	64
3,0	3,84	4	8	16	32
5,0	7,68	2	4	8	16
10,0	15,36	1	2	4	8
15,0	23,04	-	1	2	5
20,0	30,72	-	1	2	4

Source:[SEN+06]

Table 3.4 presents transmission data rates at Open Base Station Architecture Initiative (OBSAI) [Hai16]. Table 3.4 shows that OBSAI can currently provide a minimum of 768 Mbps and maximum data

rate equal to 6,144 Mbps per Remote Radio Head (RRH). The value of 614.4 Mbps is obtained dividing 152 bits, shown in figure 3.16 (messaging phase), by 247.395 ns which is the basic frame time. Dividing 128 useful message bits by 247.395 ns yields the useful OBSAI payload, which is equal to 517.39 Mbps [CPC+13, KKT15, PCSD15].

Table 3.4: OBSAI options data rate and applications in mobile broadband.

Op.	OBSAI Rate [Mbps]	Applications
1	768.0 = 1 x 614.4 x 10/8	2G/3G Radios, LTE 10 MHz 1T1R
2	1,228.8 = 2 x 614.4 x 10/8	LTE: 10 MHz 2T2R, 20 MHz 1T1R
3	3,072.0 = 4 x 614.4 x 10/8	LTE: 20 MHz 2T2R + 5 MHz 2T2R
4	6,144.0 = 8 x 614.4 x 10/8	LTE: 20 MHz 4T4R + 5 MHz 4T2R

Although OBSAI is the most complete interface for modularization base station, it has been abandoned and currently only represents 1/5 of market, while Common Public Radio Interface (CPRI), derived from OBSAI, is the most popular generic industry agreement interface, representing 4/5 $^{\text{ths}}$. It is preferred because its mapping methods are more efficient than OBSAI [dlOHLA16, Nik15].

3.4.2.2 Common Public Radio Interface (CPRI)

CPRI was launched in 2006 by a group of manufacturers (Ericsson, Huawei, NEC, NSN, and Alcatel-Lucent), it can support both electrical

interface, used in traditional base stations, and optical interface for base stations with RRH, besides to be a traditional TDM based fronthaul solution [ATC+15, I17].

Nowadays it defines the main interface provider for split functionality between BBU and RRH modules. CPRI has the following scope [ATC+15, VIAb].

1. It operates in the physical layer (L1) and the data layer (L2). The L1 defines the characteristics of the optical interface used to connect the RRH with BBU, while the L2 determines that the communication system be flexible and scalable;

2. Allows different information streams to be multiplexed over the interface, using the following protocol data plans depicted in figure 3.17:

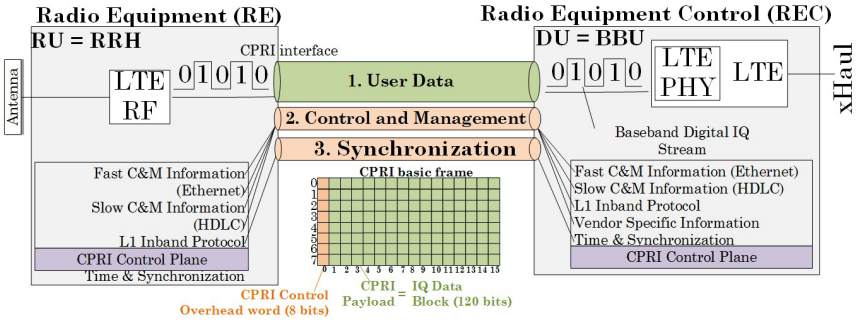

Figure 3.17: CPRI transport concept: Protocols data plans CPRI frame structure process

a) Control and Management Plan: information is sent via the In-band protocol, which carries the information along with the data generated by users. The control is used to process voice during the management of the operation,

administration, and maintenance of linkage and existing nodes;

b) Synchronization Plan: transmits the data required to alignment frames and time;

c) User Plan: RF signals are carried, from RRH (=RE) to BBU (=REC), in the form of IQ data flow in a CPRI basic frame of 260.42 ns. This basic frame is formed following four steps: Sampling, Mapping, Grouping and Framing.

3. CPRI specifies the following five topologies used in fronthaul and ilustrated in figure 3.18 [Gig17]:

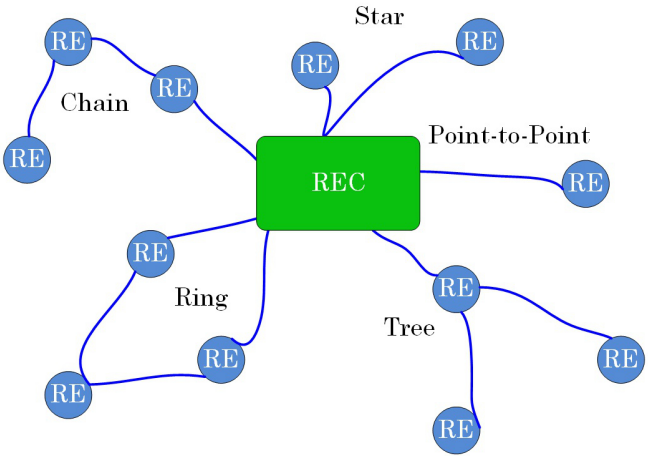

Figure 3.18: CPRI topologies: point-to-point, chain, tree, star and ring.

a) Point-to-Point: The first solution topology specified by Common Public Radio Interface (CPRI) becomes expensive when the number of fibre per sector grows quickly [CPC+13].

Besides this, delay increases with: link length, number of hops, and aggregation/demultiplexing points [JITT16];

b) Chain: this topology reduces the number of fibre in Second Generation (2G) and Third Generation (3G) systems [CPC+13, Eks12];

c) Tree: in this option the root node can be represented by Base Band Unit (BBU), and the leaves by Remote Radio Head (RRH) or small cells [PSS16];

d) Star: In this topology the substitution of active node by a passive optical power splitter/combiner which turns it into a Passive Optical Network (PON), therefore reducing installation, power consumption and maintenance costs [CPC+13, Eks12];

e) Ring: this topology allows the network to work even in the presence of a link failure on any segments [CPC+13, Eks12].

Figure 3.19 depicts the four mandatory steps performed during the construction process of a CPRI basic frame [VIAb].

The first step is to sample each Real (I) and Imaginary (Q) component RF signal. This sampling is done with a number of bits (M), which range from 4 to 20 for uplink and from 8 to 20 for downlink.

Since OFDM has a high Peak-to-Average Power Ratio (PAPR) in the time domain, CPRI needs to apply a high sampling bit resolution (15 bits) to keep quantization noise at a tolerable level. This application procedure is done multiplying both original I and Q values by 2^{15} [Wü15].

In the second step, called mapping, I and Q samples are stored, in sequence and chronological orders, inside of containers named as

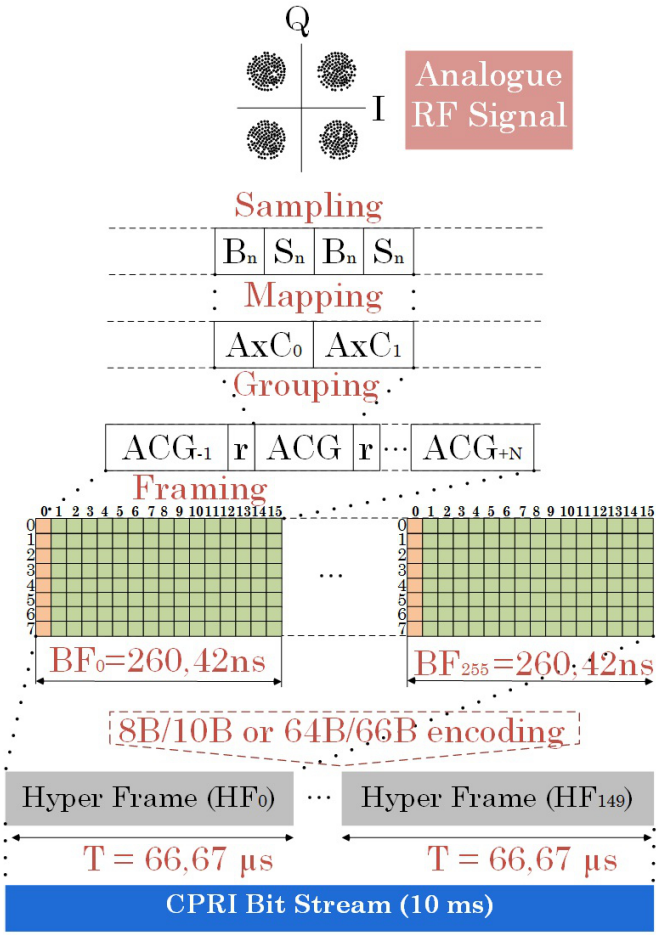

Figure 3.19: CPRI frame structure process.

antenna-carrier (AxC) with a capacity to transmit 3.84 Mbps. In a configuration, which: M = 15 bit/sample, no stuffing bits (B_n) are

used, LTE bandwidth is 10 MHz, and sampling rate of 15.36 MHz (or a 4 x chip rate of 3.84 MHz), each of the four AxC containers will transmit interleaved sequences as shown in figure 3.20.

In the third step there is a grouping of multiple containers inside a CPRI basic frame, using two options: packed and flexible positions. In the packed option, AxC containers are sent consecutively without the presence of a reserved bit (r) in between. In flexible position, the reserved bit (r) is included between AxC containers. The reserved bits are those not used by AxC containers in the IQ data block, in the basic frame [ATC+15].

AxC#1 (3.84 Mbps)	AxC#2 (3.84 Mbps)	AxC#3 (3.84 Mbps)	AxC#4 (3.84 Mbps)
$B_nI_0Q_0I_1Q_1$ .... $I_{m-1}Q_{m-1}$	$B_nI_{15}Q_{15}I_{16}Q_{16}...I_{2m-1}Q_{2m-1}$	$B_nI_{30}Q_{30}I_{31}Q_{31}$ .... $I_{3m-1}Q_{3m-1}$	$B_nI_{45}Q_{45}I_{46}Q_{46}$ .... $I_{4m-1}Q_{4m-1}$

Figure 3.20: AxC containers for LTE bandwidth of 10 MHz [dlOHLA16].

The fourth step is the basic frame composition consisting of the 120 bits from grouping's step plus 8 bits responsible for the control of information (CPRI overhead) totalling 128 bits. In the fifth step the 256 basic frame are encoded, to secure transmission, using 8B/10B or 64B/66B (in another words, 2 bits coding per 8 or 64 bits) to construct the hyper frame taking 66.67 µs. In the sixth step 150 hyper frames makes a CPRI frame taking 10 ms.

There is a nomenclature to identify position of each bit in CPRI stream. The tuple Z.X.W.Y.B, where Z is one of hyper frames, X one of 256 basic frame, W one of 16 words in basic frame, Y is the byte within a word, B indicates the bit in each byte [ATC+15].

Table 3.5 [Hai16] shows Common Public Radio Interface (CPRI) line rates, which are expressed as "Options (Op)". It shows that Common Public Radio Interface (CPRI) can currently provide a minimum of 614.4 Mbps and maximum CPRI data rate equal to 24,330.24

Mbps per Remote Radio Head (RRH). The value of 491.52 Mbps is obtained dividing 128 bits by 260.416 ns. Dividing 120 bits by 260.416 ns is equal 460.8 Mbps, which is the useful CPRI payload [CPC+13, KKT15, PCSD15].

Table 3.5: CPRI options data rate and applications in mobile broadband.

Op.	CPRI Rate [Mbps]	Applications
1	614.4 = 1 x 491.52 x 10/8	2G/3G Radios, LTE 10 MHz 1T1R
2	1,228.8 = 2 x 491.52 x 10/8	LTE: 10 MHz 2T2R, 20 MHz 1T1R
3	2,457.6 = 4 x 491.52 x 10/8	LTE: 10 MHz 4T4R, 15 MHz 2T2R, 20 MHz 2T2R
4	3,072.0 = 5 x 491.52 x 10/8	LTE: 20 MHz 2T2R + 5 MHz 2T2R
5	4,915.2 = 8 x 491.52 x 10/8	LTE: 10 MHz 8T8R, 20 MHz 4T4R
6	6,144.0 = 10 x 491.52 x 10/8	LTE: 20 MHz 4T4R + 5 MHz 4T2R
7	9,830.4 = 16 x 491.52 x 10/8	LTE: 20 MHz 8T8R
7A	8,110.08 = 16 x 491.52 x 66/64	LTE 20 MHz 8T8R
8	10,137.6 = 20 x 491.52 x 66/64	LTE carrier aggregation 5x20 MHz 2T2R
9	12,165.12 = 24 x 491.52 x 66/64	LTE carrier aggregation 3x20 MHz 4T4R

Continues on next page

Table 3.5 : *Continued from previous page*

Op.	**CPRI Rate [Mbps])**	**Applications**
10	24,330.24 = 48 x 491.52 x 66/64	LTE carrier aggregation 3x20 MHz 8T8R

Table 3.6 shows the maximum number of antenna-carrier (AxC) containers that will fit into a given CPRI link and given a specific LTE data rate using a determined bandwidth.

Table 3.6: Maximum number of antenna-carrier (AxC) containers in Common Public Radio Interface (CPRI) basic frame (260.416 ns) considering each CPRI data rate option available and each LTE data rate profile using 256-QAM.

Ch. BW [MHz]	**Samp. rate [MHz]**	**Number of AxC containers**										
LTE data rate [Mbps]		*50*	*100*	*200*	*250*	*400*	*500*	*800*	*800*	*850*	*1,000*	*2,000*
CPRI data rate [Gbps]		*0.6*	*1.2*	*2.5*	*3.1*	*4.9*	*6.1*	*9.8*	*8.1*	*10.1*	*12.2*	*24.3*
CPRI options		*1*	*2*	*3*	*4*	*5*	*6*	*7*	*7A*	*8*	*9*	*10*
1,4	1,92	8	16	32	40	64	80	128	128	160	192	384
3,0	3,84	4	8	16	20	32	40	64	64	80	96	192
5,0	7,68	2	4	8	10	16	20	32	32	40	48	96
10,0	15,36	1	2	4	5	8	10	16	16	20	24	48
15,0	23,04	-	1	2	3	5	6	10	10	13	16	32
20,0	30,72	-	1	1	2	4	5	8	8	10	12	24

Source:[dlOHLA16]

CPRI does not depend on the technology used to transmit radio signals over fibre. Literature points out two basic multiplexing architectures able to support CPRI fronthaul: TDM with proprietary multiplexing and WDM using several wavelengths [Loo13, BSTI13, DPP+13].

WDM presents two options: the first, already existing commercially, uses multiple lasers operating at different wavelengths. This option increases the complexity of the network architecture, costs and management of wavelengths. The second option uses a single source of light, known as: Self Seeding or spectrum-sliced WDM (SS-WDM). In this technique the wide range of wavelengths available simplify optical network architectures and are considered more energy efficient (green technology) [Loo13].

3.4.2.3 Open Radio equipment Interface (ORI)

ORI has been developed since 2011 by the European Telecommunications Standards Institute (ETSI) together with Next Generation Mobile Networks (NGMN). This generic open agreement interface is built upon the interface already defined by CPRI removing/adding several options and new functions [RM13].

This open interface enables the flexible combination of equipment from different manufacturers. It standardizes the way to connect digital interfaces BBU and RRH. This standard allows single-hop and multi-hop topologies. It can transmit different information flows (User Plane data, Control and Management Plane data, and Synchronization Plane data) multiplexed on the same interface. ORI links support at least one GSM (2G), (Universal Mobile Telecommunications System) Terrestrial Radio Access - Frequency Division Duplexing (UTRA-FDD) (3G), Evolved-UTRA-FDD (E-UTRA-FDD) / E-UTRA-TDD (4G)

or multiplexing combination of three of these four last technologies [PSSS14].

The ORI line bit rate starts from 1,228.8 Mbps (CPRI line bit rate option 2) and goes up to 10,137.6 (CPRI line bit rate option 8). In ORI there are three methods to mapping Antenna-carrier (AxC) Container within one basic frame: IQ sample based (method 1), WiMAX symbol based (method 2) and backward compatible (method 3). The choice of backward compatibility ensures the easy implementation of GSM, WiMAX, and LTE, in network's topologies where CPRI release 1 or 2 already exists [CSHB14, ATC+15].

Table 3.7 presents a comparison of the main features between OBSAI, CPRI and ORI. In this table, it is possible to note that OBSAI, CPRI and ORI share the same time frame and BER, but different other features.

Table 3.7: Main features comparison between OBSAI, CPRI and ORI.

Feature	**OBSAI**	**CPRI**	**ORI**
Minimum data rate [Mbps]	768	614.4	1,228.8
Maximum data rate [Gbps]	6.144	24.330	10.137
Encoding	8B/10B	8B/10B or 64B/66B	
Quantity of hyper frame	1,920	150	
Quantity of basic frame	22	256	
Time frame [ns]	247.4	260.42	

Continues on next page

Table 3.7 : *Continued from previous page*

Feature	**OBSAI**	**CPRI**	**ORI**
Time Hyper frame [µs]	5.44	66.67	
Maximum Jitter [ppb]	±0.1	±2	
Time frame [ms]	10		
Maximum Bit Error Rate (BER)	10^{-12}		

4

Emerging Xhaul Network Trends

This chapter is divided into five sections and introduces the basics features of the two techniques, named Software Defined Network (SDN) and virtualisation. Sections 4.1 and 4.2, which will be used in an evolved Centralized Radio Access Network (C-RAN) described in section 4.3. SDN and virtualisation are two important trends in the next mobile network generation. They are considered key technologies for the 5G mobile network. Their benefits are focused on satisfying the necessity for network operator to speed up their services innovation

and simplifying network management [NDK16]. Section 4.5 introduces the concepts of compress signal used to attenuate the quantity of data transited in fronthaul. Section 4.6 shows the main features of Radio over Ethernet (RoE), technique which promises to bring Ethernet interface to fronthaul segment.

4.1 Software Defined Network (SDN)

It is easy to find hardware radio equipment, however, a complete system based on this technology presents problems such as scheduling, resource allocation, troubleshooting, load balancing, security, and the cost of purchasing the hardware exceed the provided service benefits [CLSC14]. In a traditional distributed radio resource management fashion, each base station decides about its own radio resources. However, in this option, interference and radio resource managements became highly complex and suboptimal [NDK16].

Software Defined Network (SDN) is a paradigm shift that introduces an abstraction that separates the data and control planes of the network pushing all control tasks in a centralized controller, called SDN controller. This abstraction simplifies network devices and facilitates network configurations and management, because it is not necessary to deal with low level details of network devices. The use of programmable interface in SDN controllers reduces operational costs and expedites the deployment of new services. In such an approach, data planes are forwarded by devices monitored by the SDN controller using programmable interfaces [NDK16, YLJ+15].

As the figure 4.1 depicts, SDN is composed of three main layers: infrastructure layer (data plane), control layer and application layer. The infrastructure layer contains devices (such as switches, routers,

and wireless access points) without any control logic as for example: routing algorithms, like Border Gateway Protocol (BGP). In the control layer lies a controller, which encapsulates the networking logic, providing a programmatic interface for the network, implementing new functionalities and performing various management tasks. At the top of the SDN stack is the application layer consisting of all applications that use services from the controller to perform network-related tasks, such as, load balancing, Quality of Service (QoS), access control, and others.

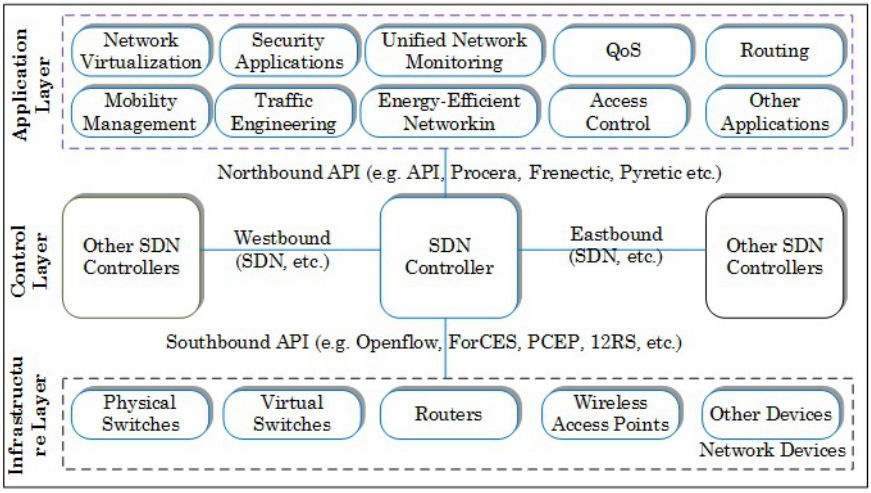

Figure 4.1: SDN architecture [NDK16].

Communications between data/application layer and control layer are done using an Application Programming Interface (API). This APIs translates information, received by the controller, into instructions. This translation is done using low-level protocols, as for example Open Flow. These instructions enable the modification of the behaviour of network devices (e.g. flow table, forwarding schemes, etc.). There are

four main types of APIs in the SDN architecture [NDK16, Yu14]:

1. The Northbound API to interface controller and application layer, enables applications to program networks and request services from them;

2. The Southbound API communicates to the controller and infrastructure layer, defining control communications including physical and virtual devices;

3. The Westbound and Eastbound APIs perform connections between controllers.

4.2 Virtualisation

There are two types of virtualisation, which cause confusion with SDN: network virtualisation, and network functions virtualisation [Yu14, NDK16].

Network virtualisation is also an abstraction, which consists of separating the network topology from the underlying physical infrastructure. This division enables multiple 'virtual' networks, e.g. Virtual Local Area Network (VLAN), deployed over the same physical equipment, therefore having a topology simpler than observed in the physical network [Yu14, NDK16].

Network functions virtualisation is the migration of functions from dedicated hardware to software, which runs on a cloud computing system. This change allows the operators to reduce costs, with equipment and energy consumption, scalability, multi-tenancy support, etc [Yu14, NDK16].

Neither of these technologies is mandatory for the operation of SDN and vice-versa, but these three technologies could benefit due to the advantages offered by each [Yu14, NDK16].

4.3 Next Generation Fronthaul Interface (NGFI)

Traditional fronthaul solutions have shown to be below both in demanded bandwidth and architecture flexibility. To combat this inefficiency, a Next Generation Fronthaul Interface (NGFI) based on Virtual Radio Access Network (V-RAN) has been proposed by China Mobile and is under study in IEEE 1914.1 task. NGFI targets to be a packet-based interface allowing that fronthaul data be packaged and transported using packet-switched networks, ensuring low bandwidth, but prevents the synchronization solution adopted for CPRI from being applied. This new interface also aims to be traffic-dependent enabling support for statistical multiplexing, antenna scale-independent interface (enabling it to be independent of the number of antennas), and the mapping between BBU and RRH should be one to many and flexible [I17, LHDG17].

This concept was originated from data centre virtualisation techniques and aims to perform base station virtualisation through the use of Network Function Virtualization (NFV). This method allows baseband resources to be deployed in multiple servers, as each physical layer (L1) server having an additional dedicated hardware accelerator that helps to meet the strict real-time requirements for wireless signal processing. while L2/L3 and applications functions are implemented in a virtualisation environment [IHD+14, oEE16].

This architecture allows that BBU resources be dynamically allocated on demand by RRH. This idea will enable load balancing mobile

traffic between BBU pools. Beyond this, there will be a BBU usage optimizing, since, such equipment is designed to always work in a maximum capacity, which in practice does not happen because traffic is greatly reduced in commercial areas at night and on weekends, and residential areas at commercial time and during holidays [CPC+13, PWLP15, IHD+14, Car15]. According to [Fre13] the possibility of multiple signals RRHs be processed by one BBU, enables greater spectral efficiency and therefore better data rates performing simpler processing in RRHs [CPC+13].

The scope of project IEEE 1914.1 is to create a standard that specifies the transport architecture for the Ethernet mobile fronthaul traffic including user data, management, and control plane traffic. Besides this, to define requirements and definitions for fronthaul networks containing data rates, timing, synchronization and quality of services are the objects of study in this work task, as well the analysis of possible functional splitting schemes, between RRH and BBU, which improve the efficiency of fronthaul segment and its interoperability on the transport level aiming to facilitate the implementation of radio functions such as massive MIMO and Coordinated MultiPoint (CoMP) transmission and reception [oEE16].

This new C-RAN layout uses NGFI, an open interface focused on redefining functions performed by BBU and RRH leading to eventual changes from/to RRH which will affect the RRH architecture. As figure 4.2 shows, this new network architecture links the Remote Radio System (RRS) to Remote Cloud Center (RCC). RRS contains the following elements: antennas, RRH and a new device called Radio Aggregation Unit (RGU), which will inherit a portion of the current BBU processing functions (the choice of these functions depends on functional split analysis). RCC will contain the rest of the BBU functions altogether with higher layer control functions, enabling

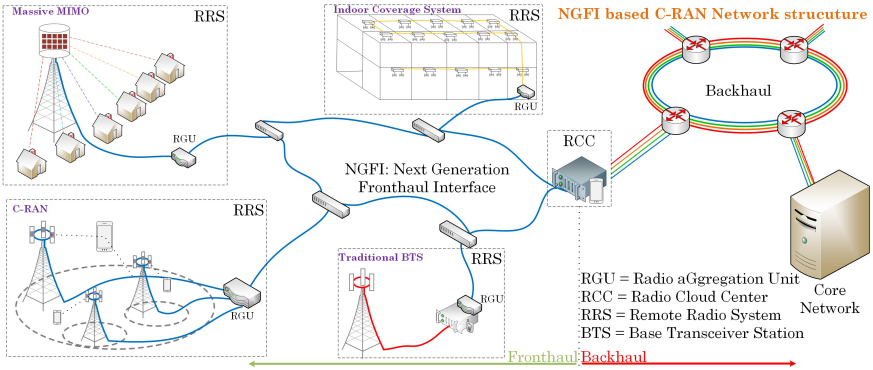

Figure 4.2: C-RAN architecture based on NGFI [KNB+16].

therefore, the following applications [IALN+16, LLS+14].

1. Indoor Coverage System (ICS): in this option the NGFI data is transported between Remote Radio System (RRS) and Remote Cloud Center (RCC) through Distributed Antenna System (DAS) utilizing tree topology. This technology is favoured by an ample building Ethernet cable resource, enabling the deployment of up to one hundred RRS;

2. Integrated Services Access Zone (ISAZ): in this approach, the fronthaul segment will be mostly a ring topology feeding six to eight macro sites, each site with three cells and each cell having from two to three carriers;

3. Dense Heterogeneous Network (Dense HetNet): in this scenario, where an extensive deployment of small cell predominates, a daisy chain topology can be used to save fibre resources.

4.4 Functional Split

As previously mentioned, in sub section 4.3, the RGU will be a beneficiary of some BBU functions. The analysis to determine which functions are transferred to RGU will be based on a functional split solution.

Considering Long Term Evolution (LTE) using MIMO with Y antennas, figure 4.3 shows a legacy C-RAN split and other potential optional solutions between RRS and RCC. Baseband processing function can be divided into user processing, which is related to traffic level, and cell processing unrelated to traffic level [oEE16].

One important functional split point (Split H) depicted in, figure 4.3, is the traditional function division used in the C-RAN scheme, which is inherited from interfaces such as OBSAI and CPRI. This case defines that, functions from: network layer (L3), data link layer (L2) and physical layer (L1) are fully realized at RCC, while time-domain RF and analogue/digital conversion functions are done by RRS [Asa15, JITT16, CSN+16].

Although this setting provides the best CoMP performance, it is also the one that demands the highest optical fronthaul bandwidth and the tightened one way latency delay and therefore sends more and more functions to be performed in the RRS. In the functional split point H, the fronthaul data rate demand is calculated by [Asa15, JITT16, CSN+16].

$$B_{UL/DL:Split_H} = 2^n \cdot 15000 \cdot N_{Sub} \cdot N_A \cdot N_B \cdot N_S \cdot N_{IQ} \cdot R_C \cdot R_L \tag{4.1}$$

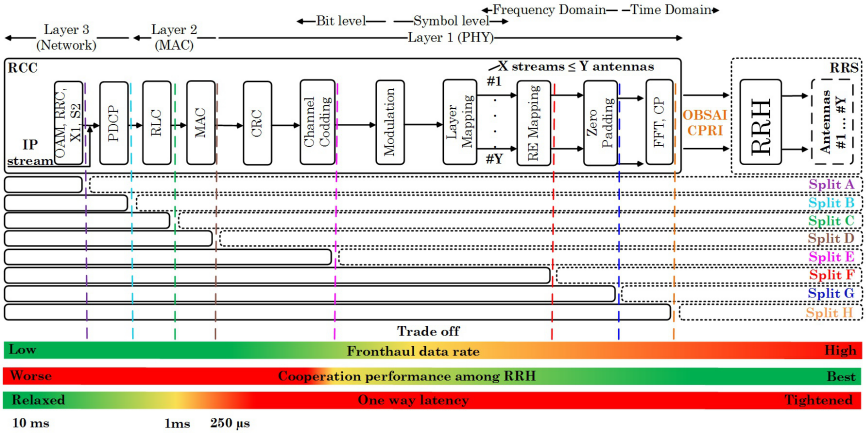

Figure 4.3: Functional split between RCC and RRS [Asa15, KKT15].

The optical CPRI originates from the electric CPRI. Since that electric CPRI was designed to meet the traditional Base Transceiver Station (BTS), which always works considering a maximum traffic, the fronthaul data rate required in this option, does not consider the case which the number of users served in the cell is less than the maximum amount of users projected, such policy generates an unnecessary data rate demand. In order to alleviate such unnecessary demand, new division options have been studied, such as the one that displaces the the cyclic prefix insertion from RCC to RRS (Split G). This configuration brings savings of approximately 6,67%. If cyclic prefix and the zero padding insertion (split F) is considered, 54.62% of the fronthaul flow stop existing.

Figure 4.3 also presents a new type of division (Split E), this alternative has been considered promising, because, at the same time, it provides a satisfactory performance of the CoMP, allowing the bits to be directly encapsulated in the Ethernet frame, and requiring a width proportional

to the number of Radio Equipment (RE) used by costumers served by the RGU. Of course, these benefits are compensated by the increase in the circuitry demanded in the construction of the RRS. In option split 5, the uplink and downlink bandwidths are calculated by [MKTO16]:

$$B_{UL:Split_E} = \sum_{n=1}^{k} \frac{1}{T_{TTI}} \cdot N_{mod-UL,k} \cdot N_{sym} \cdot N_{SC} \cdot N_{RB} \cdot N_{st-UL} \cdot N_{q-LLR} \tag{4.2}$$

$$B_{DL:Split_E} = \sum_{n=1}^{k} \frac{1}{T_{TTI}} \cdot N_{mod-DL,k} \cdot N_{sym} \cdot N_{SC} \cdot N_{RB} \cdot N_{st-DL} \tag{4.3}$$

In the split D all physical layer (L1) processing is done in RGU, no more base band IQ signals, but only digital bit sequences are sent to RGU; this setting can be considered an important limit because performing carrier aggregation in LTE-Advanced and bidirectional CoMP demands that function from layer 2 and upper layers are implemented in BBU [Asa15, Cvi14, MKTO16].

$$B_{UL:Split_D} = \sum_{n=1}^{k} \frac{1}{T_{TTI}} \cdot N_{mod-UL,k} \cdot N_{sym} \cdot N_{SC} \cdot N_{RB} \cdot N_{st-UL} \cdot N_{q-LLR} \cdot R_C \cdot \gamma \tag{4.4}$$

$$B_{DL:Split_D} = \sum_{n=1}^{k} \frac{1}{T_{TTI}} \cdot N_{mod-DL,k} \cdot N_{sym} \cdot N_{SC} \cdot N_{RB} \cdot N_{st-DL} \cdot R_C \cdot \gamma \tag{4.5}$$

In split C, whose fronthaul data rate is calculated using equation 4.5 [WRB+14], MAC functionalities are centralized, but all PHY functions are performed in RGU. However, this option does not allow the use of Coordinated MultiPoint (CoMP).

Table 4.1 presents the description and maximum values of each variable used in equations 4.1, 4.2, 4.3, 4.4, and 4.5.

Table 4.1: Parameters numerology used in equations 4.1, 4.2, 4.3, 4.5, and 4.5.

Var.	Description	4G	5G
S_R	Sampling rate [MHz]	30.72	122.88
C_B	Channel bandwidth [MHz]	20	80
N_B	Number of frequency bands	5	8
N_A	Number of antennas	8	
N_S	Number of sectors	3	
N_{IQ}	Number of IQ quantized bits	30	

Continues on next page

Table 4.1 : *Continued from previous page*

Var.	Description	4G	5G
R_C	Control word overhead	10/8 or 66/64	
R_L	Line coding (CPRI) overhead	16/15	
N_{Sym}	Number of symbols within TTI	14	
N_{SC}	Number of subcarriers per resource block (RB)	12	
N_{RB}	Number of RBs per User Equipment (UE)	6.25	
T_{TTI}	Transmission time interval (TTI) [ms]	1	
R_C	Code rate	0.094, ...,	
$N_{mod\text{-}UL,k}$	Modulation order of UE k in the uplink	2, 4 or 6	
$N_{mod\text{-}DL,k}$	Modulation order of UE k in the downlink	2, 4, 6 or 8	
$N_{q\text{-}LLR}$	Number of quantization bits for LLR	2	
$N_{st\text{-}UL}$	Number of MIMO streams in uplink	4	
$N_{st\text{-}DL}$	Number of MIMO streams in downlink	8	
γ	Ethernet Overhead for 1500 bytes	1,6%	

4.5 Compress Signal

Given the large data rates arising from the quantization of IQ signals, compression of fronthaul IQ flow has become an important topic of research. Current LTE macro base station with one cell sector, five bands, eight receive antennas and using 30 bits/baseband IQ sample requires a throughput that exceed more than 40 Gbps provided by optical fibre links. This aspect turns fronthaul links into a bottleneck. To mitigate this situation, compression techniques have been used. There are two types of compression: Lossless or Lossy.

1. Lossless, has a low compression ratio but the original signal can be fully reconstructed.

2. Lossy has a high compression, however the reconstructed signal is distorted from the original one. This distortion degree depends on compression ratio and compression algorithms.

In fronthaul there are two ways to implement the above types of compression: point-to-point and distributed. In the point-to-point compression, both uplink and downlink BBU compression are done in parallel, while in distributed compression these procedures are done in sequence [PSSS14].

For compressed E-UTRA and GSM, ORI uses CPRI IQ sample based. The data compression for E-UTRA-TDD and E-UTRA-FDD are restricted to channels with a air channel bandwidth of 10 MHz, 15 MHz, and 20 MHz. This IQ data compression is an optional feature for the Radio Equipment Control (REC) / Radio Equipment (RE) and shall be negotiated between both via Control and Management (C&M). If the transmission is carried out using compression, one process in

the REC shall be responsible for configuration and activation of the process, and the following conditions shall meet [ISG14]:

1. For LTE, the maximum one-way latency coming from the compression and decompression process should be up to 100 µs. Due to the LTE timing (HARQ) Hybrid Automatic Repeat Request requirement of a round trip time of 8 ms;

2. Error Vector Magnitude (EVM) degradation from compression / decompression should be 3% at most;

3. Compression ratio should be a minimum of 50%.

In general a compress and decompress process consists of these steps [ISG14]:

1. Down sampling process, where the ratio of output sampling rates to the original input sampling rate shall be up tp 5/8;

2. Non-linear quantization process, which consists in applying a surjective function to the I and Q sample values.

3. The decompression process is composed by: i) Inverted non-linear quantization process consisting in applying the inverse surjective function;

4. Up sampling where the sampling will be increased.

Non-linear quantization process: Due to the LTE baseband signal transmitted/received may be considered a normal distribution function *f(x)* (represented by equation 4.6), its amplitude distribution can be described via standard deviation (σ) and mean (μ), where μ is 0.

$$f(x) = \frac{1}{\sqrt{2\pi\sigma}} e^{-\frac{(x-\mu)^2}{2\sigma^2}} \tag{4.6}$$

These elements are used to characterize the Cumulative Distribution Function (CDF) of the LTE baseband signal, which determines how the different amplitudes in I/Q domain of the I/Q sampled are mapped to compressed I and Q sample values. This approach is used since it enables a fine granularity of decision levels to be used for I and Q samples of LTE baseband signal waveforms of small amplitude, and a coarse granularity to be used for I and Q samples of signal waveforms of large amplitude.

The compression function in the ORI node begins modelling, separately for I samples and Q samples, the I/Q amplitude distribution of the sampled data used for this the CDF function *g(x)* (see equation 4.7) [ISG14].

$$g(x) = \frac{1}{2}\left(1 + erf\left(\frac{x}{\sqrt{2}\sigma}\right)\right) \tag{4.7}$$

In both equations x is the integer value of the original I or Q sampled, to be compressed, and shall be within the I/Q amplitude range *[-2^N-1 ... 2^N-1 – 1]*, and the sample width, N = 15 (bits). The compression parameter value (σ) shall be configured by higher layers. Then the function *g(x)* is mapped to *h(x)* generating the compressed I and Q samples respectively, by using equation 4.8.

$$h(x) = \lceil g(x) * (2^M - 1) \rceil \tag{4.8}$$

Where, ⌈ ⌉ is ceil function, *h(x)* is the integer, within the range [0 ... $2^{M} - 1$], of the compressed I or Q sample to be generated as the result of the non linearisation process. M is the width (in bits) of the compressed I or Q sample and its value is 10.

4.6 P1904.3: Radio over Ethernet (RoE)

RoE is the alternative technology proposed for 5G fronthaul segment. It is based on a huge adoption of Ethernet interface on core networks [AMC15]. The difference of Time Division Multiplexing (TDM) packing, used by semi proprietaries (OBSAI/CPRI) or open (ORI) interfaces, RoE can provide good flexibility/scalability and achieve efficient transmission of the data generated by wireless users [oEE16].

This packaging process consists of the encapsulation of digitized Inphase, Quadrature (IQ) payload, vendor specific, and control data flows into an Ethernet frame payload field to transport them over the fronthaul segment [19015]. This technique adoption is justified because radio over Ethernet could be a generic and cost-effective technology for fronthaul transport. Furthermore, there is a natural trend of the fronthaul segment evolving to a more complex multi hop mesh network topology. This evolution will require switching and aggregation steps. These steps will be facilitated by adoption of Ethernet standards, although this method also has a natural introduction of additional latency and overhead [CSN+16, Tan16].

Standardization activities have been carried out on IEEE by a task force in IEEE Access Networks Working Group (1904.3) aiming: to design a variable rate, multipoint-to-multipoint and packet fronthaul interface, to provide specifications for the encapsulation of digitized

radio samples, header format (for vendor-specific control), and mapping structure-agnostic, for Common Public Radio Interface (CPRI) frames and other industry interfaces, from/to the Ethernet frame depicted in figure 4.4, whose variable description is found in table 4.2 [NKM+16, AMC15, 19015].

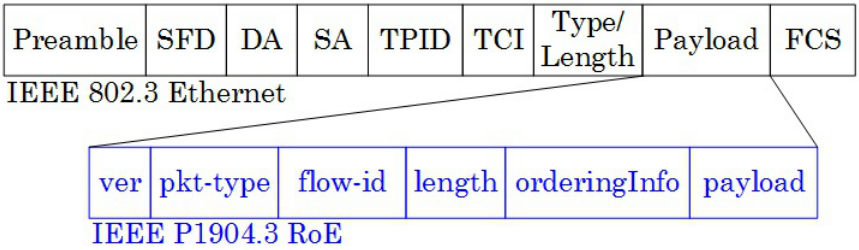

Figure 4.4: Frame format discussed by IEEE P1904.3 task force [NKM+16].

Table 4.2: Function identification of fields depicted in IEEE 802.3 Ethernet and IEEE P1904.3 Radio over Ethernet frames [Tan16].

Var.		**Feature**
IEEE 802.3	Preamble	Used for synchronization.
	SFD	Indicates start of the frame.
	DA	Stores the address of destination station.
	SA	Stores the address of source station.
	TPID	Identifies the frame as an IEEE.1Q – tagged frame.
	TCI	Sets the priority of stored information.

Continues on next page

Table 4.2 : *Continued from previous page*

Var		Feature
IEEE 802.3	Length	Covers possible extended header.
	Type/Length	Provides MAC information and number if client data types.
	Payload	Useful data from user.
	FCS	Cyclic Redundancy Check (CRC).
IEEE P1904.3	ver	Version of the RoE header being used.
	pkt-type	Contains type of RoE, such as antenna control or flow, vendor specific flow, etc.
	flow-id	Save number for the RoE packet flow for eventual multiplexing individual flows between source and destination address pair. It can identify if flows is a single AxC or a group of AxC.
	length	Covers possible extended header.
	orderingInfo	Initialized with 0, it is incremented by one on every sent packet of the contents of the packet.
	payload	Useful data from user.

Table 4.3 presents a comparison table between analogue and digital fronthaul transmission.

Table 4.3: Function identification of fields depicted in IEEE P1904.3 Radio over Ethernet frame [Tan16].

Feature	A-RoF	D-RoF
Bandwidth Utilization	Low	High
Base Station Complexity	Low	High
Implementation Complexity	Low	High
Resistance to non-linearity	Low	High
Error Vector Magnitude (EVM)	Variable	Constant

Table 4.3 shows that analogue RoF is more efficient than digital RoF in the items bandwidth utilization, base band complexity and implementation complexity, while Digital RoF is more advantageous in resistance to non-linearity and produced Error Vector Magnitude (EVM).

4.7 enhanced CPRI (eCPRI)

CPRI is extremely fronthaul data rate hungry, because it uses a permanent stream of traffic, therefore, this interface is indicated for short distances (up to 100 meters) [dG17].

The eCPRI will be based on a new functional split of the cellular base station functions, and the split point will pass so that it will be inside of the Physical Layer (i.e. Layer 1) [CPR17].

This new design, will enable a fronthaul data rate reduction ten-fold, allowing the required bandwidth to scale according to the user plane traffic, besides this, the main stream can be transported through Ethernet technology, eCPRI will then enable the use of sophisticated coordination algorithms and will also allow radio network updates by software [CPR17].

5

Numerical and Experimental Evaluations

This chapter is divided in four sections. Section 5.1 shows the numerical analysis about fronthaul demanded digital data rate using five different types of subcarrier spacing (15, 30, 60, 75 and 120) kHz. Next, the section 5.2 brings a comparison of the gains produced by three different types of compression signals, and it also shows EVM results and constellation diagrams acquired during experiment with three different lengths of fibre. The chapter continues in section 5.3 showing bandwidth results analysis considering the functional split

options approach. Section 5.4 exhibits validation results collected from experiments using analogue transmissions.

5.1 Digital Fronthaul Data Rate Calculation

As consumers demanding more and more video and other data through their mobile devices, the volume of fronthaul data traffic has increased exponentially to meet such demands. According to [Uni17], the minimum of 5G user experienced throughput in downlink will be 100 Mbps.

In accordance with the data shown in table 2.1, the 5G system has considered the possibility to keep the same amount of total/useful (1200/2048) subcarriers used in LTE for 20 MHz air channel bandwidth, therefore changing the value of the interval between two subcarriers.

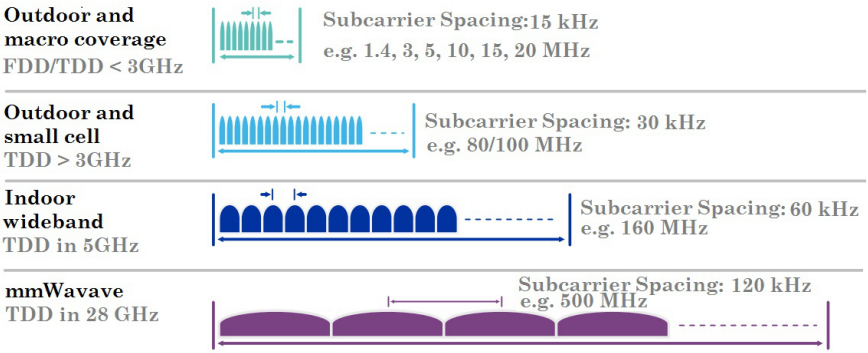

Figure 5.1: Scalable numerology with scaling of subcarrier spacing.

These new values will be governed by numerical expression $2^m \times 15{,}000$, with "m" being an integer positive or negative number. Considering this possibility this section does an analysis of the behaviour

of mobile user experienced throughput versus mobile fronthaul (MFH) digital optical fronthaul data rate for some cluster configuration.

Figure 5.1 shows the utility of a flexible subcarrier spacing. It is possible to notice that while macrocells continues using the legacy configuration from 4G (15 kHz), outdoor and small cells (30 kHz), indoor (60 kHz) and millimetre wave (120 kHz) will be served by greater spacing became facilitating the offering of higher mobile user experienced throughput.

Current research on small cells, forecasts that still in 2017 one small cell could support up to 3 aggregation bands. For this quantity of bands, figure 5.2 shows that the total mobile user throughput generated using MIMO 8x8 (1,83 Gbps) can attend up to 18 users with at least 100 Mbps each. These 18 users are more than the 16 clients supported by femto cells, but much less than 100 users supported by pico cells.

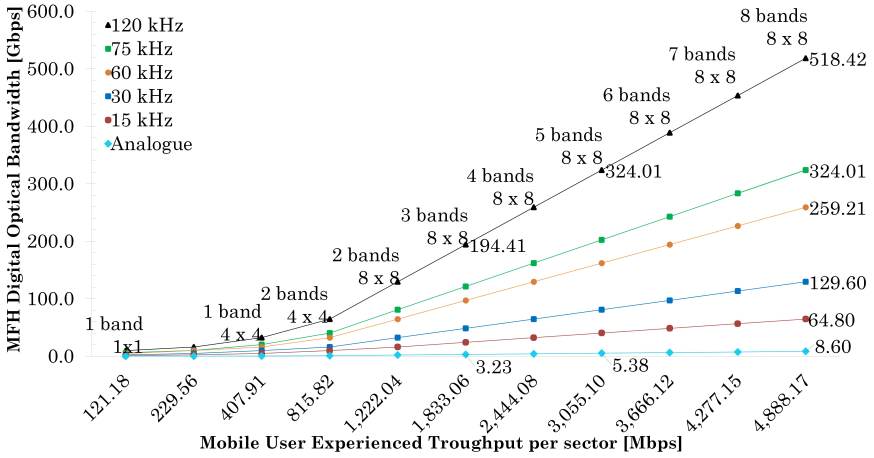

Figure 5.2: Analogue and digital optical fronthaul bandwidth for one cell site with one sector.

In figure 5.2, the line graph, whose values is calculated by equation 4.1, shows that the digital fronthaul data rate to attend to the traffic demand of only one cell site sector using different quantities of subcarrier spaces, bands and antennas, will reach 324,01 Gbps if 4G LTE-Advanced 5 bands be used, and when the number of bands is changed to 8, the digital optical fronthaul bandwidth grows by 60% reaching a maximum high than 518,42 Gbps. The graph line shows yet that, for one subcarrier spacing equal to 15 kHz and 3 carrier aggregation, the quantity of user experienced data rate generates a CPRI digital optical bandwidth on fronthaul of 24,30 Gbps, but if a subcarrier spacing is used this value reaches 194,41 Gbps. For analogue transmission the maximum bandwidth required in this case is 8.60 if 8 bands and MIMO 8x8 is used.

Table 5.1 [Itp17] shows commercial transceiver options that are able to attend currently and new mobile fronthaul bandwidth in 5G access network.

Table 5.1: Commercial dual fibre transceiver modules.

Interface	**Supporting rate [Gbps]**	**Working distance [km]**	**Optical module packaging**
CPRI	2.4576, 3.072, 4.9412	20	SFP
	6.144, 9.8304, 10.1376	20	SFP+
	24.33024	10	SFP28
Ethernet	100	40	QSFP ER
	100	40	QSFP-OTN

Continues on next page

Table 5.1 : *Continued from previous page*

Interface	**Supporting rate [Gbps]**	**Working distance [km]**	**Optical module packaging**
	100	40	CISCO CFP-100G-ER

Table 5.1 depicts that already there is Small Form-factor Pluggable (SFP) able to support the 24,3 Gbps cited in the paragraph above, and it allows these bits to be transited over optical fibre up to 40 km. Beyond, it is important to highlight the presence of Ethernet SFPs for 40 and 100 Gbps allowing transit of information over optical fibres with length up to 40 km.

The values observed in figure 5.2 on the x-axis, calculated through the equation 2.3, and using parameters presented in table 5.2, shows that mobile users will be able to experience theoretical maximum throughput ranging from 121,18 Mbps to high than 4.88 Gbps (a gap between both values is of the order of 64 times) [NK16].

Table 5.2: Parameters numerology used to obtain x-axis values showed on figure 5.2.

Var.	**Description**	**Values**
N_A	Number of antennas	1, 2, 4, 8
N_B	Number of bands	1, 2, ..., 8
U_S	Useful subcarrier	1200

Continues on next page

Table 5.2 : *Continued from previous page*

Var.	Description	Values
N_{bps}	Number of bit per symbol	8
T_{fs}	Symbol time duration [µs]	71.87

The mission of small cells on 5G network is to provide the voice and data rates of at least 50 Mbps upstream and 100 Mbps downstream. In accord with [TRV+17], to meet these requirements at least 30 small cells/km² must be deployed. Considering 100 users, these 30 small cells have the capacity to attend 3000 users /km².

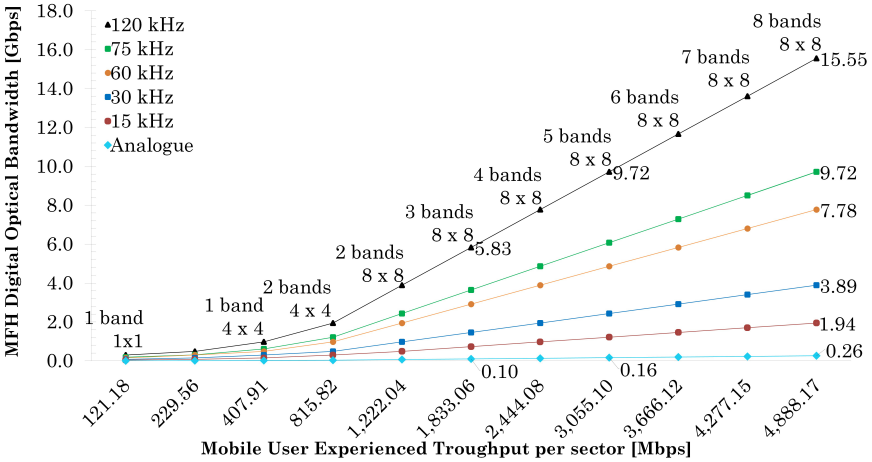

Figure 5.3: Analogue and digital optical fronthaul bandwidth for 30 small cells.

Figure 5.3, presents possible quantities of aggregated traffic for 30

small cells using five different values of subcarrier spacing. The lines graph presented in figure 5.3 shows a minimum mobile fronthaul digital optical bandwidth value equal to 36,86 Gbps, for 3 bands, using 15 kHz, 729 Gbps, when 5 bands are used, the optical bandwidth reaches 1,2 Tbps, and if 8 carrier aggregation is used together with 120 kHz of subcarrier spacing the optical overcome 15,5 Tbps.

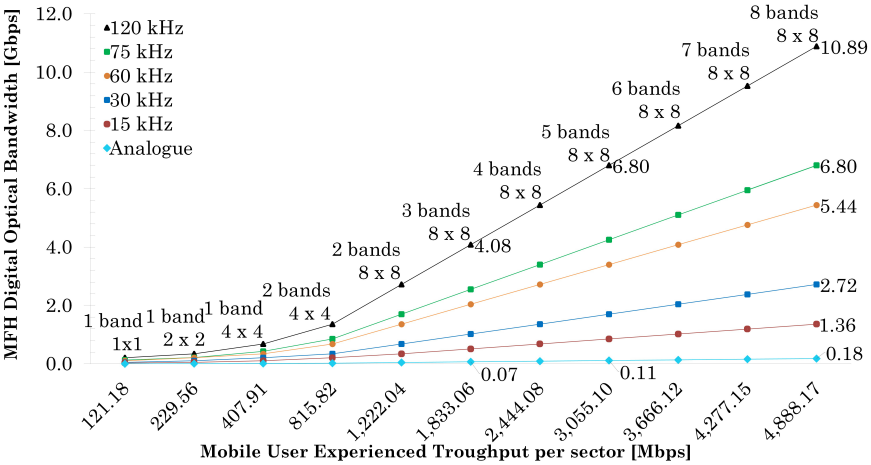

Figure 5.4: Analogue and digital optical fronthaul bandwidth for seven cell sites with three sectors.

Following same procedure adopted to analyse traffic produced by small cells, the figure 5.4 informs us that each sub cluster composed by seven cell sites containing three sectors considering the five subcarrier spacing options (15, 30, 60, 75, 120) kHz.

The figure 5.4 registers that for 15 kHz, one band, and one antenna, the total digital optical bandwidth is 25,8 Gbps. The optical bandwidth reaches 6,8 Tbps if five bands with MIMO 8x8 and 120 kHz are used. Maintain the same values for subcarrier spacing and MIMO, and

change the number of bands from five to eight the digital optical bandwidth can reach close to 11 Tbps.

The presence of small cells does not avoid the deployment of macro cells, whose design consists in development of three distinct procedures: coverage area, traffic capacity and frequency reuse using millimetre wave or sub 6 GHz bands.

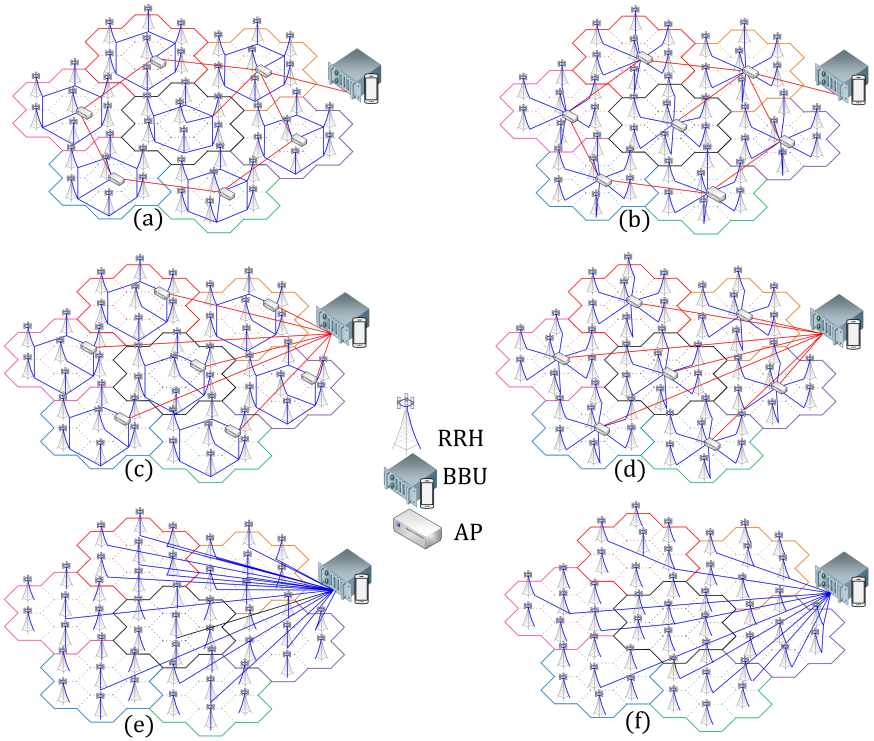

Figure 5.5: Enhanced physical topologies: (a) Ring-Ring; (b) Ring-Star; (c) Tree-Ring; (d) Tree-Star; (e)Star; (f) Star.

Based on the experience accumulated by the mobile telephone compa-

nies, figure 5.5 shows that, considering a reuse factor equal to seven, the six most common physical network topology formats used are: ring-ring, ring-star, tree-ring, tree-star, star, and daisy chain.

The graph line presented in the figure 5.6 shows that the celling aggregated traffic of whole cluster ranges can reach 76,21 Gbps. The same figure shows that for 5 bands the minimum aggregated value is about 6 Tbps and for 8 bands the floor value is 9,53 Tbps if subcarrier spacing equal to 120 kHz is used.

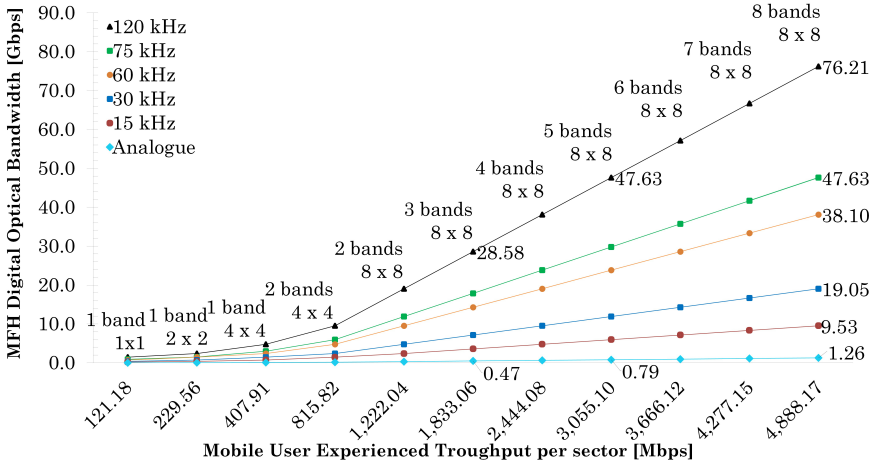

Figure 5.6: Analogue and digital optical fronthaul bandwidth generated by whole cluster showed in the figure 5.5 containing 147 sectors.

To face this huge quantity of data, the industry and academy has worked aiming to provide technologies in order to mitigate this demand. Thus, three lines of research are identified as possible solution candidates that are able to save data traffic in fronthaul, starting with two considered digital transmission (compression techniques and functional splitting) and another analogue transmission.

5.2 Compression Transmission

This subsection analyses the impact caused by compression technique over digital fronthaul bandwidth.

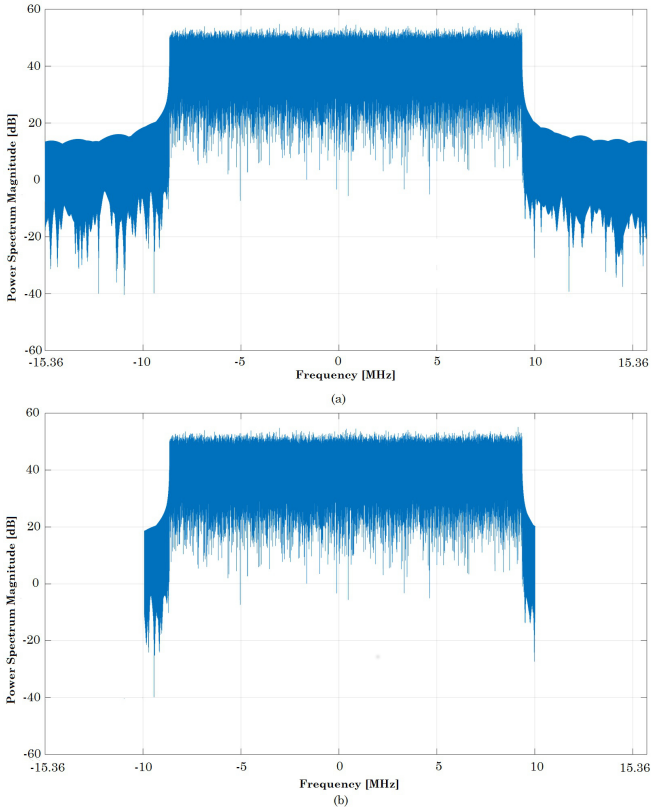

Figure 5.7: Signal spectrum: (a) with redundant spectral data; (b) without redundant spectral data.

The two basic compression ways are: reducing the sampling bits

resolution with or without redundant spectral data, using, in the last case, a low-pass filter. Figure 5.7 shows the difference between these two spectrum.

The quantity of bits used in this analysis is six because experimental results (discussed in next pages) show that if 256-QAM and smaller sampling bit resolution are used, the EVM obtained does not meet the minimum value required by the LTE standard.

Figure 5.8 registers that the use of 6 instead of 15 bits produces a digital optical bandwidth economy equal to 60.00% allowing full traffic generated by small cell with 3 bands and MIMO 8x8.

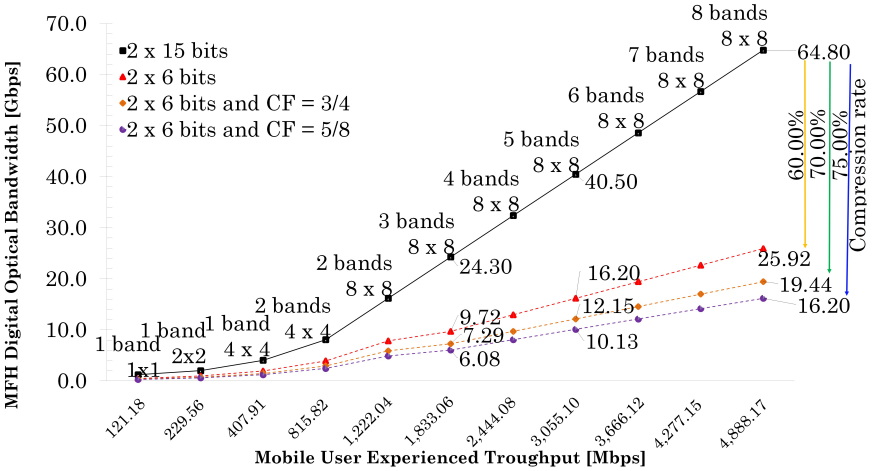

Figure 5.8: 1 small cell using subcarrier spacing equal 15 kHz.

The figure 5.8 also shows that compression rate can reach 70.00% if redundant spectral data be removed through a low-pass filter using compression factor of 3/4. If this parameter is more aggressively, defined in 5/8, the compression rate will reach 75.00%. Such compression enables, in the future, that an aggregate data flow generated by a small

cell using eight carrier aggregation and 8x8 MIMO is transmitted by an SFP with a maximum capacity of 19.44 Gbps.

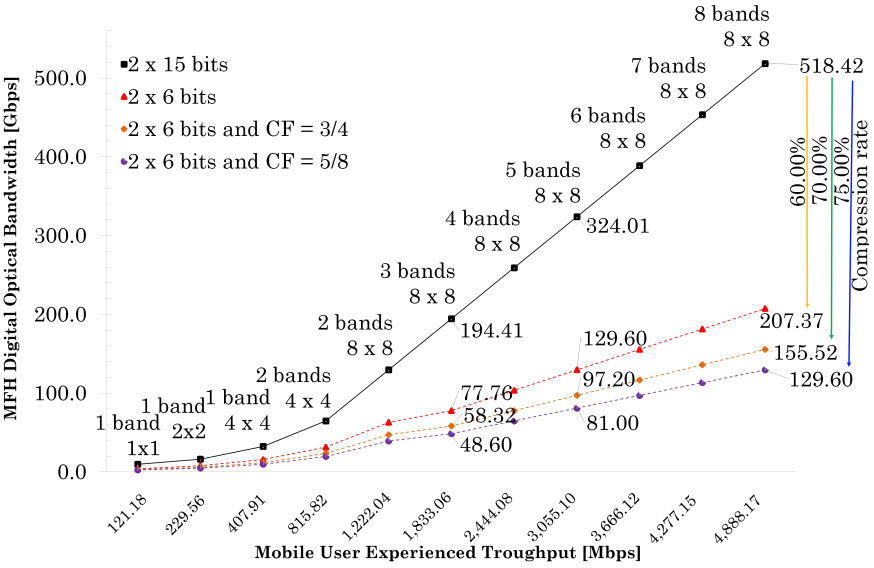

Figure 5.9: 1 small cell using subcarrier spacing equal 120 kHz.

When similar analysis is done for subcarrier spacing equal to 120 kHz, equivalent behaviour is found both for 1 or 30 small cells. Figure 5.9 shows that for 1 small cell, digital transmissions using 15 bit demands 518,42 Tbps, but if number of quantization bits is 6, the value will be 207.37 Gbps. This value can be still lower if the 6 bits be used together a compression factor of 5/8, is this case the value returns to 129.60 Gbps.

For 30 small cells, figure 5.10 indicates similar economy. A data stream of 15.55 Tbps converts respectively to 6.22 Tbps and 4,67 Tbps or 3.89 Tbps according to compression technique used.

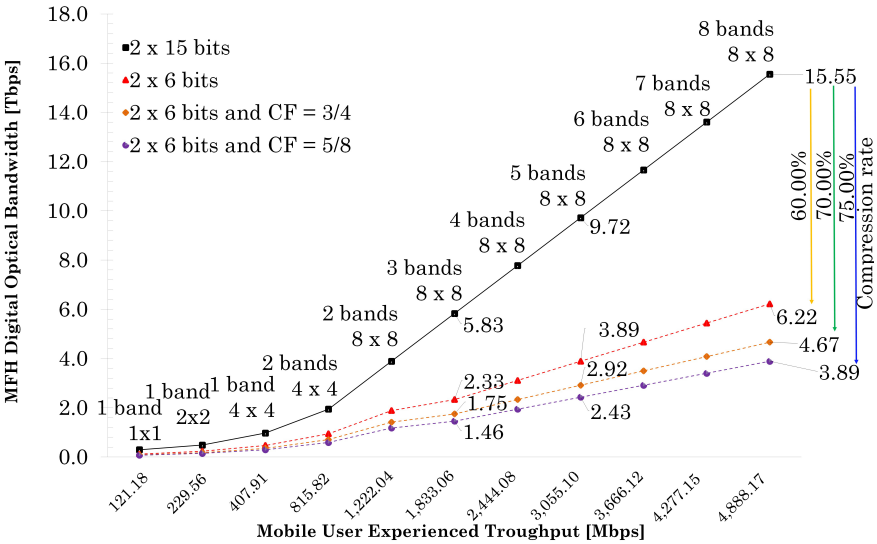

Figure 5.10: 30 small cells.

For a macro cell cluster with reuse factor equal to 7, figure 5.11 indicates equivalent results. A data stream of 10,89 Tbps converts to 4,35 Tbps, 3,27Tbps or 2,72 according to the type of compression used.

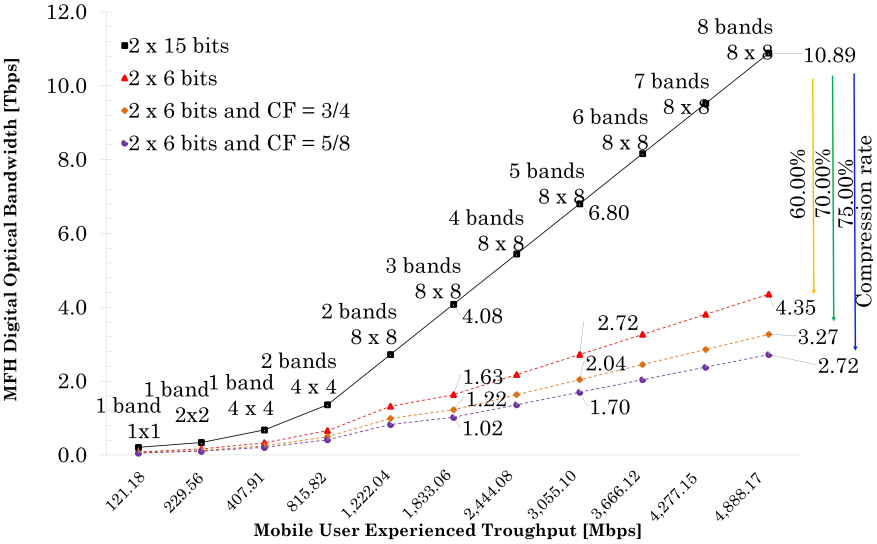

Figure 5.11: 7 cell sites with 3 sectors.

5.2.1 Compressed Fronthaul Transmission Experiment

Aiming to verify the performance of compress signal technique, using lossy approach, was performed an experiment, picture in figure 5.12, in Fraunhofer-Heinrich Hertz Institute (HHI) laboratory.

Intelectual Property (IP) lossy compression technique [Weg12] used in this experiment are based on [Weg06], and has been adopted by the Fraunhofer-HHI Remote Radio Head (RRH). Figure 5.12 shows that in this experiment the real LTE signal is generated in Matlab using off line processing.

After generation, this signal is transported one single time to RRH by Ethernet cable. In RRH happens the compression before signal be

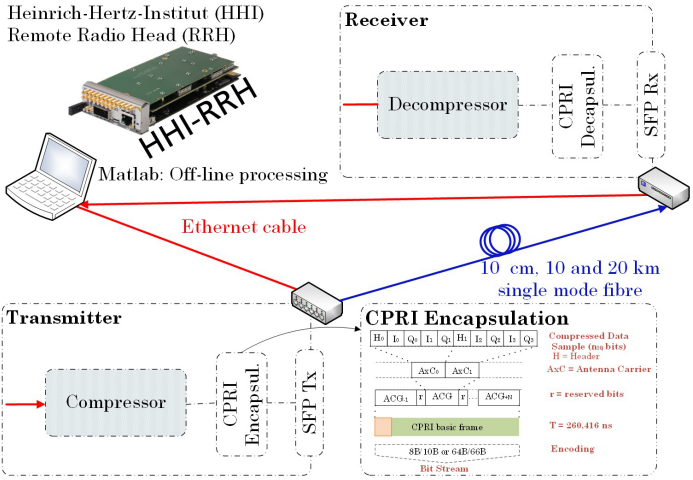

Figure 5.12: I/Q CPRI setup compression.

converted in a CPRI signal. After this conversion signal is sent to SFP operating at wavelength of 1310 nm and optical power transmission of -4.8 dBm. After this the signal is transported in 10 cm representing optical back-to-back, 10 and 20 Km. In the reception, the captured signal is unpacking from CPRI signal format, decompressed and sent to the computer, through Ethernet cable, where using Matlab EVM measurements are done and constellation diagrams are plotted.

Figures 5.13, 5.14, 5.15, and 5.16 depict the evolution of EVM as the compression ration increases.

Figure 5.13 shows that EVM evolves from almost 0 to about 4% when a maximum compression factor 3 is performed, meaning about 22,8% of EVM threshold for QPSK. The registered EVM values for different distances shows that this parameter has little influences in the EVM degradation due to the transmission to be digital. Figure 5.13 also

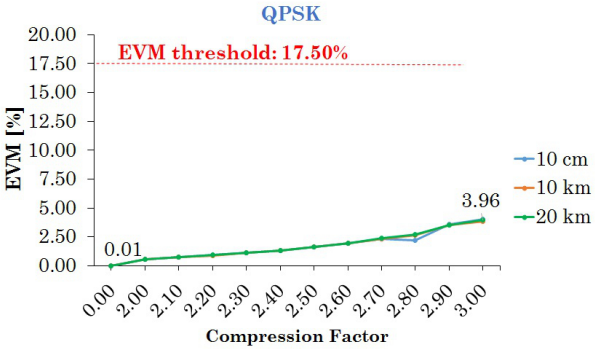

Figure 5.13: EVM measurements for optical back-to-back, after 10 and 20 km using QPSK.

shows that for QPSK the compression technique used meets the EVM requested by the LTE standard. Similar situation is shown in figure 5.14, which presents behaviour of EVM when modulation 16-QAM is used.

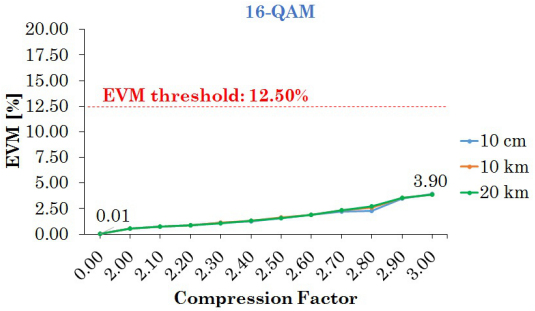

Figure 5.14: EVM measurements for optical back-to-back, after 10 and 20 km using 16-QAM.

Figure 5.14 shows that if 16-QAM modulation is used, for compression

factor 3 the EVM is nearly 4%. This value is equal to 32% of EVM threshold required for 16-QAM. For 16-QAM, EVM measurements up to 20 km present very little difference.

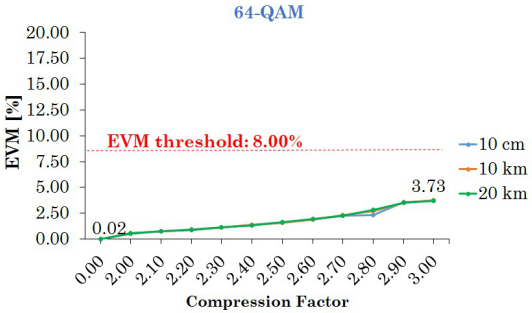

Figure 5.15: EVM measurements for optical back-to-back, after 10 and 20 km using 64-QAM.

Figure 5.15 registers similar conditions to those presented before, with EVM degradation of near 4 perceptual points for compression factor 3, however, in this case, the maximum EVM measured represents 50% of threshold EVM for 64-QAM.

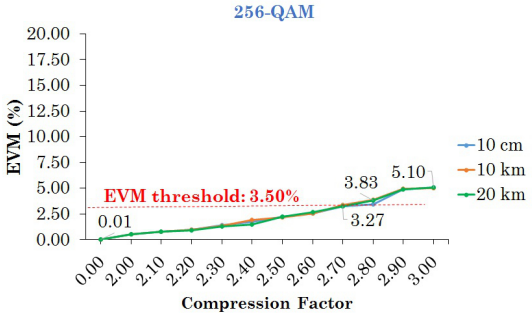

Figure 5.16: EVM measurements for optical back-to-back, after 10 and 20 km using 256-QAM.

Figure 5.16 depicts that for 256-QAM there is a paradigm shift, now for compression factor 3, the EVM measured overcome the EVM threshold required for 256-QAM, therefore the possible maximum compression factor is limited to 2.7.

Figures 5.17, 5.18, 5.19, 5.20 shows the behaviour of constellation diagram using distance of 20 km, modulations equals to QPSK, 16-QAM, 64-QAM, 256-QAM and real/equivalent bit resolutions equals to 15, 7, 6, 5 respectively, which is equivalent to compression ration equals to 0%, 52.38%, 60% and 66.67%. These values are equivalent to compression factor 0, 2.1, 2.6 and 3.

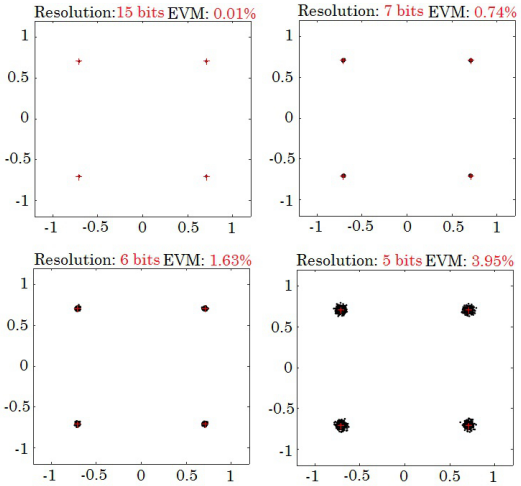

Figure 5.17: Constellation diagrams after 20 km for QPSK.

Analysing the figure 5.17, is observed for QPSK, a bit resolution subtraction of 66.67% translates into an EVM deterioration of 395%, with the EVM going from 0.01% to 3.95%.

Similar behaviour is presented by the figure 5.18, which shows that

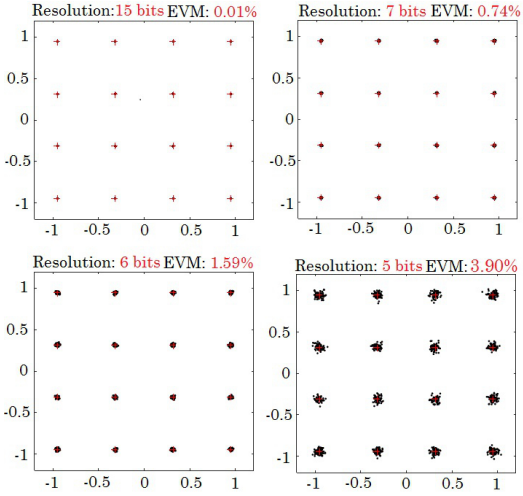

Figure 5.18: Constellation diagrams after 20 km for 16-QAM.

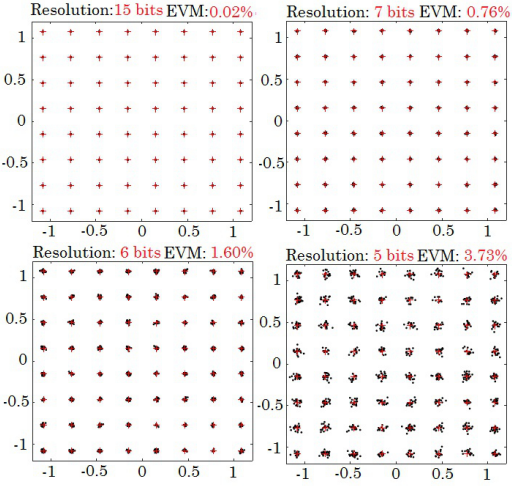

Figure 5.19: Constellation diagrams after 20 km for 64-QAM.

for 16-QAM, the same bit resolution reduction rate, but the EVM degradation is 390%, and therefore the EVM goes from 0.01% to 3.90%.

The figure 5.19 also registers an EVM degeneration for 64-QAM, but in a lesser intensity. In this case, the amount earned is 186%, with EVM leaving the level of 0.02% and reaching 3.73%.

The last case (figure 5.20), for which modulation chosen is 256-QAM, is the most worrying case, since in such situation, the decrease in the number of bits used in the sampling resolution, not only ruin the EVM, but it does so in such an intensity that the maximum value required by the LTE standard is exceeded. In this case, the decrease in EVM is equal to 255%, with the EVM departing of 0.02% and arriving at 5.10%, surpassing therefore the maximum stipulated value of 3.5%.

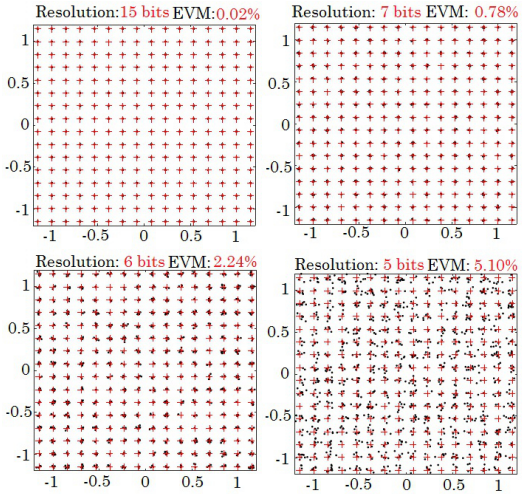

Figure 5.20: Constellation diagrams after 20 km for 256-QAM.

From this experiment it is possible to conclude that data traffic in

fronthaul over optical fibre using compress signal is possible, but for 256-QAM, the minimum bit amount used must equal 6 bits. It is also an important highlight that although data compression offers conditions to transmit data in fronthaul using fewer devices, a greater amount of compressed data implies an increase in the time required to perform the compression and decompression of the data, generating an increase in the round trip signal time. ORI standard recommends do not exceed 20 µs for LTE [ISG14].

5.3 Functional Splits Transmission

Functional split has been identified as a way to reduce the amount of digital data demanded in fronthaul. Figure 4.3, in section 4.3, shows some possible options of functional split. Based on these alternatives, this section evaluates how much economy such techniques can provide. The table 5.3 gives a summary of the quantity of samples used in 20 MHz in one frame transmitted during 1 ms.

Table 5.3: Quantity of samples per subframe for LTE bandwidth of 20 MHz.

Resource Element	**Quantity**	**%**
Reference Signal	800	2,60
Cyclic Prefix	2.048	6,67
Zero Padding	11.872	38,65
Useful Payload	16.000	52,08
Total	**30.720**	**100**

From table 5.3, it is verified that, if all cyclic prefix (used to combat multi-path fading) are added/removed in RRH, the mobile fronthaul bandwidth saved is equivalent to a total subcarrier used by LTE bandwidth 20 MHz and almost 7% of the total subcarrier used in 1 ms. If not only cyclic prefix, but also zero padding addition/removal (used to provide DFT/FFT computationally efficiency) is done in RRH this saving increases by 45.32%.

Figure 5.21 shows four possible split options of the PHY layer, which are: Split H, Split G, Split F and Split E, when a maximum number of users equal 64, 100 and 128 are used. Figure 4.3 depicts that in the first three approaches the split occurs on symbol level/cell processing domain, while the fourth (Split E) happens on bit level. Based on calculation using the equations 4.1 and 4.3, a digital mobile fronthaul comparison between these four split alternatives is achieved.

In this context the traditional CPRI approach (split H) demands the maximum bandwidth (64,80 Gbps). Next, split G presents factor reduction of 1.1, reducing therefore, the digital mobile fronthaul to 60.55 Gbps. Still in the physical layer, split F options provide an even greater economy (factor reduction 2.2), in this case the bandwidth returns to 29.4 Gbps.

The last option, split E, has the capacity to offer a factor reduction of 13.7, therefore reducing the fronthaul data rate for 4.74 Gbps if 128 users using 1050 resource elements is chosen. With the same number of resource elements and only 100 costumers this reduction achieves 17.5, representing a fronthaul data rate equal 3.70 Gbps. If 64 users are considered using the same number of resource elements the factor reduction increases to 27.3 meaning a fronthaul data rate equal 2.37 Gbps.

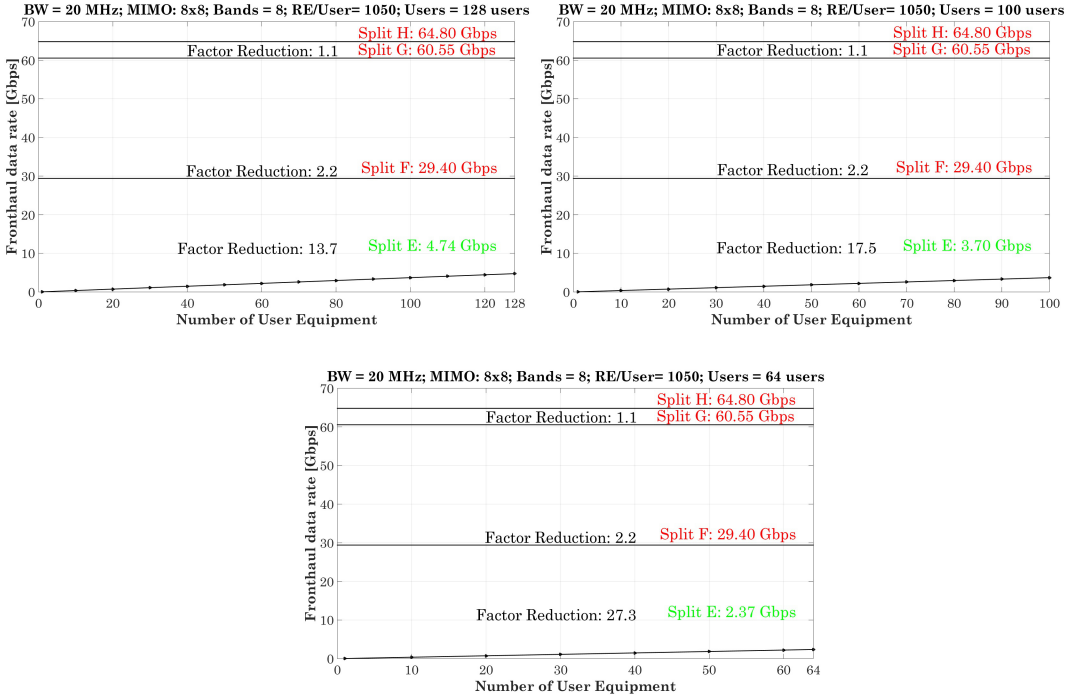

Figure 5.21: Digital Mobile Fronthaul Bandwidth for different physical split options.

In all of these alternative presented above the maximum allowed one way latency is 250 µs, in agreement with the maximum distance of approximately 25 km found for the C-RAN presented in section 3.2.

5.4 Analogue Transmission

The big advantage of analogue transmission is the small quantity of RF signal transmitted, as can be seen in figure 5.2, which shows that analogue transmission save above 86,72% when compared with digital transmission [YHH+15, SMI+14]. However, it is important to discuss potential difficulties generated by non linearities faced by operators if this type of transmission is used in fronthaul.

In order to fill this gap, this section describes an online experiment, pictured in figure 5.22, carried out in the laboratory of the French mobile operator (Orange), showing the behaviour of the analogue transmission under the influence of non-linear effects generated by the directed modulated laser when the RF power at input of the laser is increased up to achieve the non-linear region of the laser.

Figure 5.22 shows that, in IQ-Box Tx, a LTE signal using 64-QAM modulation, MIMO 2x2 configuration, and air channel bandwidth equal to 10 MHz is created. Then a CPRI signal option 2 (1,2288 Gbps) is generated based on the LTE signal created before. The CPRI signal is then sent to an optical split which replicates 3 times the same signal because Digital/Analogue Radio over Fibre Converter have 3 inputs 5.22.

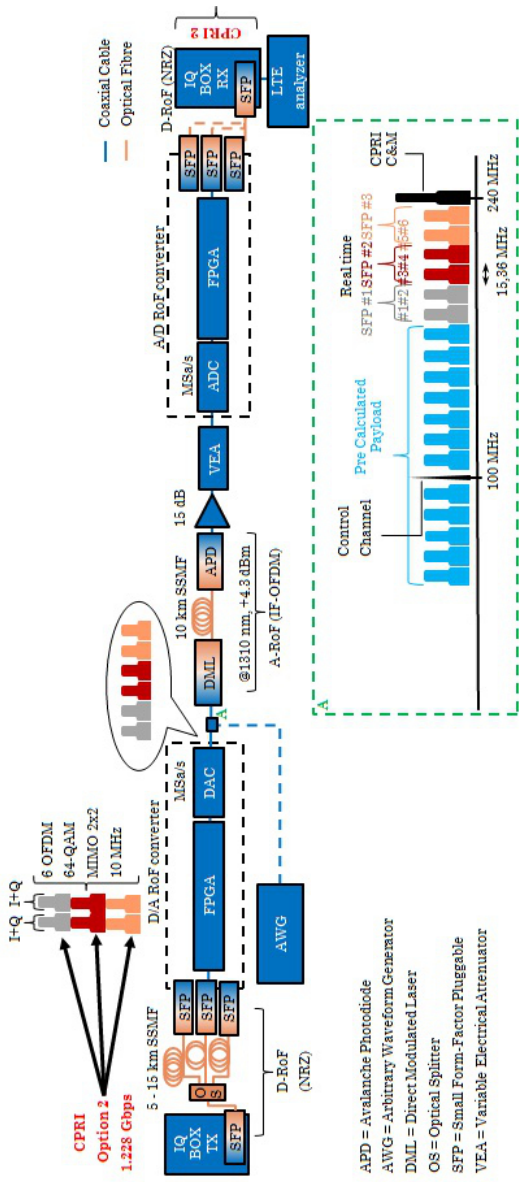

Figure 5.22: A-RoF experimental setup.

After this reproduction, signals are sent, through off-the-shelf mono-fibre SPF, over different Standard Single Mode Optical Fibre (SSMF) containing lengths equals to 5, 10, and 15 km (these 3 different lengths represent the D-RoF network segment) up to a Field Programmable Gate Array (FPGA) which does the D-RoF to A-RoF conversion.

The D-RoF/A-RoF conversion starts when the CPRI data, representing IQ time-domain samples, are transformed into two (one for each antenna) OFDM bands, each holding 10 MHz, to be transposed for an intermediate frequency.Thus, the only band initially generated in IQ-Box turns into six real time band. Along with these, is also generated one control channel low bit-rate band for the A-RoF link to be carried at 100 MHz and also one CPRI Control and Management (C&M) at 240 MHz.

Aiming to use the maximum number of frequencies operated by antennas Tx and Rx, another twelve similar signals are created by Arbitrary Waveform Generator (AWG). The similarity is achieved pre-distorting and adjusting the signal avoiding AWG frequency response, allowing the same power levels observed in real-time signals. Each band is separated from each other by a minimum space allowed by the antenna equal to 500 kHz, and the control channel is inserted between the second and third band (the inset B in figure 5.22).

This set of signals is sent to Head-End Digital to Analog Converter (DAC) where the A-RoF RF power signals are appropriately generated aiming to avoid the non-linear operation region of the laser at the same time that provides the best possible RF power to modulate a Direct Modulated Laser (DML) operating at 1310 nm and emitting in a mean optical power equal to 4 dBm.

The generated optical signal is transported over 10 km of SSMF to an Avalanche Photo Diode (APD), which converts the signal from optical

to electrical domain. After the detection by the photodiode, the signal is amplified and forwarded to a Variable Electrical Attenuator (VEA), used to set the optimum RF power at the input of the Analogue to Digital Converter (ADC) available in antenna 2. After passing this ADC the electrical analogue signal return to the CPRI format.

Figure 5.23 presents the EVM behaviour of the six real-time signals in the presence of 1 (alternately), 6, 12 and 18 bands. The figure 5.23 also present a line graph EVM evolution of D-RoF aiming to have a comparative level. The EVM measurement using one band was repeated in six different central frequencies aiming to register the EVM behaviour on whole frequency range adopted by the antennas.

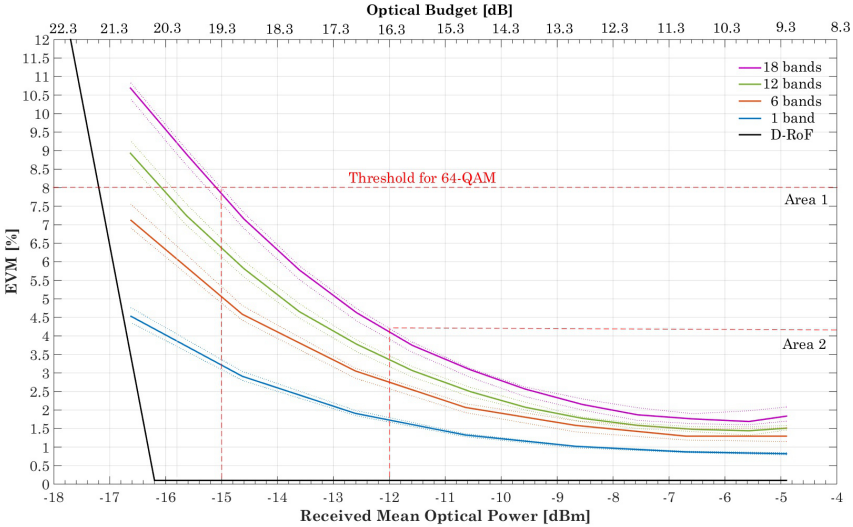

Figure 5.23: Maximum, average and minimum EVM measurements considering 1 (alternately), 6, 12 and 18 bands altogether with illustration of D-RoF EVM behaviour.

Figure 5.23 shows that, in this analogue transmission experiment, the

addition of new bands produced an EVM degradation. This worsening can be explained by the fact that A-RoF DAC provides a limited amount of RF power, therefore, a possible increase in the number of transmitted bands leads to a reduction of the individual power of each band and the consequent degradation of the Signal Noise Ratio (SNR).

This concept can be verified through figure 5.23, in received mean optical power equal to -16 dBm the gap between minimum and maximum EVM is close to 6.5 perceptual points while in -5 dBm this difference is 1.3 perceptual point.

Figure 5.23, also shows the EVM measured for the D-RoF. However, it is important to note that such EVM measurements are done in the absence of the Direct Modulated Laser (DML) and Avalanche Photo Diode (APD) used in surveying the EVM curves calculated in the analogue transmission.

In light of this, the presence of the D-RoF curve has an illustrative, but not comparative character. In the refereed curve an abrupt degradation of EVM has been detected. This fast deterioration happens because from a certain received power level, the values are incorrectly identified.

The figure 5.23 show that it is possible to transmit the six signals, therefore meeting the EVM for 64-QAM, in the presence of up to 6 different bands, if the minimum received mean optical power is -16.6 dBm. Considering that the optical power emitted by laser in transmission is 4.3 dBm, it has an optical budget equal to 20.9 dB.

For a competition of 12 bands, the minimum optical power is -15.8 dBm and its respective optical budget is 20.3 dB. When 18 bands are transmitted together, the minimum received optical power is restricted to -15 dBm and an optical budget of 19.3 dB. Area 1 show the possible

minimum received values considering 18 bands and EVM equal to 8%.

However, if an optical budget safety margin of 3 dB to accommodate extra penalties in reception (Area 2), figure 5.23 shows that the minimum received optical power required is up to -12 dBm. At this value is associated an optical budget of 16.3 dB.

Being the wavelength used in this experiment 1310nm, which has an attenuation equal to 0.4 dB/km, in the point-to-point architecture, the maximum optical fibre length is 40.75 km, which quietly meets the 20 or 25 km forecasted for fronthaul.

For only 25 km, using the same 0.4 dB/km of attenuation, the optical budget required is 10 dB. Considering a minimum received optical power equal to -12 dBm, an optical power emission equal to -2 dBm is enough to attend such length.

The biggest advantage of analogue transmission is its spectral efficiency. This conclusion is found when verifies that a single LTE downlink 10 MHz Single Input Single Output (SISO) signal requires an optical transmitter holder of at least 614.4 MHz bandwidth to pack CPRI option 1 data.

Figure 5.24 shows A-RoF signal transmitted spectrum for 1, 6 , 12 and 18 LTE signals spaced of 500 kHz. In the last situation, it needs of 189 MHz (18 $\times$ 10 MHz + 18 $\times$ 0.5 MHz), therefore in 614,4 MHz it is possible to transmit up to 58 signals (58 $\times$ 10 MHz + 58 $\times$ 0,5 MHz).

However, it must be considered that A-RoF transmission is subjected to power restrictions on both electronic (DAC, Amplifier) and optical (laser) devices, which can subtract this maximum quantity of signals before being calculated.

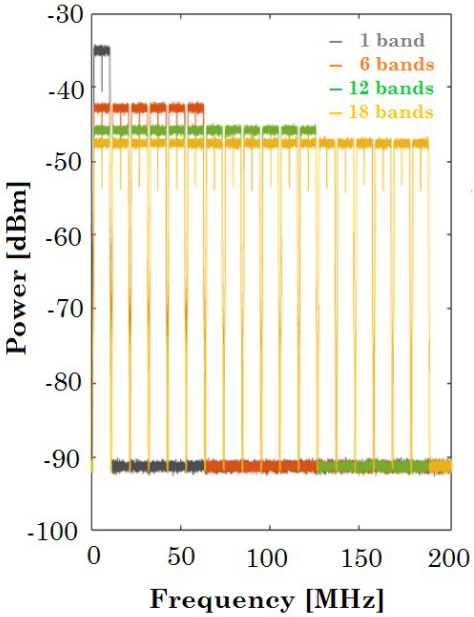

Figure 5.24: Received Electric Power A-RoF Spectrum.

Although analogue transmission has a remarkable spectral efficiency, it is important to highlight that such a data transport medium is sensitive to non-linearities effects (i.e. harmonics and intermodulation products), which are produced by devices such as laser, amplifier, and photodiode. These effects generate in-band and out-of-band degradations, therefore resulting in a worsening of the measured EVM.

Since a plural number of elements in this experiment can produce non linearities, this analysis concentrates on analysing non-linear effects produced by the direct modulated laser. This analysis is based on an experiment using similar setup shown in figure 5.22 was done.

In this experience are transmitted only 6 A-RoF bands with inter bands separations equals to: 500 kHz, 5 MHz and 10 MHz. Besides this, the RF power in Analogue to Digital Converter (ADC) was attenuated searching the best option. The results are shown in figures 5.25, 5.26, 5.27.

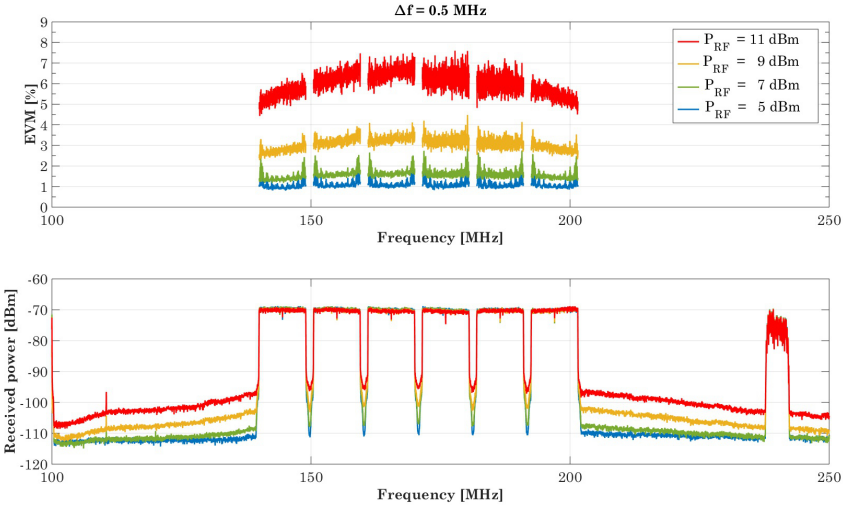

Figure 5.25: (a) EVM values per OFDM subcarrier and (b) spectrum evolution using different RF power at the laser input for Δf = 0.5 MHz.

Considering inter-band separation equal to 500 kHz, figure 5.25 demonstrates the level of EVM degradation as the RF power of the signal, which feeds the laser, is increased. Figure 5.25 (a) shows that, when the RF power (P_{RF}) levels at the input of laser is increased from 5 dBm (best case) to 11 dBm (worst case) the EVM degrades from 1% to, on average, 6%. Figure 5.25 (a) displays that the biggest EVM degeneration occurs in band numbers 3 and 4. This value better depicts the influence produced by inter-band spacing. Figure 5.25 (b)

presents the six received spectrum. By the figure 5.25 (b) is noted the strong action of out-of-band noise density non-linearity when the A-RoF inter band frequency distance is 0.5 MHz.

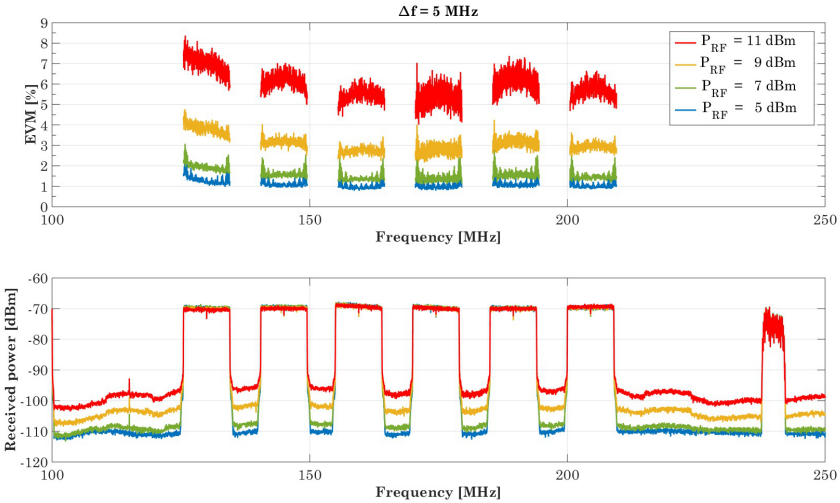

Figure 5.26: (a) EVM values per OFDM subcarrier and (b) spectrum evolution using different RF power at the laser input for Δf = 5 MHz.

Figure 5.26 (a) shows that the increase of inter-band spaces to 5 MHz produce a scattering of non-linearity, and this new situation causes the EVM to present an almost opposite behaviour verified in figure 5.25 (a). Figure 5.26 (a) shows that the increase from 0.5 MHz to 5 MHz produces an improvement of the EVM measured on the lateral subcarriers of the six signals. Figure 5.26 (b) depicts also that the spacing of A-RoF bands produces a scattering of the out-of-band noise density.

Figure 5.27 (a) confirms the thesis of the further away the signs the EVM of the sides gets better. It is noted in this figure that the EVM

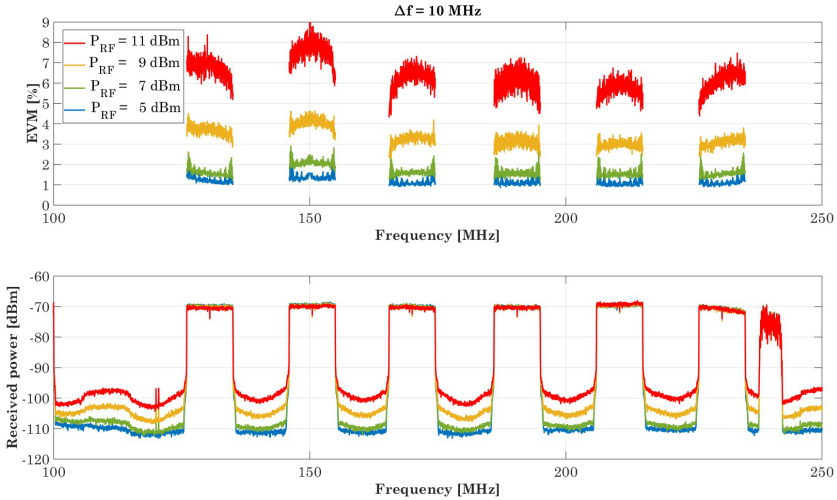

Figure 5.27: (a) EVM values per OFDM subcarrier and (b) spectrum evolution using different RF power at the laser input for Δf = 10 MHz.

measured in the edges of signal decreases faster than the same EVM showed in Figures 5.25 (a) and 5.26 (a). Figure 5.27 (b) shows also that out-of-band noise density decreases further when the A-RoF inter band distance increases to 10 MHz.

These figures also shows that the EVM within the signal remains practically unchanged. This phenomenon happens because in OFDM signal all subcarriers are separated always by the same Δf = 15 kHz apart, therefore intermodulation products generated by any pair of subcarriers will manifest at subcarriers right and left of the pair. As Δf does not changes inside of the band, OFDM signal quality continues suffering strong influence of intermodulation distortion.

6

Final Remarks

This chapter is divided in two section. Section 6.1 presents the conclusions while section 6.2 introduces potential research themes for future researches.

6.1 Summary and conclusions

A new decade come bringing the 5^{th} mobile network generation, which promises to offer mobile data volume per individual of 100 Mbps and a data volume equal to 10 Tbps/km^2.

To make this promise a reality a set of key technologies has been studied. In the access network it is possible to mention the mobile dense heterogeneous network, massive MIMO and millimetre wave, while

in the aggregation network Virtual Radio Access Network (V-RAN), an evolution of Centralized Radio Access Network (C-RAN) has been pointed as the big trend for the next mobile network generation.

All benefits offered to users by mobile 5G generations will produce as counterpart a huge quantity of data to be trafficked by fronthaul, an aggregation network segment created with C-RAN advent.

The results from section 5.1 show the enormous amount of bits that will transit over fronthaul segment when the current and pure adoption of digital CPRI transmission is used.

From these values, it is concluded that some techniques must be used to mitigate this traffic and make the transit of these signs feasible. Nowadays two digital (compression signal and functional split) and one analogue (analogue transmission) techniques are being considered to subtract the exponential values foreseen for 5G fronthaul segment.

The results presented in section 5.2 show an important digital mobile bandwidth gain of up to 72.65% on fronthaul transmissions when the compression signal technique is used.

However, such saving presents as counterpart the extra time required for compression and decompression activities, reducing the maximum distance between RRH and BBU.

The results presented in section 5.2 also shows that for 256-QAM a compression ration higher than 62.96% implies in exceeding the EVM threshold established by the LTE standard. This means that the minimum quantity of sampling bits used in CPRI is equivalent to 6 bits.

Another digital technique researched is presented in section 5.3. The results present in this section show why functional split has been considered the hottest point of research on 5G networks. The economy pro-

vided overcomes the saving produced by compression technique while ensuring the full operation of the Coordinated MultiPoint (CoMP) technique. However, new studies are demanded to show how complex and expensive RRH become if these functions are displaced from BBU to RRH.

The motivation for this preference is due to a fragility observed in analogue transmission in face of non-linearity effects produced mainly by transceivers used in such type of transmission. However, the results presented in section 5.4 do not completely rule out the use of analogue transmission, thus leaving it as a complementary technology.

When comparing the two techniques developed to deal specifically with the exponential amount of data generated by the digital transmission, it can be seen that the functional split has been overshot in relation to signal compression because it does not require the additional times for compression and decompression required in compress signal.

The analytical results shown in section 5.2 and 5.3 shows also that functional split offers an economy higher than presented by the compression of signals in the quantity of data transported in the fronthaul segment.

The analysis available in section 5.4 confirms the feasibility of analogue transmission on fronthaul segment though this type of transmission is quite sensitive to effects produced by the transmitter and receiver devices themselves. However, studies in [dVPDR+17] shows that a technique called constant envelope modulation techniques mitigates the influence of non-linearities in analogue transmission.

Although there is no certainty about which of the three data saving options presented above will prevail, it is important to point out that all three are being considered in the research developed to generate the new integrating architecture of the backhaul and fronthaul segments

presented in section A. This project stands out for using Software Defined Network (SDN) and Virtualisation, founding concepts of V-RAN technology, so such a research project is being considered a step forward in C-RAN.

6.2 Outlook for the future

To meet the 5^{th} data traffic between Remote Radio Head (RRH) and Base Band Unit (BBU) the next generation of aggregation network must necessarily consider the utilization of techniques, which minimizes the amount of data while maintaining the EVM measurements required by TS 36.104 without adding extra delays in the time it takes for the packet to perform the round trip between RRH and BBU.

Due to this functional split scenario, it has been the technique with the greatest potential to satisfy such requirements, however, the studies related to this technique are in the initial phase and therefore constitute a wide field of research to be explored.

A starting point that can be explored is to study the operation of enhanced Common Public Radio Interface (eCPRI), which is likely to subtract up to 10 times the data traffic between RRH and BBU.

Another potential topic is to study the behaviour of the traffic coming from the 30 small cells which is the minimum number of small cells required for a user to navigate on 5G networks using speeds of at least 100 Mbps.

Also can be explored the transmission of analogue and digital signal together using for this different wavelength. In this approach can be evaluated the co-existence with 24GbE, the maximum distance achieved, the minimum space between two wavelength.

The use of V-RAN to also serve the Internet of Everything (IoE) will require that the new aggregation networks serving the 5G will have sufficient intelligence to transmit at the same time, signals with bandwidth starting at 200 kHz, named Narrow Band Internet of Everthings (NB-IoE), and also hundreds of MHz the called Enhanced Mobile BroadBand (EMBB). In this research area is important to verify, for example, if signal of NB-IoE can be transmitted as guard-band of eMBB signals or in-band of regular 5G signal eMBB.

Bibliography

[19015] IEEE 1904.3. Task force standard for radio over ethernet encapsulations and mappings. Technical report, IEEE, January 2015.

[ADABV15] A. Al-Dulaimi, A. Anpalagan, M. Bennis, and A. V. Vasilakos. 5g green communications: C-ran provisioning of comp and femtocells for power management. In *2015 IEEE International Conference on Ubiquitous Wireless Broadband (ICUWB)*, pages 1–5, October 2015.

[AMC15] M. Artuso, A. Marcano, and H. Christiansen. Cloudification of mmwave-based and packet-based fronthaul for future heterogeneous mobile networks. *IEEE Wireless Communications*, 22(5):76–82, October 2015.

[Asa15] T. Asai. 5g radio access network and its requirements on mobile optical network. In *Optical Network Design and Modeling (ONDM), 2015 International Conference on*, pages 7–11, May 2015.

[ATC+15] Ericsson AB, Huawei Technologies, NEC Corporation, Alcatel Lucent, and Nokia Siemens Networks. *Common*

Public Radio Interface (CPRI); interface specification, v7.0 edition, 10 2015.

[Aya16] E. Ayanoglu. 5g today: Modulation technique alternatives. In *2016 International Conference on Computing, Networking and Communications (ICNC)*, pages 1–5, February 2016.

[AZ13] N. Ansari and J. Zhang. *Media Access Control and Resource Allocation*. Springer, 1 edition, September 2013.

[BCA+13] J. Beas, G. Castanon, I. Aldaya, A. Aragon-Zavala, and G. Campuzano. Millimeter-wave frequency radio over fiber systems: A survey. *IEEE Communications Surveys Tutorials*, 15(4):1593–1619, April 2013.

[BET+12] B. Batagelj, V. Erzen, J. Tratnik, L. Naglic, V. Bagan, Y. Ignatov, and M. Antonenko. Optical access network migration from gpon to xg-pon. In *Proc. of The Third International Conference on Access Networks ACCESS*, 2012.

[BF14] J. Bartelt and G. Fettweis. An improved decoder for cloud-based mobile networks under imperfect fronthaul. In *2014 IEEE Globecom Workshops (GC Wkshps)*, pages 1499–1504, December 2014.

[BHL+14] F. Boccardi, R. W. Heath, A. Lozano, T. L. Marzetta, and P. Popovski. Five disruptive technology directions for 5g. *IEEE Communications Magazine*, 52(2):74–80, February 2014.

[BLM+14] N. Bhushan, J. Li, D. Malladi, R. Gilmore, D. Brenner, A. Damnjanovic, R. T. Sukhavasi, C. Patel, and

S. Geirhofer. Network densification: the dominant theme for wireless evolution into 5g. *IEEE Communications Magazine*, 52(2):82–89, February 2014.

[BNP16] C. Bouras, P. Ntarzanos, and A. Papazois. Cost modeling for sdn/nfv based mobile 5g networks. In *2016 8th International Congress on Ultra Modern Telecommunications and Control Systems and Workshops (ICUMT)*, pages 56–61, Oct 2016.

[BSTI13] V. Bobrovs, S. Spolitis, I. Trifonovs, and G. Ivanovs. Spectrum sliced wdm-pon system as energy efficient solution for optical access systems. In *2013 IEEE Latin-America Conference on Communications*, pages 1–6, November 2013.

[Car15] N. Carapelle. *BaseBand Unit Hotelling Architectures for Fixed-Mobile Converged Next-Generation Access and Aggregation Networks*. Phd thesis, Politecnico di Milano, 2015.

[Cat15] D. Catania. *Performance of 5G Small Cells using Flexible TDD*. Phd thesis, Aalborg University, 2015.

[CGS13] F. Cavaliere, L. Giorgi, and R. Sabella. Overcoming the challenges of very high-speed optical transmission. Technical report, Ericsson, 2013.

[CIS17] CISCO. Ericsson mobility report. Technical report, Cisco, 2017.

[CJCB15] A. Checko, A. C. Juul, H. L. Christiansen, and M. S. Berger. Synchronization challenges in packet-based cloud-ran fronthaul for mobile networks. In *2015 IEEE*

International Conference on Communication Workshop (ICCW), pages 2721–2726, June 2015.

[CLSC14] H. H. Cho, C. F. Lai, T. K. Shih, and H. C. Chao. Integration of sdr and sdn for 5g. *IEEE Access*, 2:1196–1204, September 2014.

[CNG+17] P. Chanclou, L. A. Neto, K. Grzybowski, Z. Tayq, F.Saliou, and N. Genay. Mobile fronthaul architecture and technologies: a ran equipment assessment. In *Optical Fiber Communication Conference*, page Th4B.1. Optical Society of America, 2017.

[CPC+13] P. Chanclou, A. Pizzinat, F. Le Clech, T. L. Reedeker, Y. Lagadec, F. Saliou, B. Le Guyader, L. Guillo, Q. Deniel, S. Gosselin, S. D. Le, T. Diallo, R. Brenot, F. Lelarge, L. Marazzi, P. Parolari, M. Martinelli, S. O'Dull, S. A. Gebrewold, D. Hillerkuss, J. Leuthold, G. Gavioli, and P. Galli. Optical fiber solution for mobile fronthaul to achieve cloud radio access network. In *Future Network and Mobile Summit (FutureNetworkSummit), 2013*, pages 1–11, July 2013.

[CPR17] Common Public Radio Interface CPRI. Industry leaders agree to develop new cpri specification for 5g. Technical report, ERICSSON, HUAWEI, NEC, NOKIA, 2017.

[CSHB14] H. Chougrani, J. Schwoerer, P. H. Horrein, and A. Baghdadi. Hardware implementation of a non-coherent ir-uwb receiver synchronization algorithm targeting ieee 802.15.6 wireless band. In *ICUWB 2014 : International Conference on Ultra-WideBand*, pages 444–449, 2014.

[CSN+16] C-Y. Chang, R. Schiavi, N. Nikaein, T. Spyropoulos, and C. Bonnet. Impact of packetization and scheduling on c-ran fronthaul performance. In *GLOBECOM 2016 IEEE Global Communications Conference Exhibition and Industry Forum*, Washington UNITED STATES, 12 2016.

[Cvi14] N. Cvijetic. Optical network evolution for 5g mobile applications and sdn-based control. In *Telecommunications Network Strategy and Planning Symposium (Networks), 2014 16th International*, pages 1–5, September 2014.

[dG17] F. de Greve. Boldly forging a new frontier for fronthaul, 2017.

[DGP+15] T. A. Diallo, B. Le Guyader, A. Pizzinat, S. Gosselin, P. Chanclou, F. Saliou, A. Abdelfattath, T. A. Diallo, and C. Aupetit-Berthelemot. A complete fronthaul cwdm single fiber solution including improved monitoring scheme. In *2015 European Conference on Networks and Communications (EuCNC)*, pages 325–329, 2015.

[dlOHLA16] A. de la Oliva, J. A. Hernandez, D. Larrabeiti, and A. Azcorra. An overview of the cpri specification and its application to c-ran-based lte scenarios. *IEEE Communications Magazine*, 54(2):152–159, February 2016.

[DPP+13] U. R. Duarte, R. S. Penze, F. R. Pereira, F. F. Padela, J. B. Rosolem, and M. A. Romero. Combined self-seeding and carrier remodulation scheme for wdm-pon. *Journal of Lightwave Technology*, 31(8):1323–1330, April 2013.

[dVPDR+17] E. da V. Pereira, V. O. C. Dias, H. R. O. Rocha, M. E. V. Segatto, and J. A. L. Silva. Electrical constant envelope signals for nonlinearity mitigation in coherent-detection orthogonal frequency-division multiplexing systems. *Optical Engineering*, 56(6):066101, 2017.

[EaG13] S. M. Abd El-atty and Z. M. Gharsseldien. On performance of hetnet with coexisting small cell technology. In *Wireless and Mobile Networking Conference (WMNC), 2013 6th Joint IFIP*, pages 1–8, April 2013.

[Eks12] A. Eksim. *Wireless Communications and Networks – Recent Advances*. InTech, 1 edition, March 2012.

[Eri16] Ericsson. Ericsson mobility report on the pulse of the newworked society. Technical report, Ericsson, 2016.

[Fre13] L. Frenzel. Understanding the small-cell and hetnet movement. *Electronic Design*, 61(11):48–55, March 2013.

[FSM+15] M. Fiorani, B. Skubic, J. Maartensson, L. Valcarenghi, P. Castoldi, L. Wosinska, and P. Monti. On the design of 5g transport networks. *Photonic Network Communications*, 30(3):403–415, 2015.

[Gar17] A. A. Garba. 5g overview. Technical report, ITU, 2017.

[GCTS13] B. Guo, W. Cao, A. Tao, and D. Samardzija. Lte/lte-a signal compression on the cpri interface. *Bell Labs Technical Journal*, 18(2):117–133, September 2013.

[Gig17] Gigalight. Introduction of sfp+/sfp28 optical module of cpri common pufblic rf digital interface. Technical report, Gigalight, 2017.

[GJJ17] P. Gandotra, R. Jha, and S. Jain. Green communication in next generation cellular networks: A survey. *IEEE Access*, PP(99):1–1, 2017.

[Gui12] J. Guillory. *Radio over Fiber for the future Home Area Networks*. Phd thesis, University of Paris-Est, 2012.

[Hai16] D. H. Hailu. Cloud radio access networks (c-ran) and optical mobile backhaul and fronthaul. Master's thesis, Norwegian University of Science and Technology, 2016.

[Haq14] S. Haque. Fiber to the antenna a closer look at benefits and issues in integrated optical and wireless networks. Master's thesis, BRAC University, 2014.

[HH15] E. Hossain and M. Hasan. 5g cellular: key enabling technologies and research challenges. *IEEE Instrumentation Measurement Magazine*, 18(3):11–21, 2015.

[Hu16] L. Hu. *Opportunities in 5G Networks: A Research and Development Perspective*. CRC Press, 1 edition, 7 2016.

[Hua10] Huawei. Next-generation pon evolution, 2010.

[Hun84] R. G. Hunsperger. *Integrated Optics: Theory and Technology*. Springer-Verlag, 2 edition, April 1984.

[Hus14] S. Hussain. *An Innovative RAN Architecture for Emerging Heterogeneous Networks: The Road to the 5G Era*. Phd thesis, University of New York, 2014.

[HvVH17] V. Houtsma, D. van Veen, and E. Harstead. Recent progress on standardization of next-generation 25, 50, and 100g epon. *Journal of Lightwave Technology*, 35(6):1228–1234, March 2017.

[I17] Chih-Lin I. Ran revolution with ngfi (xhaul) for 5g. In *Optical Fiber Communication Conference*, page W1C.7. Optical Society of America, 2017.

[IALN+16] China Mobile Research Institute, Alcatel-Lucent, Nokia Networks, ZTE Corporation, Broadcom Corporation, and Intel China Research Center. Next generation fronthaul interface. Technical report, China Mobile Research Institute, June 2016.

[IHD+14] C. L. I, J. Huang, R. Duan, C. Cui, J. X. Jiang, and L. Li. Recent progress on c-ran centralization and cloudification. *IEEE Access*, 2:1030–1039, August 2014.

[IKT13] D. Iida, S. K.and J. K., and J. Terada. Dynamic twdm-pon for mobile radio access networks. *Opt. Express*, 21(22):26209–26218, November 2013.

[INF12] INFINERA. Super-channels: Dwdm transmission at 100gb/s and beyound. Technical report, Infinera, 2012.

[Ins] China Mobile Research Institute. *C-RAN The Road Towards Green RAN*. China Mobile.

[iP15] iCIRRUS Project. Intelligent converged network consolidating radio and optical access around user equipment. Technical report, CORDIS, 2015.

[iP16] iJOIN Project. Interworking and joint design of an open access and backhaul network architecture for small cells based on cloud networks. Technical report, CORDIS, 2016.

[ISG14] ETSI Industry Specification Group ISG. *Open Radio equipment Interface; ORI interface Specification*, v4.1.1 edition, 10 2014.

[IT15] ITU-T. *Radio-over-fibre (RoF) technologies and their applications*, 2015.

[Itp17] Itprice. The best cisco global price list checking tool. Technical report, CISCO, 2017.

[Iva13] T. Ivanković. Heterogeneous networks in theory and practice. In *Information Communication Technology Electronics Microelectronics (MIPRO), 2013 36th International Convention on*, pages 452–455, May 2013.

[JITT16] M. Jaber, M. A. Imran, R. Tafazolli, and A. Tukmanov. 5g backhaul challenges and emerging research directions: A survey. *IEEE Access*, 4:1743–1766, April 2016.

[JL13] A. H. Jung and B. K. Lee. Centralized optical routing based on digitized radio-over-fiber technique for wireless backhauling. In *2013 18th OptoElectronics and Communications Conference held jointly with 2013 International Conference on Photonics in Switching (OECC/PS)*, pages 1–2, June 2013.

[JMZ+14] V. Jungnickel, K. Manolakis, W. Zirwas, B. Panzner, V. Braun, M. Lossow, M. Sternad, R. Apelfrojd, and

T. Svensson. The role of small cells, coordinated multipoint, and massive mimo in 5g. *IEEE Communications Magazine*, 52(5):44–51, May 2014.

[KH16] K. KwangOk and C. HwanSeok. Real-time demonstration of extended 10g-epon capable of 128-way split on a 100 km distance using oeo-based pon extender. In *2016 International Conference on Information and Communication Technology Convergence (ICTC)*, pages 930–932, Oct 2016.

[KKT15] J. Kani, S. Kuwano, and J. Terada. Options for future mobile backhaul and fronthaul. *Optical Fiber Technology*, 26, Part A:42 – 49, 2015. Next Generation Access Networks.

[KLH13] Heejung Kim, Sungwon Lee, and Kyung Hee. A survey on the key enabling technologies for the 5g mobile broadband networks, 2013.

[KNB+16] R. Knopp, N. Nikaein, C. Bonnet, F. Kaltenberger, A. Ksentini, and R. Gupta. Prototyping of next generation fronthaul interfaces (ngfi) using openairinterface. Technical report, Open Air Interface, September 2016.

[KPSD10] G. Kardaras, Tien Thang Pham, J. Soler, and L. Dittmann. Analysis of control and management plane for hybrid fiber radio architectures. In *Communication Technology (ICCT), 2010 12th IEEE International Conference on*, pages 281–284, November 2010.

[KRM+16] G. Khanna, T. Rahman, E. Man, E. Riccardi, A. Pagano, A. Chiado, S. Calabro, B. Spinnler,

D. Rafique, U. Feiste, H. de Waardt, B. Sommerkorn-Krombholz, N. Hanik, T. Drenski, M. Bohn, and A. Napoli. Single-carrier 400g 64qam and 128qam dwdm field trial transmission over metro legacy links. *IEEE Photonics Technology Letters*, PP(99):1–1, 2016.

[LCCV13] J. Ling, D. Chizhik, C. S. Chen, and R. A. Valenzuela. Capacity growth of heterogeneous cellular networks. *Bell Labs Technical Journal*, 18(1):27–40, June 2013.

[LETM14] E. G. Larsson, O. Edfors, F. Tufvesson, and T. L. Marzetta. Massive mimo for next generation wireless systems. *IEEE Communications Magazine*, 52(2):186–195, February 2014.

[LGN+16] J. Liu, H. Guo, H. Nishiyama, H. Ujikawa, K. Suzuki, and N. Kato. New perspectives on future smart fiwi networks: Scalability, reliability, and energy efficiency. *IEEE Communications Surveys Tutorials*, 18(2):1045–1072, November 2016.

[LHDG17] H. Li, L. Han, R. Duan, and G. M. Garner. Analysis of the synchronization requirements of 5g and corresponding solutions. *IEEE Communications Standards Magazine*, 1(1):52–58, March 2017.

[LLJ+15] L. B. Le, V. Lau, E. Jorswieck, N-D. Dao, A. Haghighat, D. I. Kim, and T. Le-Ngoc. Enabling 5g mobile wireless technologies. *EURASIP Journal on Wireless Communications and Networking*, 2015(1):1–14, 2015.

[LLN15] C. Lim, , K. L. Lee, and A. Nirmalathas. Review of physical layer networking for optical-wireless integration. *Optical Engineering*, 55(3):031113, 2015.

[LLS+14] L. Lu, G. Y. Li, A. L. Swindlehurst, A. Ashikhmin, and R. Zhang. An overview of massive mimo: Benefits and challenges. *IEEE Journal of Selected Topics in Signal Processing*, 8(5):742–758, October 2014.

[LN10] C. Lim and A. Nirmalathas. Optical-wireless integration: Technologies for physical layer networking. In *Wireless Communications and Networking Conference Workshops (WCNCW), 2010 IEEE*, pages 1–5, April 2010.

[Loo13] M. Loomis. Network architectures for cpri backhauling. In *Optical Fiber Communication Conference/National Fiber Optic Engineers Conference 2013*, page OTu2E.4. Optical Society of America, 2013.

[LPJ13] K. Lee, J. H. Park, and H.yun D. Jung. Comparison of digitized and analog radio-over-fiber systems over wdm-pon networks. In *2013 International Conference on ICT Convergence (ICTC)*, pages 705–706, October 2013.

[LZ16] F-L. Luo and C. J. Zhang. *Signal Processing for 5G: Algorithms and Implementations*. Wiley, 1 edition, 2016.

[LZZ+13] L. Lei, Z. Zhong, K. Zheng, J. Chen, and H. Meng. Challenges on wireless heterogeneous networks for mobile cloud computing. *IEEE Wireless Communications*, 20(3):34–44, June 2013.

[MET15] METIS. Ict-317669 metis, deliverable 8.4 version 1 metis final project report, April 2015.

[Mit14] J. E. Mitchell. Integrated wireless backhaul over optical access networks. *Journal of Lightwave Technology*, 32(20):3373–3382, October 2014.

[MKTO16] K. Miyamoto, S. Kuwano, J. Terada, and A. Otaka. Analysis of mobile fronthaul bandwidth and wireless transmission performance in split-phy processing architecture. *Opt. Express*, 24(2):1261–1268, Jan 2016.

[NDK16] V. G. Nguyen, T. X. Do, and Y. Kim. Sdn and virtualization-based lte mobile network architectures: A comprehensive survey. *Wireless Personal Communications*, 86(3):1401–1438, 2016.

[Net16] Fiber Optic Social Network. Disadvantages and advantages of dwdm and cwdm system. Technical report, FOMSN, 2016.

[Nik15] N. Nikaein. *LATENCY, COOPERATION, AND CLOUD IN RADIO ACCESS NETWORK*. Phd thesis, University of Nice, 2015.

[NK16] G. Nakkoul and M. S. H. Kaikobad. Implementing linear predictive coding based on a statistical model for lte fronthaul. Technical report, China Mobile Research Institute, 2016.

[NKM+16] S. Nishihara, S. Kuwano, K. Miyamoto, J. Terada, and A. Ootaka. Study on protocol and required bandwidth for 5g mobile fronthaul in c-ran architecture with mac-phy split. In *2016 22nd Asia-Pacific Conference on Communications (APCC)*, pages 1–5, August 2016.

[NW13] D. Novak and R. Waterhouse. Advanced radio over fiber network technologies. *Optics Express*, 21(19):23001–23006, September 2013.

[ODK16] T. O. Olwal, K. Djouani, and A. M. Kurien. A survey of resource management toward 5g radio access networks. *IEEE Communications Surveys Tutorials*, 18(3):1656–1686, 2016.

[oEE16] IEEE Institute of Electrical and Electronics Engineers. P1914.1 - standard for packet-based fronthaul transport networks. Technical report, IEEE, June 2016.

[OJFM11] A. Osseiran and W. Mohr J. F. Monserrat. *Mobile and Wireless Communications for IMT-Advanced and Beyond*. Wiley, 1 edition, August 2011.

[OOF+14] R. S. Oliveira, R. S. Oliveira, C. R. L. Francês, J. C. W. A. Costa, D. F. R. Viana, M. Lima, and A. Teixeira. Analysis of the cost-effective digital radio over fiber system in the ng-pon2 context. In *Telecommunications Network Strategy and Planning Symposium (Networks), 2014 16th International*, pages 1–6, September 2014.

[PCSD15] A. Pizzinat, P. Chanclou, F. Saliou, and T. Diallo. Things you should know about fronthaul. *Journal of Lightwave Technology*, 33(5):1077–1083, March 2015.

[PHV15] D. Pompili, A. Hajisami, and H. Viswanathan. Dynamic provisioning and allocation in cloud radio access networks (c-rans). *Ad Hoc Networks*, 30:128 – 143, 2015.

[PK11] Z. Pi and F. Khan. An introduction to millimeter-wave mobile broadband systems. *IEEE Communications Magazine*, 49(6):101–107, June 2011.

[PPP15] 5G PPP. *The 5G Infrastruture Public Private Partnership: the next generation of communication networks and services*, 2015.

[Pro15a] 5G-Crosshaul Project. 5g-crosshaul: The 5g integrated fronthaul/backhaul. Technical report, CORDIS, 2015.

[Pro15b] 5G-X-Haul Project. Dynamically reconfigurable optical-wireless backhaul/fronthaul with cognitive control plane for small cells and cloud-rans. Technical report, CORDIS, 2015.

[Pro16a] Cloud Radio Net Project. Cloud wireless networks: An information theoretic framework. Technical report, CORDIS, 2016.

[Pro16b] Sonata Project. Sonata nfv: Agile service development and orchestration in 5g virtualized networks. Technical report, CORDIS, 2016.

[PSL+16] M. Peng, Y. Sun, X. Li, Z. Mao, and C. Wang. Recent advances in cloud radio access networks: System architectures, key techniques, and open issues. *IEEE Communications Surveys Tutorials*, 18(3):2282–2308, March 2016.

[PSS16] N. Panwara, S. Sharmaa, and A. K. Singhb. A survey on 5g: The next generation of mobile communication. *Physical Communication*, 18, Part 2:64 – 84, 2016. Special Issue on Radio Access Network Architectures and Resource Management for 5G.

[PSSS14] S. H. Park, O. Simeone, O. Sahin, and S. Shamai Shitz. Fronthaul compression for cloud radio access networks:

Signal processing advances inspired by network information theory. *IEEE Signal Processing Magazine*, 31(6):69–79, November 2014.

[PWLP15] M. Peng, C. Wang, V. Lau, and H. V. Poor. Fronthaul-constrained cloud radio access networks: insights and challenges. *IEEE Wireless Communications*, 22(2):152–160, April 2015.

[RIG+17] V. Rakovic, A. Ichkov, N. Grosheva, V. Atanasovski, and L. Gavrilovska. Analysis of virtual resource allocation for cloud-ran based systems. In *2017 20th Conference on Innovations in Clouds, Internet and Networks (ICIN)*, pages 60–64, March 2017.

[RM13] A. Raikwar and A. K. Mishra. Towards unified vlsi architectures of radio-interfaces in distributed base transceiver stations. In *Control, Automation, Robotics and Embedded Systems (CARE), 2013 International Conference on*, pages 1–6, December 2013.

[RRS09] K. N. Sivarajan R. Ramaswami and G. H. Sasaki. *Optical Networks A Pratical Perspective*. Wiley, 3 edition, September 2009.

[RVR15] RF, Wireless Vendors, and Resources. Massive mimo | m-mimo basics | massive mimo advantages. Technical report, RFWireless-World, 2015.

[Sah09] S. Saha. Obsai interoperability in multi-vendor wimax base station architecture environment. Master's thesis, Helsinki University of Technology, 2009.

[Sal16] T. Salman. Cloud ran: Basics, advances and challenges. Technical report, Washington University in St. Louis, 2016.

[Sau14] M. Sauter. *From GSM to LTE-Advanced: An Introduction to Mobile Networks and Mobile Broadband*. Wiley, 2 edition, August 2014.

[SEN+06] Hyundai Syscomm, LG Eletronics, Nokia, Samsung ELectronics, and ZTE Corporation. *Open Base Station Architecture Initiative (OBSAI); BTS System Reference Document*, v2.0 edition, 2006.

[SHL+14] J. Shin, S. Hong, J. Y. Lim, S. Cho, H. Y. Rhy, and G. Y. Yi. Cwdm networks with dual sub-channel interface for mobile fronthaul and backhaul deployment. In *16th International Conference on Advanced Communication Technology*, pages 1099–1102, February 2014.

[SKGR15] S. Sun, M. Kadoch, L. Gong, and B. Rong. Integrating network function virtualization with sdr and sdn for 4g/5g networks. *IEEE Network*, 29(3):54–59, May 2015.

[SL15] V. Savic and E. G. Larsson. Fingerprinting-based positioning in distributed massive mimo systems. In *2015 IEEE 82nd Vehicular Technology Conference (VTC2015-Fall)*, pages 1–5, September 2015.

[SMI+14] N. Shibata, T. Murakami, K. Ishihara, T. Kobayashi, J. i. Kani, J. Terada, M. Mizoguchi, Y. Miyamoto, and N. Yoshimoto. 256-qam 8 wireless signal transmission with dsp-assisted analog rof for mobile front-haul in lte-b. In *2014 OptoElectronics and Communication*

Conference and Australian Conference on Optical Fibre Technology, pages 129–131, July 2014.

[SNRZ17] H. Si, B. L. Ng, M. S. Rahman, and J. Zhang. A novel and efficient vector quantization based cpri compression algorithm. *IEEE Transactions on Vehicular Technology*, PP(99):1–1, February 2017.

[SS14] H. Son and S. M. Shin. Fronthaul size: Calculation of maximum distance between rrh (at cell site) and bbu (at co). Technical report, NetManias, 2014.

[STP+13] A. Saadani, M. El Tabach, A. Pizzinat, M. Nahas, P. Pagnoux, S. Purge, and Y. Bao. Digital radio over fiber for lte-advanced: Opportunities and challenges. In *Optical Network Design and Modeling (ONDM), 2013 17th International Conference on*, pages 194–199, April 2013.

[Str16] E. C. Strinati. Next generation of wireless networks. Technical report, Community Research and Development Information Service, 2016.

[Tan16] W. Tangtrongpairoj. *Radio over Fiber based Wireless Access Technology for Flexible Channel Resource Allocation*. Phd thesis, Nara Institute of Science and Technology, 2016.

[TAS+16] A. Tzanakaki, M. Anastasopoulos, D. Simeonidou, I. Berberana, D. Syrivelis, T. Korakis, P. Flegkas, D. C. Mur, I. Demirkol, J. Gutiérrez, E. Grass, Qing Wei, E. Pateromichelakis, A. Fehske, M. Grieger, M. Eiselt, J. Bartelt, G. Lyberopoulos, and E. Theodoropoulou. 5g infrastructures supporting end-user and operational

services: The 5g-xhaul architectural perspective. In *2016 IEEE International Conference on Communications Workshops (ICC)*, pages 57–62, May 2016.

[Tel03] International Telecommunication Union Telecommunication. *ITU-T Recommendation G.694.2 Spectral grids for WDM applications: CWDM wavelength Grid*, 2003.

[Tel12] International Telecommunication Union Telecommunication. *ITU-T Recommendation G.694.1 Spectral grids for WDM applications: DWDM Frequency Grid*, 2012.

[TGC+16] Z. Tayq, B. Le Guyader, P. Chanclou, S. Gosselin, D. Abdourahmane, D. P. Venmani, C. Aupetit-Berthelemot, S. Pachnicke, M. Eiselt, A. Autenrieth, and J. Elbers. Fronthaul performance demonstration in a wdm-pon-based convergent network. In *2016 European Conference on Networks and Communications (EuCNC)*, pages 250–254, 2016.

[TKK+14] T. Taniguchi, T. Kobayashi, S. Kuwano, J. i. Kani, J. Terada, and H. Kimura. Mobile optical network for future radio access. In *2014 12th International Conference on Optical Internet 2014 (COIN)*, pages 1–2, August 2014.

[TKT+14] T. Tashiro, S. Kuwano, J. Terada, T. Kawamura, N. Tanaka, S. Shigematsu, and N. Yoshimoto. A novel dba scheme for tdm-pon based mobile fronthaul. In *Optical Fiber Communications Conference and Exhibition (OFC), 2014*, pages 1–3, March 2014.

[TR14] N.D. Tripathi and J. H. Reed. *Cellular Communications: A Comprehensive and Practical Guide*. Wiley-IEEE Press, 1 edition, October 2014.

[TRV+17] R. Tucker, M. Ruffini, L. Valcarenghi, D. R. Campelo, D. Simeonidou, L. Du, M. C. Marinescu, C. Middleton, S. Yin, T. Forde, K. Bourg, E. Dai, E. Harstead, P. Chanclou, H. Roberts, V. Jungnickel, S. Figuerola, T. Takahara, R. Yadav, P. Vetter, D. A. Khotimsky, and J. S. Wey. Connected ofcity: Technology innovations for a smart city project [invited]. *IEEE/OSA Journal of Optical Communications and Networking*, 9(2):A245–A255, February 2017.

[TSF+17] T. Tsutsumi, Y. Sakai, T. Fujiwara, H. Ou, Y. Kimura, T. Sakamoto, K. I. Suzuki, M. Kubota, and A. Otaka. Field measurement and analysis of long-reach and high-splitting-ratio 10g-epon with optical amplifier in central office. *Journal of Lightwave Technology*, 35(10):1775–1784, May 2017.

[TvWA+16] M. Tercero, P. von Wrycza, A. Amah, J. Widmer, M. Fresia, V. Frascolla, J. Lorca, T. Svensson, M. H. Hamon, S. Destouet Roblot, A. Vijay, M. Peter, V. Sgardoni, M. Hunukumbure, J. Luo, and N. Vucic. 5g systems: The mmmagic project perspective on use cases and challenges between 6ghz and 100 ghz. In *2016 IEEE Wireless Communications and Networking Conference*, pages 1–6, April 2016.

[Uni17] International Telecommunication Union. Draft new report itu-r m.[imt-2020.tech perf req] - minimum re-

quirements related to technical performace for imt-2020 radio interface(s). Technical report, ITU, 2017.

[VGMM14] C. Vitale, R. Gupta, V. Mancuso, and A. Morelli. A prototyping methodology for sdn-controlled lte using labview sdr and ns3, 2014.

[VIAa] VIAVI. *Optimizing Small Cells and the Heterogeneous Network (HetNet).*

[VIAb] VIAVI. *Radio Frequency Analysis at FiberBased Cell Sites.*

[VIAc] VIAVI. *Radio Frequency Analysis at FiberBased Cell Sites with an OBSAI Interface.*

[Wü15] D. Wübben. Final definition and evaluation of phy layer approaches for ranaas and joint backhaul-access layer. Technical report, ICT, 2015.

[WAS15] T. Wan and P. Ashwood-Smith. A performance study of cpri over ethernet with ieee 802.1qbu and 802.1qbv enhancements. In *2015 IEEE Global Communications Conference (GLOBECOM)*, pages 1–6, December 2015.

[Weg06] Q. W. Wegener. Adaptive compression and decompression of bandlimited signals, March 7 2006. US Patent 7,009,533.

[Weg12] A. W. Wegener. Compression of baseband signals in base transceiver system radio units, December 11 2012. US Patent 8,331,461.

[WHG+14] C. X. Wang, F. Haider, X. Gao, X. H. You, Y. Yang, D. Yuan, H. M. Aggoune, H. Haas, S. Fletcher, and E. Hepsaydir. Cellular architecture and key technologies

for 5g wireless communication networks. *IEEE Communications Magazine*, 52(2):122–130, February 2014.

[Wik14] Wikiwand. Wavelength-division multiplexing. Technical report, Wikipedia, 2014.

[WIK16] FIBER OPTIC WIKI. Dwdm disadvantages and dwdm advantages. Technical report, Fowiki, 2016.

[WNG10] D. Wake, A. Nkansah, and N. J. Gomes. Radio over fiber link design for next generation wireless systems. *Journal of Lightwave Technology*, 28(16):2456–2464, August 2010.

[WRB+14] D. Wubben, P. Rost, J. S. Bartelt, M. Lalam, V. Savin, M. Gorgoglione, A. Dekorsy, and G. Fettweis. Benefits and impact of cloud computing on 5g signal processing: Flexible centralization through cloud-ran. *IEEE Signal Processing Magazine*, 31(6):35–44, Nov 2014.

[YHH+15] Chenhui YE, Xiaofeng Hu, Xiaoan Huang, Qingjiang Chang, Xiao Sun, Zhensen Gao, Simiao Xiao, and Kaibin Zhang. A first demonstration of a pon-based analog fronthaul solution supporting 120 20mhz lte-a signals for future het-net radio access. In *Asia Communications and Photonics Conference 2015*, page ASu3E.2. Optical Society of America, 2015.

[YLJ+15] M. Yang, Y. Li, D. Jin, L. Zeng, X. Wu, and A. Vasilakos. Software-defined and virtualized future mobile and wireless networks: A survey. *Mobile Networks and Applications*, 20(1):4–18, 2015.

[YLLN13] Y. Yang, F. Li, C. Lim, and A. Nirmalathas. Radio-over-fiber technologies for future mobile backhaul supporting cooperative base stations. In *Microwave Symposium Digest (IMS), 2013 IEEE MTT-S International*, pages 1–3, June 2013.

[Yos13] N. Yoshimoto. Operator perspective on next-generation optical access for high-speed mobile backhaul. In *Optical Fiber Communication Conference and Exposition and the National Fiber Optic Engineers Conference (OFC/NFOEC), 2013*, pages 1–3, March 2013.

[Yu14] H. Yu. *Software-Defined Networking in Heterogeneous Radio Access Networks.* 2014.

[ZM13] J. Zander and P. Mähönen. Riding the data tsunami in the cloud: myths and challenges in future wireless access. *IEEE Communications Magazine*, 51(3):145–151, March 2013.

[ZOY14] K. Zheng, S. Ou, and X. Yin. Massive mimo channel models: A survey. *International Journal of Antennas and Propagation*, 2014(2):1–110, June 2014.

[ZSL14] X. Zhang, D. Shen, and T. Liu. Review of linearization techniques for fiber-wireless systems. In *Wireless Symposium (IWS), 2014 IEEE International*, pages 1–4, March 2014.

Annex A: 5G-Crosshaul Project

Various cloud computing researchers have lately been studied in European projects. In [iP16], radio access network functionalities are centralized using an open information technology platform, which is based on a cloud infrastructure, aiming for a joint design and optimisation of access and backhaul using management and operation algorithms integrating small cells and centralised processing.

A converged and wireless network approach aiming to flexibly connect small cells to the core network is investigated in [Pro15b]. In it, an optical/wireless architectures, network management, and software-defined cognitive control plane for mobile scenarios are studied.

In [iP15] is proposed an intelligent Centralized Radio Access Network (C-RAN), whose connections between RRH and BBU is achieve by optical fibre, using flexible Ethernet in the midhaul. This approach aims to minimize costs while offering self-optimizing network functions that maximise network resource utilisation and energy efficiency.

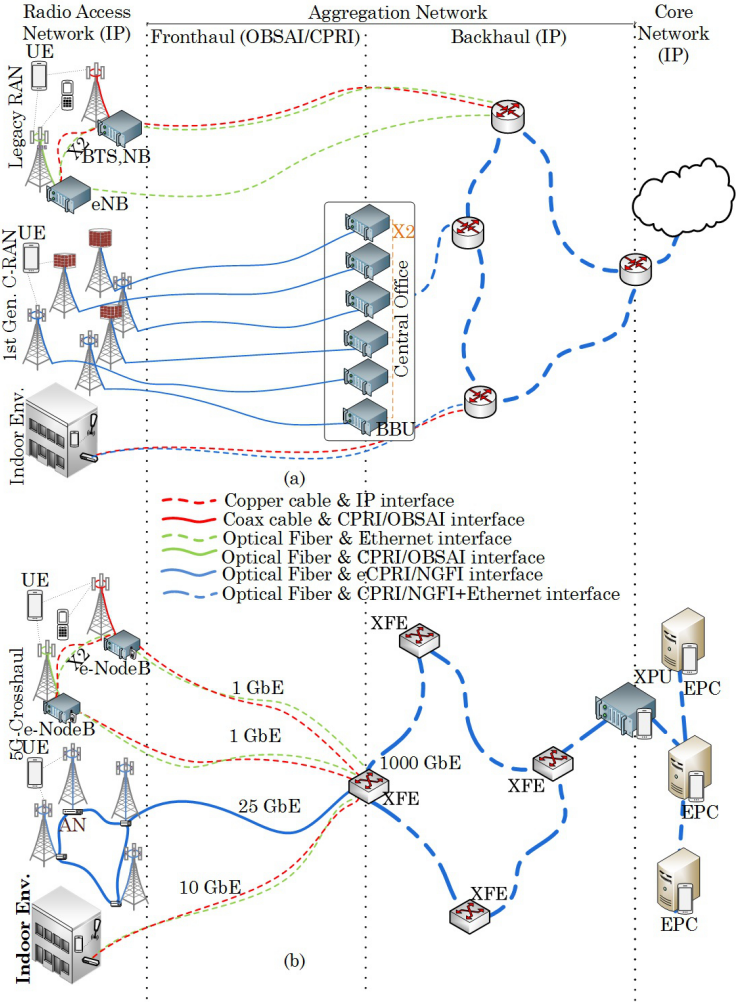

Figure A.1: Mobile system architecture: (a) legacy D-RAN and traditional C-RAN; (b) 5G-Crosshaul.

To develop a Network Function Virtualization (NFV) framework to provide a programming model and development tool chain for virtualised services is the target of [Pro16b].

Focused on conducting a new theoretical study about ultimate communications limits and the potential of different cloud radio networks structures, the research conducted in [Pro16a] also expects to introduce optimal strategies for systems migrated to the cloud whose connection is then achieved using backhaul/fronthaul option.

The novel 5G architecture proposed by the 5G-Crosshaul project [Pro15a] can be considered an evolution of the traditional C-RAN concept proposed by China Mobile in 2010.

Figure A.1(a) shows that in the 4G legacy network, the signal from/to antennas was transported in a CPRI frame from/to eNodeB, then eNodeB forwarded/received a signal to the core network inside of one Ethernet frame. In an second stage, C-RAN architecture, pushed the baseband processing (e-NodeB) to a central office distant up to 25 km from the antenna. In the latter Figure A.1(b) depicts that 5G-Crosshaul architecture, baseband processing is performed based in a virtualised BBU hostelled in data centrers following the Software Defined Network (SDN) and Network Function Virtualization (NFV) paradigms.

The 5G-Crosshaul technologies present the following advantages:

1. To provide 1000 times higher wireless area capacity than observed in 2010, the multi-layer switch, named 5G-Crosshaul Forwarding Element (XFE), provides an efficient bandwidth transmission, through traffic multiplexing, by using different levels of granularity from Mbps to Gbps;

2. To facilitate the deployment of a massive number of devices, 5G-Crosshaul data plane will enable connection, to same network, through XFE switch using copper, wireless or fibre;

3. To reduce energy consumption by up to 90% (as compared to 2010), data plane architecture will allow centralization/concentration baseband processing on a reduced number of nodes, to optimize computational resources in 5G-Crosshaul Processing Unit (XPU) node and to permit that switching granularity can be achieved considering performance metrics and energy related criteria;

4. 5G-Crosshaul data plane offers a programmable transport platform acting several layers (packet, time slot, wavelength) enabling differentiated services;

5. The adoption of one Software Defined Network (SDN) / Open Flow enables reproduction of IP, Ethernet or MultiProtocol Label Switching (MPLS) networks behaviour, more specifically on the packet forwarding function. This feature also allows automation, management and configuration of networking rules and policies such as traffic separation, dynamic instantiation of functions, Virtual Local Area Network (VLAN) to tunnel mapping;

6. Enables new models of network virtualisation and multi-tenancy;

7. The concept of multi-tenancy, used by 5G-Crosshaul, which various users share the same network, increases efficiency and reduces CapEx and OpEx costs;

8. Flexibility of interconnections of distributed 5G radio access systems and core network functions, stored on network cloud nodes;

9. Simplifies network operations and allows a wide optimisation of Quality of Service (QoS) offered by the system.

The 5G-Crosshaul technologies have to address huge challenges described below:

1. How to distribute, dynamically and in the best possible way, functions belonging to the Baseband Unit (BBU), considering the network layout and traffic conditions;

2. How to operate and optimize, in a homogeneous way, a 5G network containing high technological heterogeneity;

3. How to apply, rigorously, and/or support QoS requirements, so different, depending on services requested by users and/or the network;

4. How to provide a convergence, backhaul/fronthaul, without disregarding the constant evolutions of switch, frame structure, synchronization mechanisms and evolution of physical technology;

5. How can you reduce the cost of last-mile, low-cost technologies by providing multi-tenancy and system-wide optimization while still providing an algorithm-based infrastructure design;

6. How to maximize the flexibility offered by the dynamic reconfiguration of physical parameters, routing and placement of functions to maximize the use of assets and at the same time reduce energy consumption.

5G-Crosshaul project presents the following novelties:

1. A control infrastructure, named Crosshaul Control Infrastructure (XCI), which is a unified and abstract network model allowing a control plane integration;

2. A unified data plane containing new technologies with high transmission capacity, through deterministic-latency switch architectures named Crosshaul Forwarding Element (XFE);

3. Routing and traffic algorithms able to meet 5G requirements such as latency and jitter;

4. Applications to reduce network management;

5. Optimization techniques allowing Quality of Experience (QoE);

Recent predictions show that in 2020 there will be considerable growth in the capillarity of mobile networks through use of small cells. The promising technologies to address this mobile network densification are Software Defined Network (SDN) / Network Function Virtualization (NFV).

In the face of this new reality, a modern way of integrating fronthaul/backhaul technologies has been considered a key point for the proper functioning of 5G networks. The integration of both these segments will be quite beneficial because it will allow the use of the same infrastructure, leading to a fall in total costs.

Considering such demand, a new 5G-Crosshaul architecture has been developed aiming to integrate fronthaul/backhaul segments in a flexible, software-defined reconfigured, and packet based 5G transport network keeping an architecture compatibility with the current and most popular open source SDN controllers used, namely Open Daylight (ODL) and Open Nerwok Operating System (ONOS).

5G-Crosshaul's area of expertise extends its domain for three sub-areas: processing plane, control plane, and data plane.

A.1 Processing Plane

It is in this plane that 5G-Crosshaul Processing Unit (XPU) is localized. XPU is a logical unit in charge of hosting baseband processing or computing operations such as instantiation and management of virtual network functions by network function virtualisation. XPU hosts BBUs and also might serve as caches. The various services, which are possible to host in XPUs, are responsible for the signifiers flexibility provided by Crosshaul architecture.

A.2 Control Plane

The control plane is centralized in the 5G-Crosshaul Control Infrastructure (XCI). The XCI concentrates all intelligence to provide control and management functions that execute different types of resources contained in 5G-Crosshaul infrastructure.

XCI is the 5G transport Management and Orchestration (MANO). Based on SDN precepts, it supplies a unified platform, used by orchestration layer applications, to monitor and/or to program data plane by means of a set of functions allowing automated and on-demand virtual network slices, and chains of virtual network functions. The combination of these elements enables a dynamic and convergent 5G fronthaul and backhaul virtual infrastructure within a multi-tenancy environment.

Figure A.2 presents with more details of the acting of XCI in a 5G-Crosshaul environment.

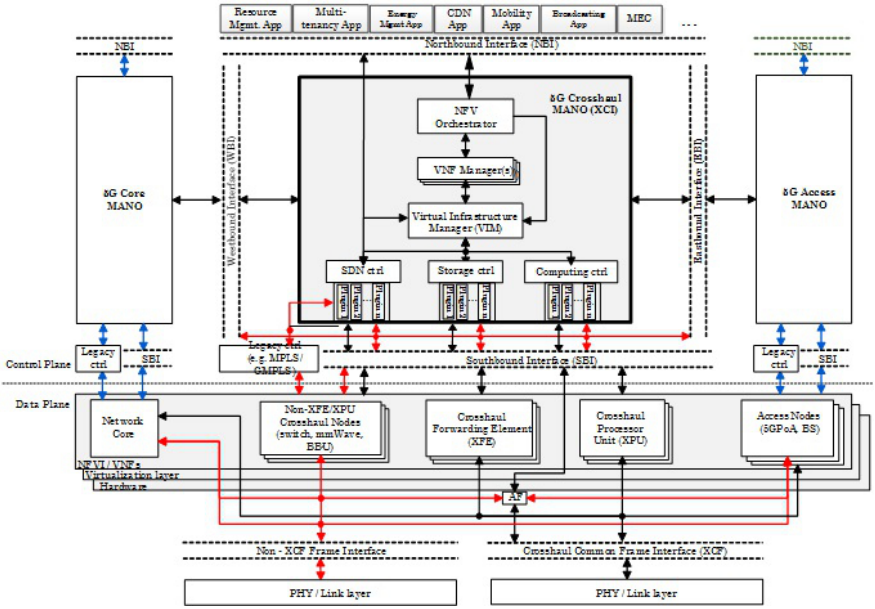

Figure A.2: 5G-Crosshaul system architecture.

XCI is composed of three main blocks: Network Function Virtualisation Orchestration (NFVO), Virtual Network Functions Managers (VNFMs), Virtualised Infrastructure Manager (VIM). The figure A.2 shows the XCI four points interfaces: northbound, southbound, eastbound and westbound.

In the Westbound Interface (WBI) and Eastbound Interface (EBI) there are only Crosshaul APIs, which only interact with controllers, out of scope of the 5G-Crosshaul domain. The reason for this interaction is to monitor potential conditions occurring in Radio Access Network (RAN) and/or Core Network (CN) domains, which can affect the Crosshaul architecture performance.

XCI offers, in the Northbound Interface (NBI), Application Programming Interface (API)s such as REST, NETCONF, or RESTCONF, which are used to program and monitor data plane, while the Southbound Interface (SBI) is based on APIs such as OpenFlow, OF-Config, OVSDB and SNMP, which are used to interact with data plan, controlling and managing: the PHY configuration of the different link technologies (transmission power on wireless links), the packet forwarding behaviour executed by all the 5G-Crosshaul Forwarding Element (XFE) inside of 5G-Crosshaul network and the 5G-Crosshaul Processing Unit (XPU).

A.3 Data Plane

To have a unified and radio technology independent transport architecture, 5G-Crosshaul network offers switches with big capacity (XFEs), as shown in figure A.3.

These devices can be interconnected using heterogeneous links, which can be via wired (i.e. copper or fibre) or wireless (i.e. mmWave and optical wireless, also known as free space optics).

Wireless connections (Scenario 1) are used in two opposite cases: rural areas, where the cost of new implementations is prohibitive, and densely populated cities where the deployments of cables, for logistics reasons are not possible, or high costs with digging and road works are required.

Having fixed access infrastructures (Scenario 2), operators tend to reuse such infrastructure. However, this reuse is not easy due to the fact that the majority of this infrastructure was designed for much smaller requirements, than those demanded by 5G networks. The

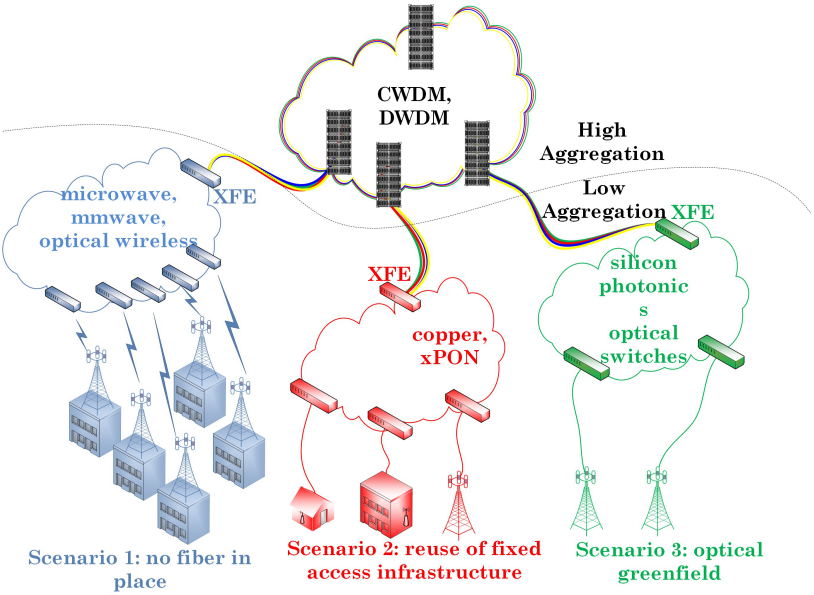

Figure A.3: 5G-Crosshaul technology map.

operator's insistence on using this option, necessarily implies, in new device investments, aiming to target low latency, symmetric up/down streams and high bandwidth. This option has been considered mainly for indoor approach.

Scenario 3 always occurs if no infrastructure exists. In such condition, a complete new network, using modern technologies and devices, is deployed, enabling high performance.

5G-Crosshaul data plane logical architecture, illustrated in figure A.4, is controlled by 5G-Crosshaul Control Infrastructure (XCI) and it contains six main components, namely: 5G-Crosshaul Common Frame (XCF), 5G-Crosshaul Packet Forwarding Element (XPFE),

5G-Crosshaul Circuit Switching Element (XCSE), 5G-Crosshaul Forwarding Element (XFE), and Adaptation Function (AF).

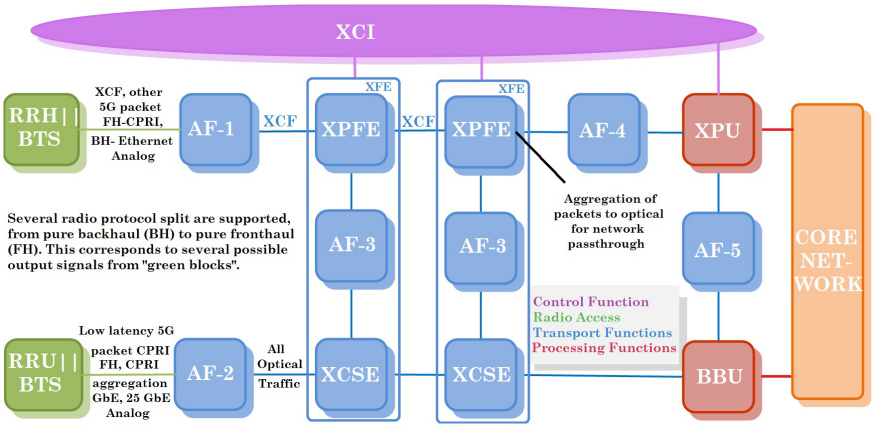

Figure A.4: 5G-Crosshaul data plane architecture.

The XCF is a transport/packet frame format interface based on Ethernet standard facilitating reuse of current switch, however, XCF also enables the deployment of generic switches. XCF improves Ethernet because it includes an apparatus to manage time-sensitive applications, which are activities online that speed tends to make a dramatic difference in customer experience. The XCF design enables it to be compatible with different current physical interface technologies existent in the transport network. XCF is designed to carry both fronthaul and backhaul data over heterogeneous links, such as, Ethernet (IEEE 802.3), mmWave radio and WiFi (IEEE 802.11).

XCF also supports various functional splits of the radio protocol stacks and multi-tenancy streams, which are flows of different tenants. The XCF has low protocol overhead allowing the flows to be sent by multiple paths towards one destination bringing multiplexing gains. XCF is

compatible with legacy technologies besides transport synchronization information. Based on these features the Ethernet frame has been considered the option to be used by XCF.

The figure A.5 shows that XCF is a frame format used by 5G-Crosshaul Packet Forwarding Element (XPFE), which is a packet forwarding. The same figure A.5 depicts that besides XCF, XPFE also contains other components such as a common control plan agent that is responsible for connecting XPFE with the 5G-Crosshaul Control Infrastructure (XCI). Common device agent in charge of connecting with system peripheral and presenting to the control infrastructure information such as CPU usage, GPS position, RAM occupancy and so on. Mappers for each physical interface. Physical interfaces, which transmit data on the link. XPFE exploits the statistical multiplexing gain in a new generation packet which is based on fronthaul interfaces.

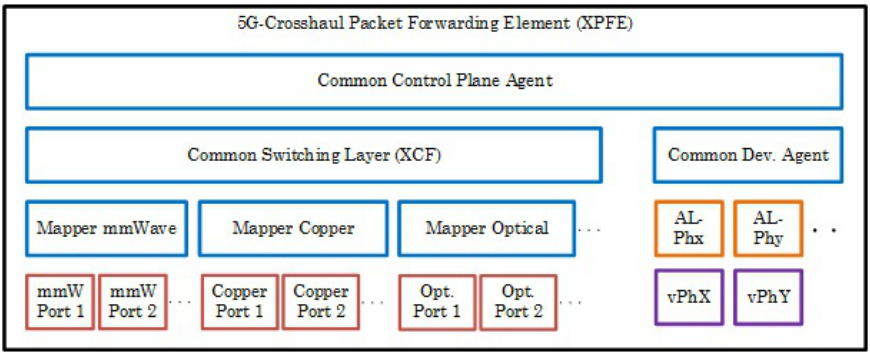

Figure A.5: XPFE functional architecture.

Another important component present in 5G-Crosshaul data plane architecture is the 5G-Crosshaul Circuit Switching Element (XCSE). XCSE is used to offload the XPFE and cross-connect constant bit rate fronthaul traffic, such as CPRI. XCSE can be divided into two sub-switches at different traffic granularity. In optical networks, the

coarsest sub-switch can be Optical Add&Drop Multiplexer (OADM), Reconfigurable Optical Add&Drop Multiplexer (ROADM) or Optical Cross-Connect (OXC), and the finest one can be Optical Transport Network (OTN) switch.

XPFE and XCSE are the two elements that compose the 5G-Crosshaul Forwarding Element (XFE), and "the bridge" that links both these elements is an Adaptation Function (AF), named AF-3. Such option is used always that XCF traffic on XPFE layer needs to be offload, to avoid congestion and therefore avoid loss of packets. In this situation AF-3 aggregates a set of packets into big pipes, which can be managed by the XCSE, as shown in figure A.4, which is not based on the 5G-Crosshaul Common Frame (XCF).

On the other hand, the Adaptation Function (AF) connects Remote Radio Unit (RRU) or Base Transceiver Station (BTS). AF-1 has the purpose to be a media adaptation (from air to fibre) and translation of vendor specific radio interface such as (CPRI, OBSAI, ORI, Ethernet, etc.) into the proposed 5G-Crosshaul Common Frame (XCF), which will be switched by one 5G-Crosshaul Packet Forwarding Element (XPFE).

The AF-2 function is to map the radio interface in one protocol, i.e G.709 (OTN), G.989 (NG-PON2), used by the 5G-Crosshaul Circuit Switching Element (XCSE). The AF-2 utilization is indicated when a packet conversion to threaten compliance, with stringent requirements, is required by interfaces such as CPRI, OBSAI or ORI. In this case, AF-2 also performs media adaptation functions and maps the radio interface in one protocol which will be used by the circuit switch.

AF-4 is triggered whenever the interface between XPFE and XPU does not happen through XCF. AF-5 will be used when a pre-existing BBU needs to communicate with 5G-Crosshaul Processing Unit (XPU).

5G-Crosshaul architecture has the capacity to address the formidable challenges on the future 5G network. It allows an integration of front-back haul segments, besides combing the best latency performance by circuit switching, but also statistical multiplexing for high 5G traffic load by packet switching features.